o-Nitrobenzyl-based polymer materials with light-regulated multi-functions

Dissertation

zur Erlangung des Grades

des Doktors der Ingenieurwissenschaften

der Naturwissenschaftlich-Technischen Fakultät

der Universität des Saarlandes

von

Xinhong Xiong

Saarbrücken

2021

Tag des Kolloquiums:	23. February 2022
Dekan:	Prof. Dr. Jörn Eric Walter
Berichterstatter:	Prof. Dr. Aránzazu del Campo Bécares Prof. Dr. Guido Kickelbick
Akad. Mitglied:	Dr. Lola Gonzales-García
Vorsitz:	Prof. Dr. Karen Lienkamp

o-Nitrobenzyl-based polymer materials with light-regulated multi-functions

Xinhong Xiong

geb. in Dangyang, China

DISSERTATION

INM-Leibniz Institut für neue Materialien, Saarbrücken

Acknowledgements

I am a slow walker, but I never walk backwards (Abraham Lincoln). For me, the whole period of the PhD is an important part of my life. Although the thesis come a little bit late and many difficulties are encountered, I got the most beloved angel in my life. I am so lucky that I met so many kind, gentle, and lovely people, who gave me help, encouragement and always warm my heart in the last five years. Therefore, it is a great pleasure to convey my deepest and sincerest gratitude to them all here.

First and foremost, I would like to thank Dr. Jiaxi Cui for being a great advisor to me. It is you who gave me the opportunity to start my PhD five years ago. What I have learnt from you in both scientific research and life is priceless. I am deeply impressed by your extraordinary creativity, unmatched enthusiasm, and great taste of science. Your profound knowledge and patient guidance not only help me in my research, but also broaden my horizon and save me a lot of precious time. Without your encouragement, your affirmation, and your respect, I will not have confidence in completing the thesis. Also, you always tried your best to support my career choice which helped me to come out from the confusion. No matter as a mentor or friend, your suggestions are always great for me. Thousands of words can't express my gratitude to you. Being your student is my greatest fortune.

Prof. Dr. Aránzazu del Campo Bécares, thank you so much for being my first supervisor, supporting my work, and providing me a better condition to complete the doctoral thesis.

Ms. Qiyang Jiang, I am lucky to know you and it was very nice experience to share my happiness and sadness with you. Thank you for taking care of me in life, enlightening me when I am confusing, encouraging, and helping me when I am in trouble. Of course, as the godmother of my baby, you give endless love to her and always consider more

comprehensively which helped me to make the right choices. Thank you, my sincere friend.

Dr. Jingnan Zhang, you are one of the most exciting friends in my mind. Whenever I need help, you never say No and are always the first one to give me a hand. Your sunny smile brought me infinite happiness which made my life not so boring. Thank you and hope you can find a position you really like.

Dr. Lu Han, a kind and lovely girl. Your optimistic attitude is always encouraging me to go forward. It was really a good memory to work with you and celebrate the birthday together. While I only overlapped with you for two years, we have continued our friendship. I believe you will achieve great success in your career.

Dr. Huaixia Zhao, an elder sister who helped me a lot in my experiments. I am deeply impressed by your hard-working, self-discipline, and rigorous attitude to scientific research. I hope you have a prosperous scientific future.

Dr. Jun Feng and Ms. Xi Zheng, a kind couple, thanks for helping me a lot in starting and adjusting the new life in Saarbrücken. I hope both of you can gain what you want in future.

Dr. Bin Li, thank you for selflessly sharing your experience with me, which helps me avoid a lot of failures. I believe you will have a great success in China soon.

Dr. Xianqiang Pei, thank you for helping me in both work and life, especially when I delivered the baby, you stopped your work and sent me to the hospital timely. Hope everything is fine with your new lab and you can get great scientific achievements in the future.

Many thanks to Dr. Yijun Zheng, Dr. Xiaozhuang Zhou, Dr. Baiju Pazhamkalathil Krishnan, Dr. Lizbeth Ofelia Prieto López, Dr. Fatih Puza, Dr. Haoran Ma, Dr. Anle Wang, Ms. Zeyu Fu, Ms. Danfeng Zhang and other colleagues in the group of Dynamic Biomaterials for spending the wonderful and unforgettable time with you in Germany.

Your encouragement and help really mean a lot to me. I wish you all the best in the future.

I would like to say thanks to Jieqiang Zhang and Feifei Xue, my special friends, who always encourage me to pursue my dream. Thanks a lot for your instructions when I felt confused and frustrated. I could always get inspiration by talking with you. I wish we can continue our relationship forever.

Last but not the least, I would like to express my love and thanks to my family members, especially to my father and mother, father in law, and mother in law for shouldering my responsibility all the time. Undoubtedly, you are always the greatest support and motivation to drive me forward. I would like to thank my wise husband, Lulu Xue, for continuous accompany and infinite love. You always support me in whatever I want to do. I appreciate everything you did for me. The road ahead is still long, let's go together.

Ziyu Xue, my lovely daughter, now you are three years old. You are the best gift that God gave to me. I hope you grow up healthily, happily and chase your dream bravely. I will always support you without any hesitation. This thesis is dedicated to my beloved angel.

Xinhong Xiong

07. 07. 2021, in Saarbrücken

Abstract

o-Nitrobenzyl (*o*NB)-based polymers have been used as photodegradable materials/surfaces, and responsive biomaterials. While previous studies have mainly focused on the photodegradation of the material by intercalating *o*NB derivatives in the polymer chains, this thesis pays attention to the utilization of *o*NB photolysis to tailor the properties of materials, including interface functions, network topology, and bulk properties. To this end, two kinds of *o*NB based molecules with multifunctional units were designed and synthesized: 2-bromo-N-(2-nitro-3, 4-dihydroxyphenethyl)-2-methylpropanamide (**NO_2-BDAM**, nitrodapomine based initiator) and 2-((2-bromo-2-methylpropanoyl)oxy)ethyl 4-(4-(1-(acryloyloxy)ethyl)-2-methoxy-5-nitrophenoxy) butanoate (**vinyl-*o*NB-Br**, photolabile inimer). In part 1, NO_2-BDAM, in combination with $Mn_2(CO)_{10}$ as a visible light-sensitive additive, was used to control the growth and detachment of polymer brushes independently. In part 2, vinyl-*o*NB-Br was introduced into a double network material for in situ regulating topology from connected double network (c-DN) to disconnected double network (d-DN) by light exposure. In the last part, vinyl-*o*NB-Br was used to graft and detach polymer brushes from a network, leading to the change of network topology and material toughness. These results contribute to the topic of functionalized *o*NB based polymer systems and tunable topological polymer networks, providing useful strategies both in chemistry and materials.

Zusammenfassung

o-Nitrobenzyl (*o*NB)-basierte Polymere wurden als photoabbaubare Materialien/Oberflächen und responsive Biomaterialien verwendet. Während sich frühere Studien hauptsächlich auf den Photoabbau des Materials durch die Interkalation von *o*NB-Derivaten in den Polymerketten konzentrierten, widmet sich diese Arbeit der Nutzung der *o*NB-Photolyse, um die Eigenschaften von Materialien, einschließlich Grenzflächenfunktionen, Netzwerktopologie und Volumeneigenschaften, anzupassen. Zu diesem Zweck wurden zwei Arten von oNB-basierten Molekülen mit multifunktionellen Einheiten entworfen und synthetisiert: 2-Brom-N-(2-nitro-3,4-dihydroxyphenethyl)-2-methylpropanamid (NO_2-BDAM, Nitrodapomin-basierter Initiator) und 2 -((2-Brom-2-methylpropanoyl)oxy)ethyl 4-(4-(1-(Acryloyloxy)ethyl)-2-methoxy-5-nitrophenoxy)butanoat (vinyl-*o*NB-Br, photolabiles Inimer). In Teil 1 wurde NO_2-BDAM in Kombination mit $Mn_2(CO)_{10}$ als Additiv für sichtbares Licht verwendet, um das Wachstum und die Ablösung von Polymerbürsten unabhängig voneinander zu kontrollieren. In Teil 2 wurde vinyl-*o*NB-Br in ein Doppelnetzwerkmaterial eingebracht, um die Topologie in situ vom verbundenen Doppelnetzwerk (c-DN) zum getrennten Doppelnetzwerk (d-DN) durch Lichteinwirkung zu regulieren. Im letzten Teil wurde Vinyl-oNB-Br zum Aufpfropfen und Ablösen von Polymerbürsten aus einem Netzwerk verwendet, was zu einer Änderung der Netzwerktopologie und Materialzähigkeit führte. Diese Ergebnisse tragen zum Thema funktionalisierte *o*NB-basierte Polymersysteme und abstimmbare

topologische Polymernetzwerke bei und liefern nützliche Strategien sowohl in der Chemie als auch in den Materialien.

List of Abbreviations

ATR-FTIR	Attenuated total reflection-Fourier transform infrared
AIBN	2, 2'-Azobisisobutyronitrile
AA	Acrylic acid
AC	Acryloyl chloride
ACN	Acetonitrile
Au	Gold
BIBB	2-Bromoisobutyryl bromide
BA	Butyl acrylate
$CHCl_3$	Chloroform
$CDCl_3$	Chloroform-$_d$
c-DN	connected-Double network
d-DN	disconnected-Double network
DA·HCl	Dopamine hydrochloride
DEEA	Di(ethylene glycol) ethyl ether acrylate
DMAP	4-(Dimethylamino)pyridine
DCM	Dichloromethane
DMF	*N,N*-Dimethylformamide
DMSO	Dimethyl sulfoxide
DMSO-$_{d6}$	Dimethyl sulfoxide-$_{d6}$
DN	Double network
EG	Ethylene glycol
EBIB	Ethyl α-bromoisobutyrate
EA	Ethyl acetate
EDC·HCl	1-(3-Dimethylaminopropyl)-3-ethylcarbodiimide Hydrochloride
GPC	Gel permeation chromatography
HCl	Hydrochloride
HDDA	1,6 -Hexanediol diacrylate
HPLC	High performance liquid chromatography

List of Abbreviations

H_2SO_4	Sulfuric acid
HEBiB	2-Hydroxyethyl 2-bromopropionate
HO-*o*NB-COOH	4-[4-(1-Hydroxyethyl)-2-methoxy-5-nitrophenoxy] butyric acid
I-819	Irgacure 819
K_2CO_3	Potassium carbonate
LC/MSD	Liquid chromatography/mass selective detector
$Mn_2(CO)_{10}$	Dimanganese decacarbonyl
Mn	Number-average molecular weight
Mw	Weight-average molecular weight
NO_2-BDAM	2-Bromo-N-(2-nitro-3, 4-dihydroxyphenethyl)-2-methylpropanamide
$NaNO_2$	Sodium nitrite
NIPAAm	*N*-Isopropylacrylamide
$NaHCO_3$	Sodium bicarbonate
Na_2SO_4	Sodium sulphate
$NaIO_4$	Sodium periodate
N_2	Nitrogen
NMR	Nuclear magnetic resonance
*o*NB	ortho-Nitrobenzyl
OXGA	2-Oxoglutaric acid
PE	Petroleum ether
PP	Polypropylene
PTFE	Polytetrafluoroethylene
PDI	Polydispersity index
PAAm	Polyacrylamide
PAMPS	Poly(2-acrylamido-2-methylpropanesulfonic acid)
PSAPS	Poly(3-sulfopropyl acrylate potassium salt)
STEM	Structurally tailored and engineered macromolecular
SLIPS	Slippery liquid infused porous surface
SEC	Size-exclusion chromatography

List of Abbreviations

SiO_2	Quartz
Si	Silicon
Ti	Titanium
TEA	Trimethylamine
TFA	Trifluoroacetic acid
THF	Tetrahydrofuran
Tris-HCl	Tris(hydroxymethyl) aminomethane -Hydrochloride
UV	Ultraviolet
VA-044	2,2′-Azobis[2-(2-imidazolin-2-yl) propane] dihydrochloride
Vinyl-*o*NB-COOH	4-(4-(Acryloyloxymethyl)-2-methoxy-5-nitrophenoxy) butanoic acid
Vinyl-*o*NB-Br	2-((2-Bromo-2-methylpropanoyl)oxy) ethyl 4-(4-(1-(acryloyloxy)ethyl)-2-methoxy-5-nitrophenoxy) butanoate
WCA	Water contact angle
XPS	X-ray photoelectron spectrometer
3D	Three-dimensional
4D	Four-dimensional
RAFT	Reversible addition-fragmentation chain transfer polymerization
NMP	Nitroxide-mediated polymerization
ROMP	Ring-opening metathesis polymerization

Whenever it is not stated here, all other abbreviations have their usual default meaning.

Contents

Motivation and scope of this thesis

o-Nitrobenzyl (*o*NB) derivatives are photo-responsive molecules that can undergo photolysis to release a leaving group. The introduction of these molecules in polymer materials can endow polymers with photo-responsiveness to change various properties. While most of current studies focus on the utilization of *o*NB groups as simple photocleavable units, there are also several attempts to multifunctionalize the *o*NB derivatives for enabling more capabilities to the *o*NB-based polymer systems. For example, nitro-catechol derivatives that contain both catechol and *o*NB structures allow their polymers to show both interesting adhesion and photolysis functions. In this thesis, multifunctional *o*NB derivatives are designed and synthesized for the preparation of smart polymeric materials. *o*NB derivatives respond to UV light and undergo photolytic cleavage, but they are stable when exposed to wavelengths in the visible region, e.g., 460 nm. Harnessing responsiveness to different wavelengths within a single material is expected to develop next-generation smart platforms with wavelength selective functions. For this, this thesis presents three polymer systems with tunable properties under different light wavelengths, i.e. coating and creating surface patterns, tuning double network topologies, and regulating mechanical properties of network materials.

In the first part of this thesis, a multifunctional nitrodopamine-based initiator (NO_2-BDAM) is designed for surface coating, grafting polymer brushes and detaching them from the surface. When NO_2-BDAM is combined with visible-light sensitive dimanganese decacarbonyl ($Mn_2(CO)_{10}$), it is possible to graft polymer brushes to a surface under visible light (460 nm), and then to remove the formed polymer brushes using UV light (360 nm). This transition provides a window to evaluate the polymer molecular weight obtained from the grafting-from method and the density of grafted polymer brushes. This method can also be used to make surface patterns.

Furthermore, this strategy can be applied to regulate the network topology of poly(di(ethylene glycol) ethyl ether acrylate) (PDEEA) elastomer by grafting crosslinked polymers to form a connected double network (c-DN) structure. Such c-DN can be in situ converted into a disconnected double network (d-DN) structure by UV light irradiation. The study of this thesis indicates that the change in topology from c-DN to d-DN had little impact on the mechanical property of the elastomer. The above methodology has also been applied to graft polymer brush side chains from a network. The photolysis reactions allow for on-demand detachment of the grafted polymer chains to regulate the network topology from bottlebrush-like topology to simple network topology. The attached polymer brushes can toughen the materials, while the detaching would weaken the toughening performance. The photolabile group-based strategies alternate the systems' property irreversibly. In summary, the work in this thesis is presented as follows:

1) **Chapter 1** elaborates on the general state of the art within this field, in which the research status of *o*NB derivatives based platforms, and different investigation aspects from responsive surfaces to functional polymer networks, as well as their potential applications so far, are introduced.
2) **Chapter 2** describes the approach to regulate surface properties. The multi-functional initiator NO_2-BDAM, which contains a catechol structure for surface modification, alkyl bromide group for radical grafting polymerization, and *o*-nitrophenyl ethyl connecting group for photolysis, was designed and synthesized. Further applying $Mn_2(CO)_{10}$ as an initiating system, visible light (460 nm) for triggering the site-specific growth of polymer brushes and UV (365 nm) light for photocleavage of the polymer chains to detach the grafted polymers from the surface have been deeply studied. The applicability of the current method on different monomers and various substrates is investigated. At last, potential

applications of this approach to create desired surface patterns are demonstrated.

3) **Chapter 3** reports a similar light wavelength-selective approach to regulate the network topology of poly(di(ethylene glycol) ethyl ether acrylate) (PDEEA) based double network elastomer by incorporating an orthogonal light-responsive inimer (2-((2-bromo-2-methylpropanoyl)oxy)ethyl 4-(4-(1-(acryloyloxy)ethyl)-2-methoxy-5-nitrophenoxy) butanoate, vinyl-*o*NB-Br). Vinyl-*o*NB-Br possesses three functional moieties, i.e., acrylate-based double bond for incorporation within a network, Br group for further photo-induced grafting polymerization, and *o*NB moiety for photocleaving. After swelling the as-prepared elastomer in a mixture containing monomer, crosslink-linker, and photoinitiator, tethered Br group from vinyl-*o*NB-Br can initiate in situ polymerization to generate a second network which is connected to the first one to construct a double network elastomer (typically involves a c-DN structure). Then, the disconnection of the second network to transform the c-DN to d-DN microstructure in situ was studied. The mechanical property of PDEEA elastomer with different topologies of DN structures (from c-DN to d-DN) was explored. At last, the influence of connecting points number between the second network and the first network on the mechanical property of PDEEA elastomer was evaluated.

4) **Chapter 4** illustrates the regulation of elastomer topology from bottlebrush-like network topology to semi-interpenetrating network topology for tuning its toughness. Based on the inimer-containing structures described in Chapter 3, a network consisting of poly(*N*-isopropylacrylamide) (PNIPAAm) brushes can be prepared using 460 nm light to induce in situ grafting polymerization. The PNIPAAm side chains can be detached from the backbones by UV irradiation to form a semi-interpenetrating topological network. The toughening mechanism of materials has been detailed investigated by changing the grafting mass density

of PNIPAAm brushes. Interestingly, by extracting out the detached polymer chains, the network can convert to its original state, showing a promising approach to one-cycle reversibility in the modification of material's mechanical properties.

5) Finally, a conclusion about using *o*-nitrobenzyl derivatives to regulate materials' properties through wavelength-selective approaches, and a brief outlook for further development of polymer platforms to dynamically regulate their properties is exposed in **Chapter 5**.

Chapter 1

1. Introduction

Photo-responsive polymers can change their properties under a light stimulus.[1-3] Different molecular properties can be regulated by light, including conformation,[4-7] amphiphilicity,[8-10] polarity,[11-13] charge,[14-16] optical chirality,[17-18] conjugation[19] etc. When properly designed, the light-induced molecular change can trigger a macroscopic change of material properties like plasticity, shape, solid/liquid transition, solubility, wettability, optical properties, adhesion, and conductivity.[20-22] A photo-responsive functional group (chromophore) can be designed to be combined into the polymer chains to form photo-responsive polymers. The response, depending on properties of the chromophore, can be classified as reversible or irreversible. Reversible systems are referred as the switchable two photostationary states for tuning material properties and are based on molecular switches, while irreversible systems are based on irreversible, typically photocleavage reactions. Although photolabile molecules can't reversibly switch to their original state, there are still some advantages of photolabile chromophore systems, such as 100% photoconversion can be achieved since no equilibrium between two states is involved. Photocleavable groups have been used to photo-induced micropatterns,[23-28] photodegrade materials,[29-30] photoresist,[31-32] control drug delivery,[33-39] cell encapsulation and tissue adhesion.[40-42]

When photolabile groups are included in a polymer chain, they are cleaved upon light exposure. Owing to the position where the chromophore is localized in the chain, different light-induced molecular processes can be realized, for example, charge generation in the side groups,[43] activations of catalyst and "click" reactant, formation of caged groups,[44] depolymerization and chain shortening, etc.[45]

Typical examples of photolabile protecting groups (*o*-nitrobenzyl,[46] coumarin-4-

ylmethyl derivatives,[47] and phenacyl esters,[48] pyrenylmethyl,[49] and 2-napthoquinone-3-methides[50]) are represented in Figure 1. Depending on the structure of the group, different photolysis mechanisms are possible. Coumarin-4-ylmethyl leaves a coumarin byproduct which is solvent-trapped.[47] Upon irradiation, phenacyl esters undergo cleavage by the scission of homolytic C-O bond to give a phenacyl derivative radical and an acyloxy radical. The rapid H atom transfer to the acryloxy radical to yield the carboxylic acid and p-methoxyacetophenone as the photoproduct.[51] 2-Napthoquinone-3-methides generate a highly reactive radical which can selectively react with vinyl compounds incorporating electron-donating group (i. e., oxygen) via very rapid Diels-Alder addition reaction, resulting in the coupling of two species.[50] Incorporating this group on polymer side chains enables light-induced reactivity, which is useful in photolithography.

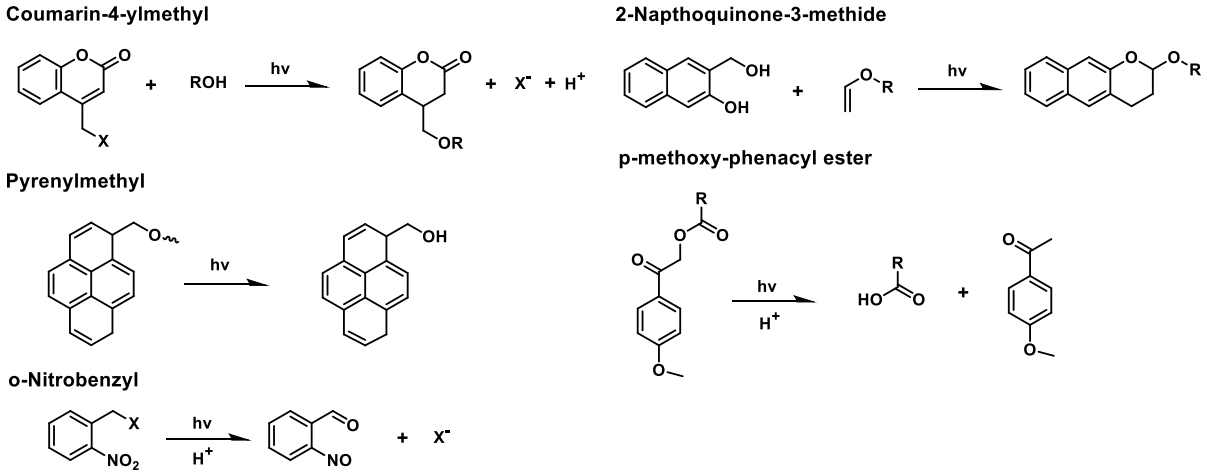

Figure 1. Typical examples of irreversible photo-responsive groups.

Among the various types of photolabile groups, *o*-nitrobenzyl derivatives undergo light-induced intramolecular oxidation resulting in the released functionality and a nitrosocarbonyl byproduct. These compounds have gained increased use in the fields of chemistry and polymer science to achieve spatial control of molecular and polymer properties using light irradiation. Since the pioneering work by Barltrop[46] and Patchornik,[52] *o*NB analogs developed for the protection of different groups have been

used for caged surfaces/interfaces, functional crosslinked networks, and dynamic biomaterials.[24, 53-60]

The photolysis mechanism of *o*NB is described as following: the ground state of NB-derived molecule **1** converts into its excited state (**1***) when exposed to 300-365 nm light irradiation. Then, an intramolecular hydrogen abstraction is generated to form the *aci*-nitro intermediate **2**. This decay efficiency mainly depends on the substitution, solvent, pH, and irradiation energy as well. After that, an irreversible cyclization of **2** results in the formation of intermediate **3**, followed by its ring-opening process to generate hemiacetal intermediate **4**. At last, intermediate **4** releases the leaving group (LG) and 2-nitrobenzaldehyde byproduct **5** forms (Figure 2).[61]

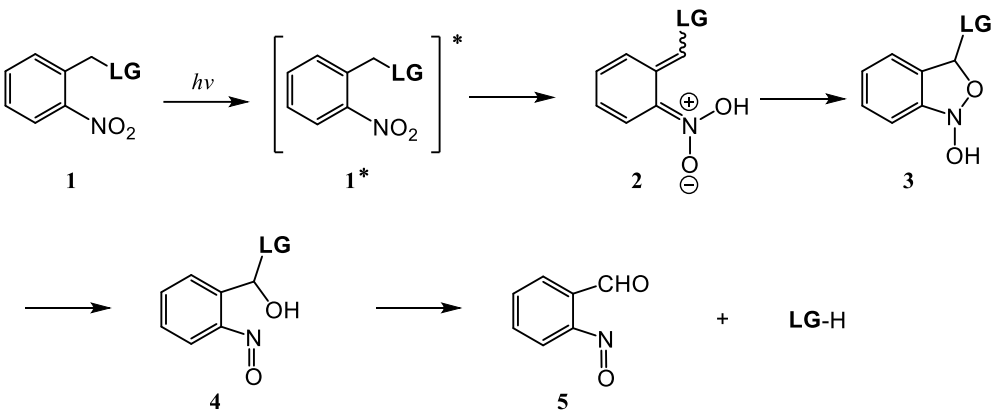

Figure 2. Mechanism of *o*NB photolysis and deprotection of organic molecules. Reproduced with permission.[61] Copyright 2013, Wiley-VCH.

1.1 *o*NB-derived smart polymers

*o*NB derivatives have been incorporated into functional polymers, including *o*NB-terminated polymers, *o*NB side chains polymers, *o*NB-derived block polymers, and *o*NB-based supramolecular polymers.[57] A whole variety of *o*NB protected functionalities has been explored, including amides, amines, carbamate, carbonates, ethers, and alcohol ester.[62]

1.1.1 *o*NB ester-based polymers

The first trial of using *o*NB esters as photolabile polymers was reported by Petropoulos in 1977,[63] in which photodegradable poly(*o*-nitrobenzaldehyde acetals) prepared by condensing *o*-nitrobenzaldehyde with a series of glycols was described. Followed by this study, a series of *o*NB ester-based polymers have been developed.[64-67]

1.1.1.1 *o*NB ester-based end-capped polymers

Attachment of a single *o*NB group to the end of a polymer chain has been used to regulate the properties of functional polymers. Almutairi and co-workers developed self-immolative polymeric nanomaterials to on-demand release payloads upon exposure (Figure 3a).[68] UV excitation photocleaved the *o*NB from the polymer headgroups. The backbones of the polymers then underwent depolymerization and degradation to fully disassemble and degrade the polymer into small molecules. In this case, the encapsulated payloads are released. To release the payloads more efficiently, Liu and co-workers reported self-immolative polymersomes (SIPsomes) formed through self-assembly of amphiphilic block polymers containing a hydrophobic poly(benzyl carbamate) and a hydrophilic poly(N,N-dimethylacrylamine) terminated with *o*NB ester (Figure 3b).[69] Upon UV light exposure, the caging *o*NB moiety is removed, triggering a head-to-tail cascade depolymerization of the hydrophobic block. As a consequence, the SIPsomes are disintegrated to carbon dioxide, water soluble aminobenzyl alcohol, and poly(*N*, *N*-dimethylacrylamine), co-releasing guest-loaded drugs. *o*NB was also applied as photo-responsive shell to poly(amidoamine) (PAMAM) dendrimers (Figure 3c). Wei and co-workers described the synthesis of PAMAM dendrimer peripherally attached by *o*NB esters with nearly 100% grafting efficiency. The photosensitive *o*NB shell can be released efficiently upon 365 nm UV irradiation, leading to a change in solubility (from hydrophobic to hydrophilic) and the release of loaded guest molecules, such as salicylic acid and Adriamycin. It has been found that the release of salicylic acid is greater with UV exposure than that without, exhibiting

the necessity of caged shell for smart molecular encapsulation platform.[70]

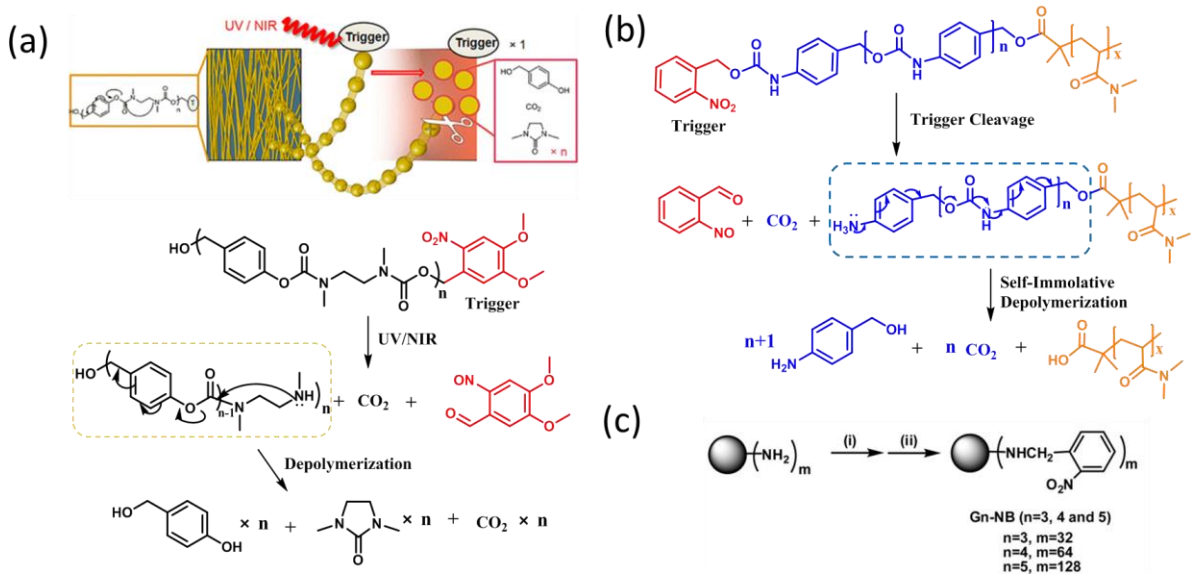

Figure 3. Examples of *o*NB ester-based end capped polymers. (a) Self-immolative polymersomes formed by *o*NB caped polymer. (b) Self-immolative polymersomes formed by *o*NB caped amphiphilic block polymers. (c) PAMAM dendrimer peripherally attached by *o*NB esters. Reproduced with permission.[68-70] Copyrights 2012, 2014, American Chemical Society. Copyright 2010, Wiley-VCH.

1.1.1.2 *o*NB ester-based side-chain polymers

Among different kinds of *o*NB ester-based photo-responsive polymers, those that have *o*NB groups introduced as side-chains are the most widely used ones. Eto and co-workers have reported positive photosensitive polyimide precursors containing pendant *o*NB side groups. *o*NB-based diacid chlorides were derived from the reactions between tetracarboxylic dianhydrides and *o*-nitrobenzyl alcohols, then which can react with diamines by polycondensation technique to form photosensitive resist (Figure 4a).[31] By varying the monomer's stoichiometry, polymers with different molecular weights are formed. They found that the sensitivity of photosensitive polyimide to organic solvent decreases with increasing the molecular weight of the polymers after exposed under UV light, because of the increased of hydrophilic groups (-COOH) generated from photolabile moieties in the side chains.

Nitro-aromatic groups have an inhibitory effect in radical polymerization owing to the reaction between *o*NB and free radicals to form stable nitroxyl radicals that cannot induce further polymerization. It is found that it is difficult for acrylate-type *o*NB monomer to undergo controlled radical polymerization, while methacrylate-based *o*NB monomer can be polymerized with low molecular weight (~ 11000 g/mol) and relatively high polydispersity index (PDI ~1.5).[71] Gohy and co-workers have systemically investigated the controlled-radical polymerization (CRP) of photosensitive *o*-nitrobenzyl acrylate (NBA) and *o*-nitrobenzyl methacrylate (NBMA) through three typical CRP techniques, i.e. atom transfer radical polymerization (ATRP), reversible addition-fragmentation chain transfer polymerization (RAFT), and nitroxide-mediated polymerization (NMP) (Figure 4b).[71] They found no polymerization by RAFT and NMP, and only low-molecular-weight polymers with broad distribution form in ATRP. In contrast to NBA, NBMA seems much more promising in polymerization due to its higher reactivity. When it is used for the ATRP, characteristic features of a living/controlling polymerization can be observed in optimized polymerization conditions and polymers with higher molecular weight (17000g /mol) and narrow polydispersity index (PDI ~1.13) are obtained.

Besides, to avoid the inhibitory effect during radical polymerization, ring-opening metathesis polymerization (ROMP) is utilized as a more robust technique to synthesize polymers with photocleavable *o*NB ester side chains (Figure 4c).[72] *o*NB moiety can be firstly incorporated into the norbornene-based monomers, followed by undergoing polymerization with Grubbs's ruthenium carbine catalyst. With this technology, the monomers can be consumed within minutes to hours with predictable molecular weight (< 20 000 g/mol) and narrow PDI (< 1.17).

In addition, *o*NB groups can also be hung as the side chain of conjugated polymer chains. *o*NB groups can be first attached to thiophene, and the obtained monomer can

then be co-polymerized with 5,5'-bis(trimethylstannyl)-2,2'-bithiophene under catalyst (Figure 4d).[73] The formed conjugated polymer shows great solubility in organic solvent with the photocleavable property.

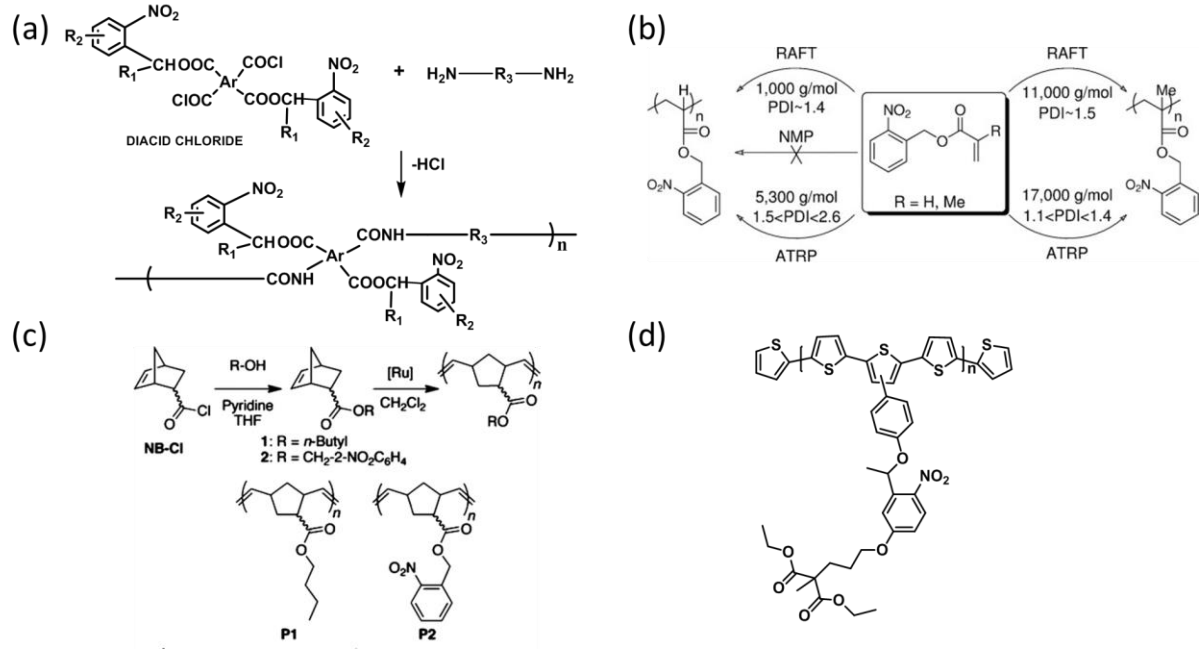

Figure 4. Examples of photo-responsive polymers with *o*NB in the side chains. (a) Polycondensation is used to polymerize *o*NB-derived polymers. (b) Radical polymerization is widely used for the formation of *o*NB side-chain polymer. (c) Ring-opening metathesis polymerization technique used for generating *o*NB side-chain polymer. (d) *o*NB side chains can be attached to the conjugated polymers. Reproduced with permission.[31, 71-73] Copyrights 1991, 2011, 2017, American Chemical Society. Copyright 2009, Wiley-VCH.

With the development of these techniques for efficient polymerization of *o*NB moiety in the side chain, a series of functional polymers were obtained. For example, *o*NB groups can be grafted on the side chains to form bottlebrush polymers. Zhang and co-workers have developed UV-cleavable bottlebrush polymers through 'grafting to' strategy by using poly(3-azido-2-hydroxypropyl methacrylate) as the polymer backbone and *o*NB propargyl-capped polystyrene as the side chains, respectively (Figure 5a).[74] Owing to the bottlebrush structure, the molecular weight of the obtained

*o*NB-derived polymer can be up to over 100000 g/mol, which is very rare for *o*NB-based polymers. Therefore, the high molecular weight bottlebrush polymer makes it more viscous (intrinsic viscosity: 12 mL/g). Upon UV irradiation, the significant cleavage of bottlebrush polymer chains leads to a rapid decrease in molecular weight and a large decrease in the intrinsic viscosity of bottlebrush polymer (from 12 mL/g to 7.39 mL/g).

Furthermore, *o*NB-based side chains have also been incorporated into photo-based generators to make poly(olefin sulfone)s depolymerize under a light. Naka and co-workers have investigated photo-induced depolymerization of poly(olefin sulfone)s that bear *o*NB-protected bases in the side chain (Figure 5b).[75] A series of polymers with different spacer-length and molecular weight have been prepared by varying the monomers and polymerization conditions. After UV irradiation, the conjugated basic group on the side chain is exposed, resulting in the depolymerization of poly(olefin sulfone)s turn back to olefin monomer and sulfur dioxide. The length of the spacer of the *o*NB side chain on poly(olefin sulfone)s shows an inconspicuous degradation phenomenon, which may owe to the cancellation of the freedom movement of the photo-based generators with different connecting spacer units.

Li and co-workers have reported the dual responsive *o*NB-based amphiphilic polymer by partially cleaving polyhedral oligomeric silsesquioxane (POSS) terminated by PNBMA side chains (Figure 5c).[76] After short UV illumination, PNBMA can be partially converted into poly(methacrylic acid) (PMAA), and random copolymer POSS-P(NBMA-*co*-MAA) is obtained. The resulting copolymer can self-assemble into spherical micelles with tunable morphology regulated by pH and UV irradiation. The formed micelles can be further exposed to UV light for reorganizing their assemblies to release the guest molecules into water.

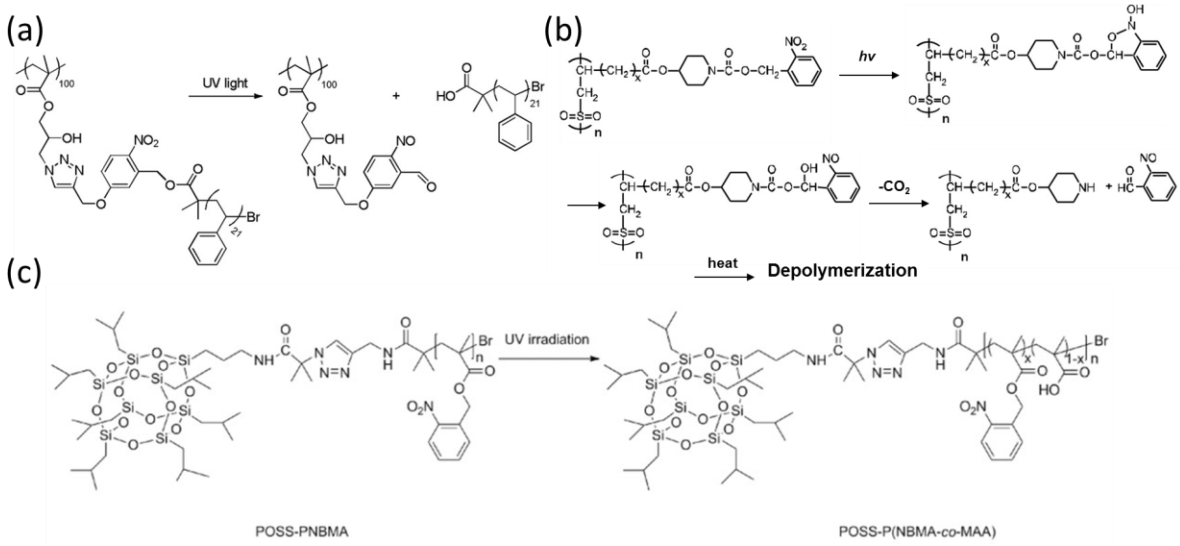

Figure 5. Examples of other functional polymers with *o*NB groups as the side chains. (a) Functional bottlebrush polymers with *o*NB side chains. (b) *o*NB used as a photo-base generator for photo-induced depolymerization. (c) Dual response of POSS-P(NBMA-co-MAA) by pH and UV light. Reproduced with permission.[74-76] Copyrights 2013, 2015, 2017, Wiley-VCH.

1.1.1.3 *o*NB ester-based block polymers

Photolabile block copolymers have been studied due to their self-assembling properties and their guest molecules loading performances. *o*NB-derived block copolymers are formed either by using a designed polymer as the macro-initiator to copolymerize the *o*NB-based monomer or using *o*NB moiety as the linker to connect two different polymers. The inclusion of the *o*NB as part of the backbone allows cleavage of the blocks and distortion of the self-assembly capability of the molecule. Zhao and co-workers firstly investigated the photo-controlled release of hydrophobic guest molecules from polymer micelles using *o*NB-based amphiphilic block copolymers (Figure 6a).[77] In their design, poly(ethylene oxide) (PEO) is kept as the hydrophilic block, while introducing PNBMA as the hydrophobic block. Under one-photon UV (365 nm) or two-photon near-infrared (700 nm) irradiation, the chromophore is detached and the hydrophobic PNAMA block is converted into hydrophilic PMMA. In this way, the photo-controlled release and delivery of

encapsulated hydrophobic guests are realized. During this process, the intensity of light irradiation, the length of *o*NB-based polymer block (molecular weight), and particle crosslinking of micellar aggregate are designed to regulate the dissociation of the block copolymer micelles. In a similar design, photocleavable *o*NB-based linkage was used to connect a cationic group which could effectively form pDNA/salt-stable polyplexes with sizes appropriate.[78] Irradiation-induced cleavage in this block copolymer facilitates pDNA release and efficient nucleic acid delivery.

Poly(ethylene oxide) and polystyrene (PS) blocks are also connected by a photolabile *o*-nitrobenzyl linker.[45] Light exposure cleaves the polymer backbone and separates the hydrophilic and hydrophobic blocks (Figure 6b), which has been successfully carried in both liquid and solid states. This block copolymer can be annealed to generate a vertically aligned cylindrical morphology. After UV irradiation and washed by methanol/water, the film leads to a nanoporous PS structure.[79] These diblock copolymers can be obtained either by copper (I)-catalyzed azide-alkyne cycloaddition of the two pre-synthesized blocks or by ATRP polymerization. The former method is preferred if the composition of the copolymer needs to be tailored.[80-81]

Ring-opening polymerization was used to prepare *o*NB-derived block copolymer with 3-methyl-3-nitrobenzyl-trimethylene carbonate-bearing numerous nitrobenzene photolabile groups with poly(*N*-isopropylacrylamide) (PNIPAAm) as the macroinitiator (Figure 6c).[82] It can self-assemble into spherical micelles in an aqueous solution. The hydrophobic and hydrophilic chain lengths influence the micelle size and subsequent guest molecule loading efficiency. Upon light irradiation, a burst occurs of the particles due to the rapid degradation of the micellar core, which can be used to release the encapsulated molecules.

Another dual-responsive block copolymer connected by *o*NB moiety was formulated via ring-opening polymerization of ε-caprolactone by using 5-propargylether-2-

nitrobenzyl alcohol as the initiator and then “click” reacting with azide-terminated poly(ethylene glycol) (Figure 6d).[83] The obtained poly(ε-caprolactone)-acetal-nitrobenzyl ester-poly(ethylene glycol) (PCL-PEG) possesses linkages of both light-triggerable *o*NB and acid-labile acetal. This block copolymer can self-assemble into spherical polymeric nanoparticles, which undergo fast degradation due to the cleavage of acetal and *o*NB linkages under acid and light responsiveness.

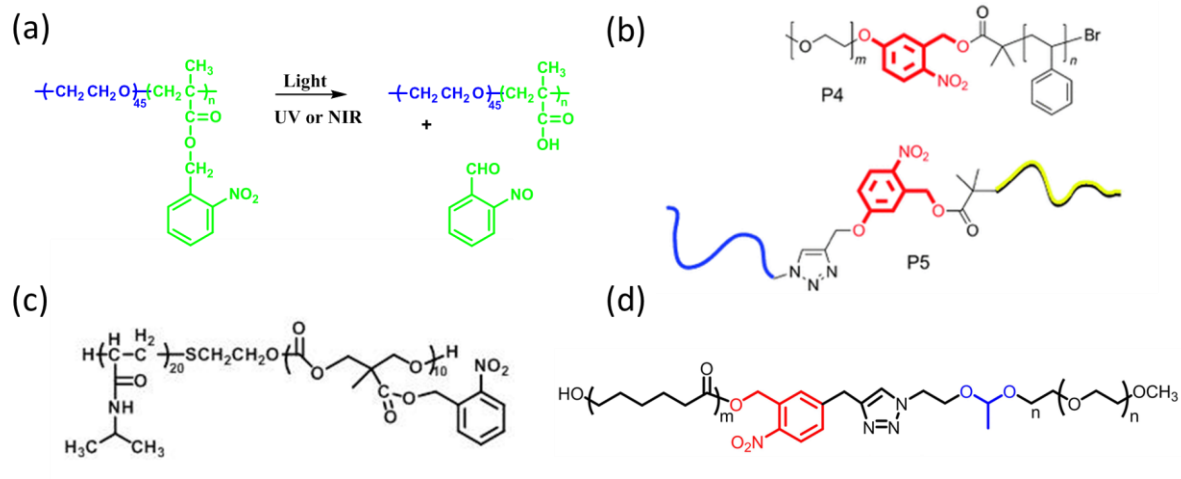

Figure 6. Examples of *o*NB ester-based block copolymers. (a) PEO-based macroinitiator is used to co-polymerize *o*NB monomer. (b) *o*NB moiety can be used as a linker to connect two different polymers. (c) Ring-opening polymerization is used to prepare temperature and light dual responsive polymer. (d) Ring-opening polymerization and click reaction are applied to form *o*NB-derived block copolymers. Reproduced with permission.[45, 77, 82-83] Copyrights 2006, American Chemical Society. Copyrights 2011, Wiley-VCH. Copyrights 2015, Elsevier B.V. Copyrights 2019, Springer.

1.1.1.4 *o*NB ester-based supramolecular polymers

In 1998, photo-controlled molecular weights of supramolecular polymers were first reported (Figure 7a).[84] These were obtained by the self-assembly of telechelic polymers 2-ureido-4-pyrimidone (UPy) units as the terminal. UPy can build up long chainsdimerize by quadruple H-bonding with high affinity (Km of 2.2×10^{6} M^{-1} in chloroform).[85] A chloroform solution of UPy terminated polymer behaves like a solution

of a conventional covalently linked polymer. The degree of polymerization, viscosity, shearing effects, and viscoelastic properties are regulated by the ratio of extra added monofunctional UPy, which end-caps the growing chains.[85] The ability of UPy to dimerize can be prevented by protecting the UPy end-groups with the photolabile group (*o*NB). As a result, the polymerization and depolymerization processes can be tuned by UV light irradiation. This photo-triggering H-bonding strategy was applied to prepare light-responsive material with self-healing ability.[86] Recently, Cui and co-workers have synthesized a silanizing agent which was functionalized with *o*-nitrobenzyl protected UPy for studying the UPy dimerization underwater (Figure 7b).[86] For this purpose, a photo-activated surface was prepared by modifying *o*NB protected UPy on a substrate. It has been found that UPy-based copolymer can stably bond to the activated substrate even underwater. The sample idea has been further expanded to photo-responsive hydrogel thin film.[87]

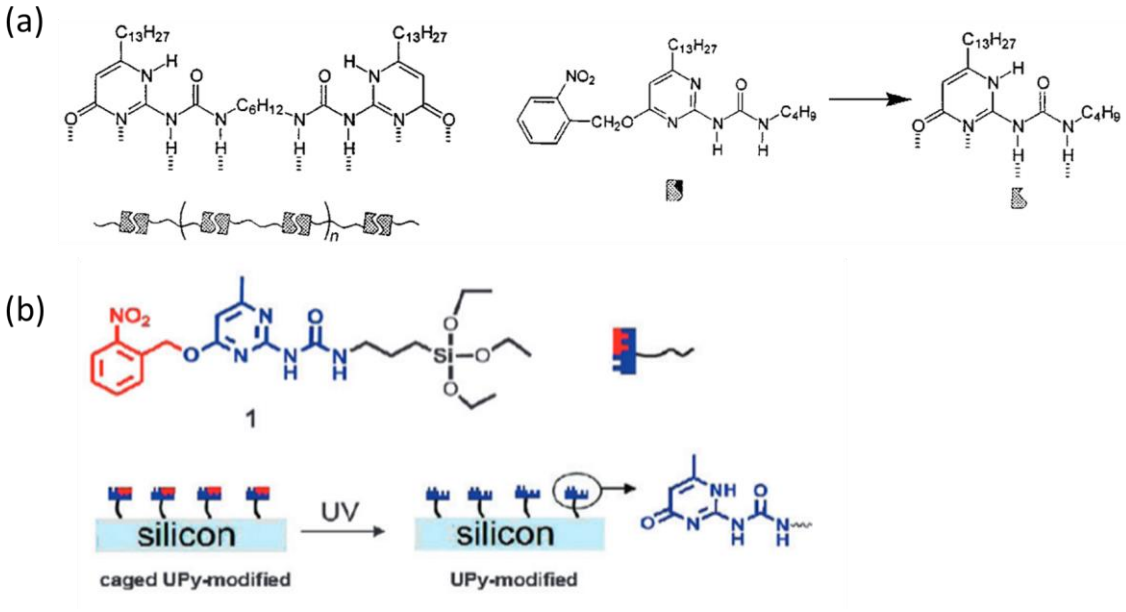

Figure 7. (a) Supramolecular polymer consisting of two UPy units and monofunctional UPy unit with *o*NB-based photolabile protected group. (b) Silanizing agent functionalized with *o*NB protected UPy and its dimerization underwater. Reproduced with permission.[84, 86] Copyrights 1998, 2012, The Royal Society of Chemistry.

1.1.2 *o*-Nitrodopamine based polymers

o-Nitrodopamine based molecules and polymers are *o*NB derivatives that combine the photo-cleavable properties of the *o*NB group and the adhesive properties of the dopamine functionality.[88-92] Nitrodopamine derivatives display photo-responsiveness under UV light. Four-arm PEG-nitrodopamine hydrogel films have been prepared by either covalently self-crosslinking under oxidative conditions or metal-mediated crosslinking by adding Fe^{3+} cations (Figure 8).[92] Upon UV irradiation, photo-induced debonding of Fe^{3+}-crosslinked gel is more effective than that of covalently self-crosslinked gel, which may because the free catechols in the covalently crosslinked gel could interfere with the reactive intermediates during the photolysis process and cause side reactions to decrease the overall photocleavage yield, thus metal-coordinated gel required fewer exposure doses for complete removal.

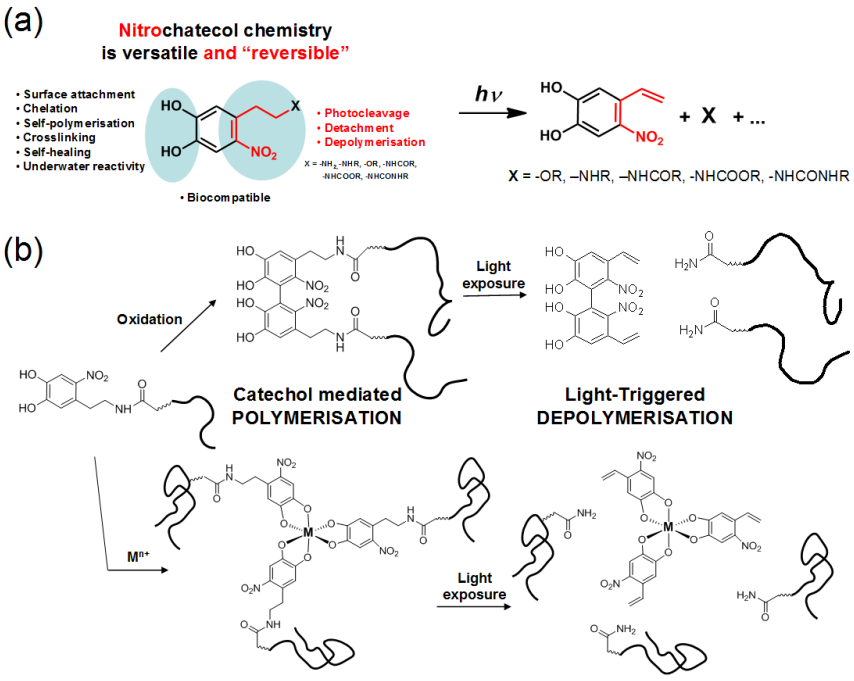

Figure 8. Photocleavage mechanisms of nitrodopamine derivatives. (a) Photolytic reaction of the *o*-nitrophenyl ethyl moiety. (b) Different strategies used to trigger bonding (through oxidation of catechol groups or formation of metal complexes) and debonding of PEG-nitrodopamine derivatives upon light. Reproduced with permission.[92] Copyright 2012, Wiley-VCH.

1.1.3 Application of *o*NB-based polymers

Light-induced dissociation at the polymer level of *o*NB derivatives can be reflected on the macroscopic level of material properties, which has been used in various applications.

1.1.3.1 Controlled drug delivery

Polymer micelles or vesicles can be formed through self-assembly of photolabile block copolymers, which can be used as carriers for controlled drug delivery. Figure 9 demonstrates the basic mechanism for photocleavable polymer micelles, that is, light exposure induces the changes in solubility of the block polymer modified with the photolabile group and, the micelles disassembly as a consequence.[37-38]

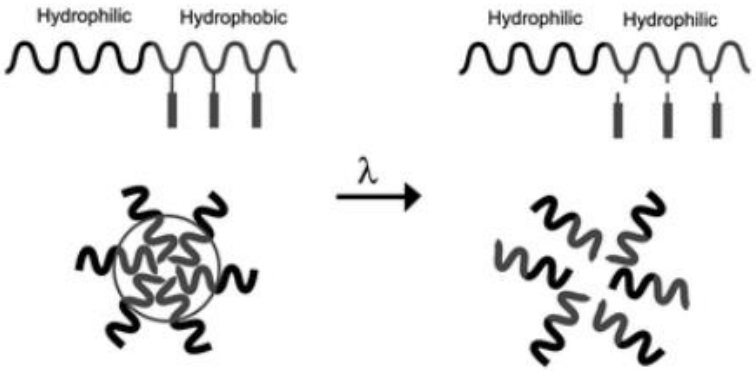

Figure 9. Schematic illustration of photolabile block copolymer micelles that can be dissociated irreversibly to transform the hydrophobic block into a hydrophilic one upon light irradiation. Reproduced with permission.[38] Copyright 2009, The Royal Society of Chemistry.

*o*NB-based block copolymers are one of the most typical examples. Kondo and co-workers have described photosensitive polymer micelles made from amphiphilic block copolymers composed by poly[N-(2-hydroxypropyl) methacrylamide] (PHPMA) and poly(4,5-dimethoxy-2-nitrobenzyl methacrylate) (PDNMA) (Figure 10a).[33] Spherical block copolymer micelles are formed by the self-assembly of PHPMA-b-PDNMA with a diameter of 130-200 nm to encapsulate antitumor drug 5-fluorouracil (5-FU). When exposed to UV light, the micellar size decreases gradually, and 5-FU is released with

time-dependence, following a clear sigmoid curve.

However, the short penetration length of UV light in tissue, and its phototoxic effect on living cells are not favorable for use in bio-applications. Exposure with near-infrared (NIR) light would be more convenient. One possibility is to use two-photon excitation, but for most chromophores, photoreaction occurs with low efficiency, and have low two-photon-absorption cross sections and requires high power femtosecond pulse lasers. To overcome this limitation, Lanthanide doped upconverting nanoparticles (UCNPs) have been added to photoresponsive micelles (Figure 10b and 10c).[34] UCNPs can absorb NIR light and convert it into higher-energy photons in the UV and visible regions. These are absorbed by the *o*NB groups in the core-forming block. After photocleavage reaction, the core becomes hydrophilic and the micelles dissociate and then the payloads are released.

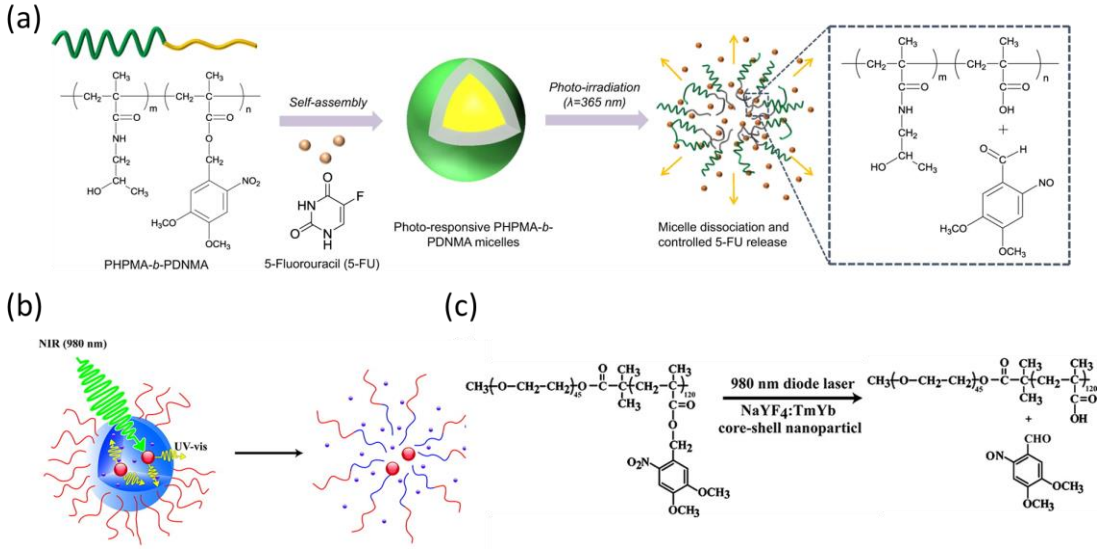

Figure 10. *o*NB-based block copolymers for drug delivery. (a) Illustration of the self-assembly and disassembly of 5-FU loaded PHPMA-b-PDNMA micelles and the corresponding payload release upon UV irradiation. (b) Photosensitive micelles that encapsulate upconversion nanoparticles (UCNPs) and allow excitation in the NIR. UCNPs absorb NIR and convert it to UV-vis light to trigger the release of the drug along with the dissociation of micelles. (c) Polymer systems used in (b). Reproduced with permission.[33-34] Copyright 2011, American Chemical Society. Copyright 2020, nature Publishing Group.

Drugs can not only be encapsulated in the block copolymer micelles, but can also be attached to the polymer chains through covalently bonds. Sung and co-workers have developed photo-degradable nanoparticles composed of an amphiphilic methoxy(polyethylene glycol)-b-poly(ε-caprolactone)-co-poly(azido-ε-caprolactone-g-ortho-nitrobenzyl retinoic ester) copolymer with a hanging photo-sensitive *o*NB linker to attach retinoic acid (RA), a well-known morphogen in human development, for delivering payloads upon irradiation (Figure 11a).[35] *o*NB linker can be efficiently degraded under gradient UV irradiation, and as a result, the loaded RA is released into mouse embryoid bodies (Figure 11b).[35] This photo-gradient strategy is promising to tune the gradient delivery of morphogens ranging from nanomolar to micromolar in biological systems. With a similar strategy, Lee and co-workers have developed a photo-responsive system to co-deliver a covalently bonded and a physically encapsulated drug (Figure 11c).[36] Alkyne-functionalized pyrene with *o*NB moiety can be attached to the copolymer backbone, which self-assembles to yield spherical micelles with physically load coumarin. Upon UV irradiation, the cleavage of *o*NB linker leads to individual releasing of these two model drugs, demonstrating potentials to deliver multiple therapeutics with controllable release performance.

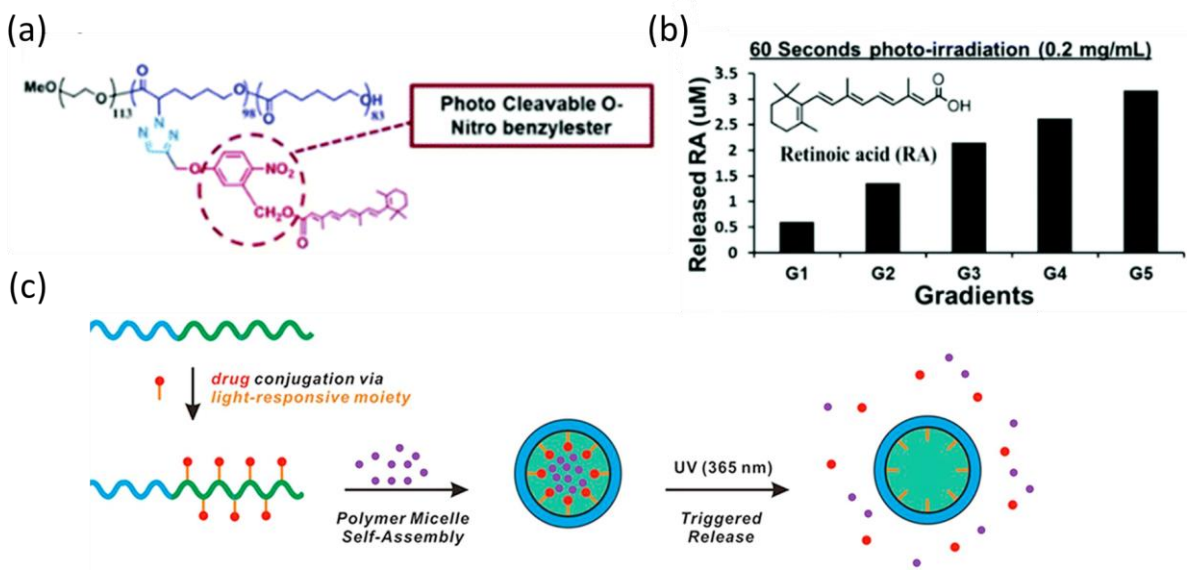

Figure 11. *o*NB-derived copolymers for gradient and multiple deliveries of drugs. (a) Schematic illustration of the photolabile copolymer bonded with RA via the *o*NB linker. (b) Gradient release of RA from copolymer micelles upon gradient photo-irradiation. (c) Schematic representation of block copolymer conjugated with the drug through photocleavable linkers, encapsulation of a dye within polymeric micelle, and subsequent individually releasing of physically entrapped dye and photo-dissociated drug upon UV irradiation. Reproduced with permission.[35-36] Copyright 2017, The Royal Society of Chemistry. Copyright 2014, Elsevier B.V.

1.1.3.2 Functional micropatterns

Owing to the photolysis properties of *o*NB-derived polymers, functional micropatterns can be constructed by selective light irradiation. *o*NB-based photo-responsive polymers are good candidates for making hydrogel and cell patterns.[25-28] Figure 12a shows an example that combines both photo-induced formation of thiol-ene network and photo-induced degradation of nitrobenzyl spacers. The hydrogel is prepared by visible light ($\lambda > 400$ nm) induced “click” reactions without inducing any photocleavage of the nitrobenzyl links. And upon UV light ($\lambda < 400$ nm) irradiation, the covalent links are photocleaved, which can be used to create the second pattern (Figure 12a and 12b).[26] Furthermore, the functional *o*NB ester-based polymers can be modified on the

material surface and used for cell patterns. Another strategy for constructing cell patterns on titanium substrates is achieved by combining the upconversion nanoparticles (UCNPs), photocleavable nitrobenzyl, and the bio-adhesive ligand arginine-glycine-aspartic acid (RGD). Upon irradiation with the NIR light (980 nm) through a photomask, UCNPs can in situ transfer NIR light into UV light, which results in the photocleavage and detachment of the unsheltered cells, forming the cell pattern finally (Figure 12c and 12d).[25]

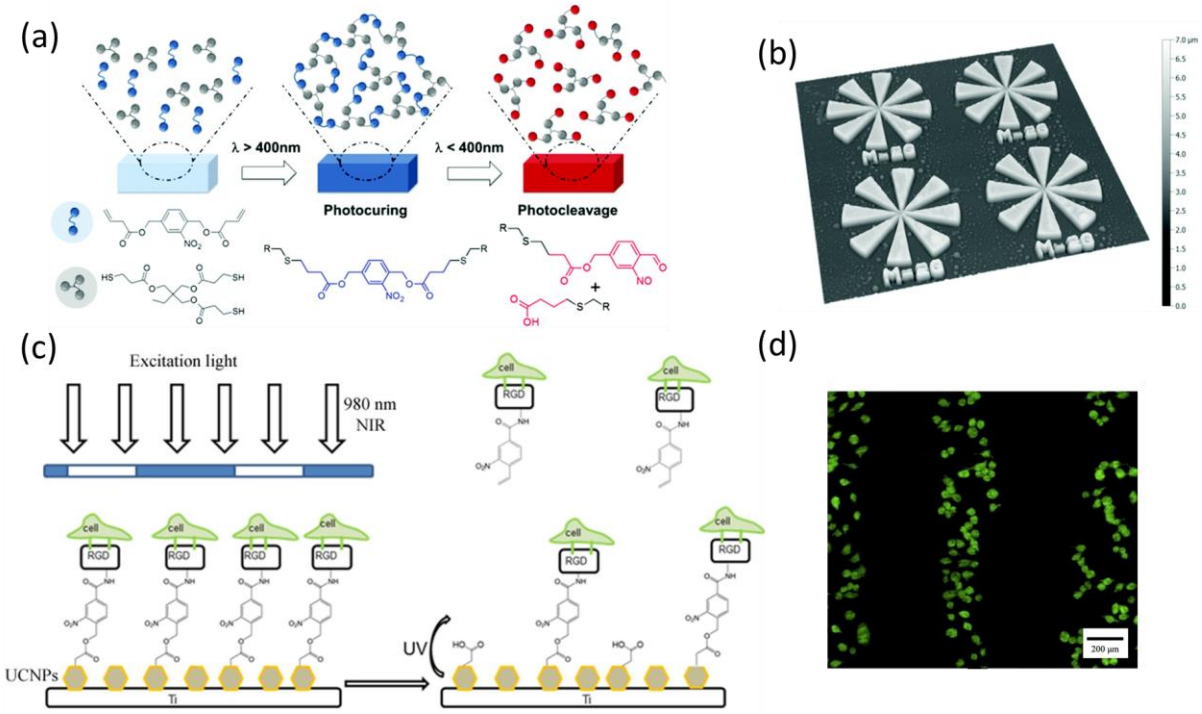

Figure 12. Photo-induced formation and photo-cleavage of thiol-ene networks for the design of switchable hydrogel patterns in (a) and (b). The process of the construction of cell patterned surface in (c) and (d). Reproduced with permission.[25-26] Copyright 2014, American Chemical Society. Copyright 2017, Elsevier B.V.

1.1.3.3 *o*NB-based photodegradable materials

*o*NB-derived photodegradable materials are polymers containing photolabile *o*NB groups in the main chain which can undergo chain dissociation upon light irradiation. Diblock copolymer of poly(ethylene oxide) (PEO) and polystyrene (PS) with a

photodegradable *o*NB linker has been used to prepare ordered self-assembly nanostructures.[79, 93] When PS was used as the continuous phase, the copolymer self-assembles into highly ordered hexagonally packed cylinders oriented perpendicular to the substrate. UV irradiation cleaves the two blocks by the photolysis reaction of *o*NB. Removal of the free PEO block by washing with water leads to the formation of a nanoporous template.[94] Diblock photodegradable copolymers can be obtained by using two kinds of click reactions and used as a potential for the development of drug delivery systems and biomaterials.[95] Another kind of photodegradable polymers, polymers with a metal-metal bond (i.e. iron and molybdenum) in main chains of polyesters and polyamides, are sensitive to visible light. Such photodegradable polymer films are interesting for agriculture since the film can be degraded with daily light and does not need to be removed.[53]

These photodegradable properties can also be integrated with other components to broaden their applications. For example, a photodegradable dendritic amphiphilic nanocontainer with a hydrophilic and a lipophilic unit connected by the photocleavable group has been developed (Figure 13).[29] Light-induced cleavage of the photolabile hydrophobic groups leads to loss of hydrophilic-lipophilic balance to dissociate the micellar aggregates. Therefore, these amphiphilic dendrimers have been used for encapsulating and light-controlled delivering of Nile red.

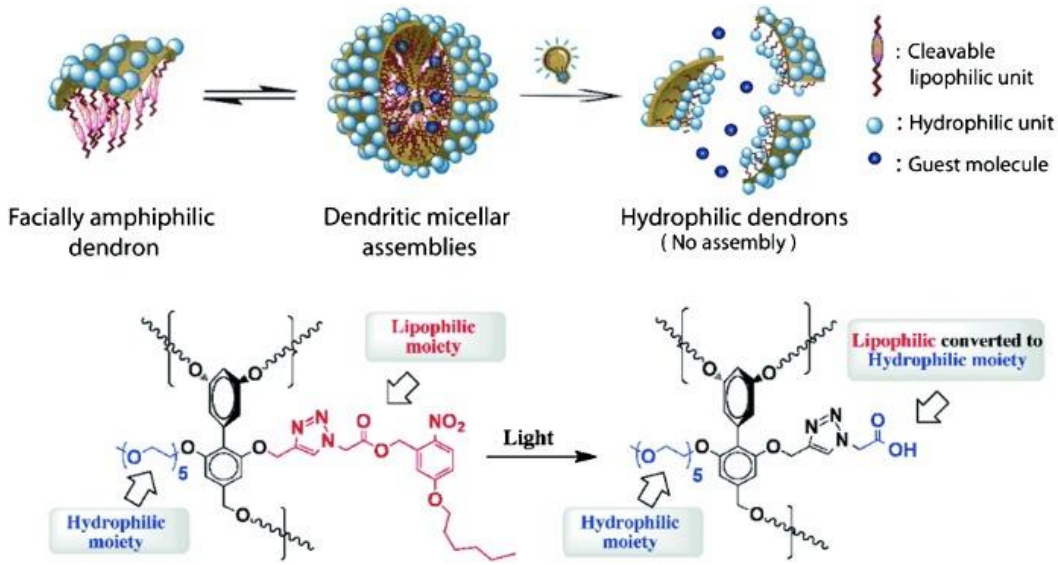

Figure 13. Schematic illustration of the light-induced disassembly of dendritic micellar assemblies by using hydrophobic *o*NB as the linkage. Upon light irradiation, the lipophilic group converted to hydrophilic moiety to break the hydrophilic-lipophilic balance to release the loaded guest molecules. Reproduced with permission.[29] Copyright 2011, Wiley-VCH.

Moreover, photodegradable hydrogels containing poly(ethylene glycol) chains crosslinked with photocleavable nitrobenzyl units have been applied as 3D scaffolds for cell growth with light-tunable mechanical properties (Figure 14).[30, 54, 96] Micrometric resolution of the photodegradation process is possible to occur by using scanning lasers and two-photon excitation. The cell migration is directed by the created 3D channels with reduced crosslinking inside the hydrogel. The elasticity and mechanical properties of the photodegradable materials containing nitrobenzyl units with different functional groups can also be weighed before and after light irradiation.[55, 97] A unique hydrogel-nanoparticle hybrid scaffold containing three distinct components that trigger on-demand release of small molecule drugs. Upon light-irradiation, the photo-triggerable compound is activated to cause the cleavage of the covalently-bound drug and then be released from the hydrogel.[98] Moreover, image-guided, targeted, and dually locked photodegradable materials can release the anticancer drug and be employed for the real-time monitoring of the prodrug and in vitro cellular imaging by

one- and two-photon excitation.[56]

Photodegradable hydrogels are promising for creating 4D biomaterials for different tissue-engineering applications.[42] Such photodegradable biomaterials have been applied for directed cell function and modulating cell phenotype as consequence of softening of the hydrogel network after controlled photodegradation.[99-102] Selective photodegradation on one side of these thin hydrogel films leads to self-folding structures which are actuated by swelling that can be used for 3D cell culture.[41] Owing to the controllable degradation, it is possible to make gradient patterned stiffness.[103]

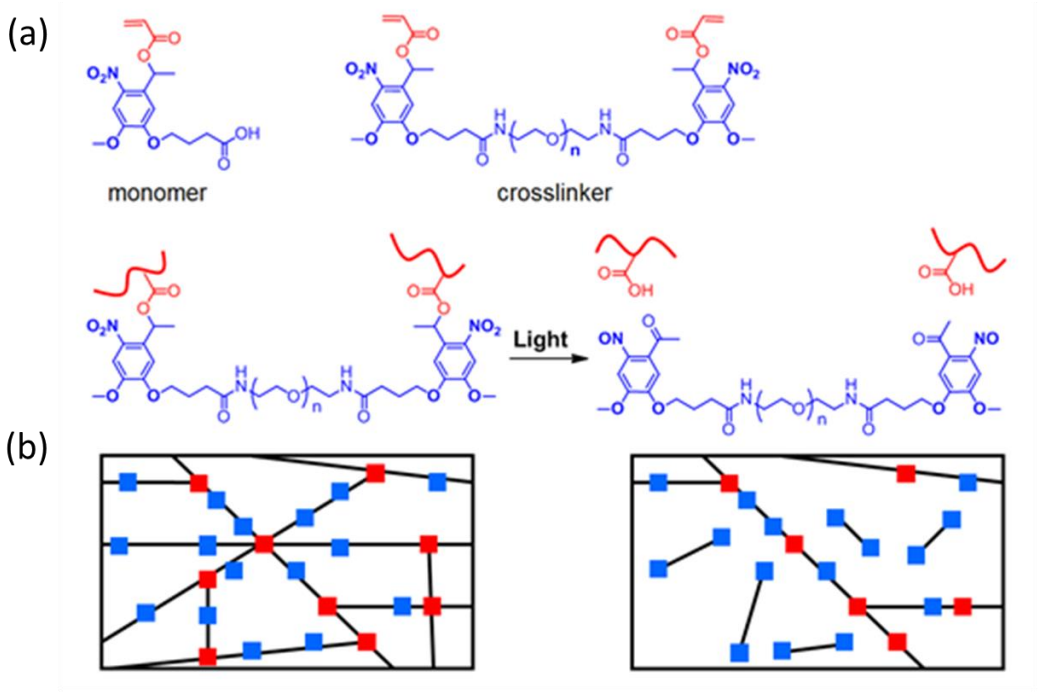

Figure 14. Light-induced degradation of *o*NB-based crosslinker to dynamically tune the properties of hydrogels. (a) *o*NB-based monomer and crosslinker used for generation of photosensitive hydrogel. (b) Network structures changed after light irradiation. Reproduced with permission.[30] Copyright 2009, AAAS.

1.2 *o*NB-derived responsive polymer brushes

Polymers formed on a surface can be defined as “polymer brushes”, which are densely attached with anchor sites to a surface.[104] Therefore, introducing polymer chains onto

the material surfaces can not only significantly tune surface properties, but also render obtained polymer brushes with new functionalities.[105] Polymer brushes were received attention in 1950s since Waarden, M. Van Der found that carbon black particles in liquid paraffin can be stabilized by the adsorption of dodecylbenzene,[106] indicating that grafting polymer molecules onto colloidal particles can prevent flocculation effectively. Among various functional flat surfaces, *o*NB-derived polymer brushes show representative photo-responsive characters to tune surface properties. Until now, different strategies have been developed to construct *o*NB-derived brushes on surfaces, including growing *o*NB-based side-chain polymer brushes and linking other kinds of polymers onto the surface through *o*NB linker.[24, 57-58, 107]

With special design, *o*NB-derived photocleavable polymer would generate ionizable carboxylic or amine groups upon light irradiation, which can be further used to change the wetting and swelling ability of polymer brushes.[24, 43] Cui and co-workers have reported the in situ modulation of the swelling performance of polymer brushes by integrating the photolysis of poly(4,5-dimethoxy-2-nitrobenzyl methacrylate) (PNVOCMA) based photosensitive polymers in the side chain (Figure 15a).[24, 108] The resulting polymer brushes are neutral and hydrophobic owing to the aromatic group. Upon UV irradiation, NVOC moiety is removed and a polyanion (PMAA) chain is generated. When this surface is irradiated through a mask, a surface pattern with different wettability and swelling performance is generated. The negatively charged polymer brushes can swell and collapse with pH response. Meanwhile, different wetting states (different photoconversion degrees) can be developed by the regulation of the exposure dose. Therefore, the wettability of the surface can be changed from hydrophobic to hydrophilic (Figure 15b).[109]

Besides, free amine groups can also be caged by introducing another photoremovable protecting group in this system. Thereby, poly(2-[(4,5-Dimethoxy-2-

nitrobenzoxy)carbonyl]aminoethyl methacrylate) (PNVOCAMA) has been used to fabricate the photoresponsive surface (Figure 15c).[43] Under UV irradiation, the NVOC group is removed to generate a polycation (poly(2-aminoethyl methacrylate, PAMA). At the pH of 4, the highly charged brush shows a swollen conformation to adsorb a large amount of solvent, while increasing the pH, the charged ammonium group is converted into non-charged amine to collapse the polymer brush.

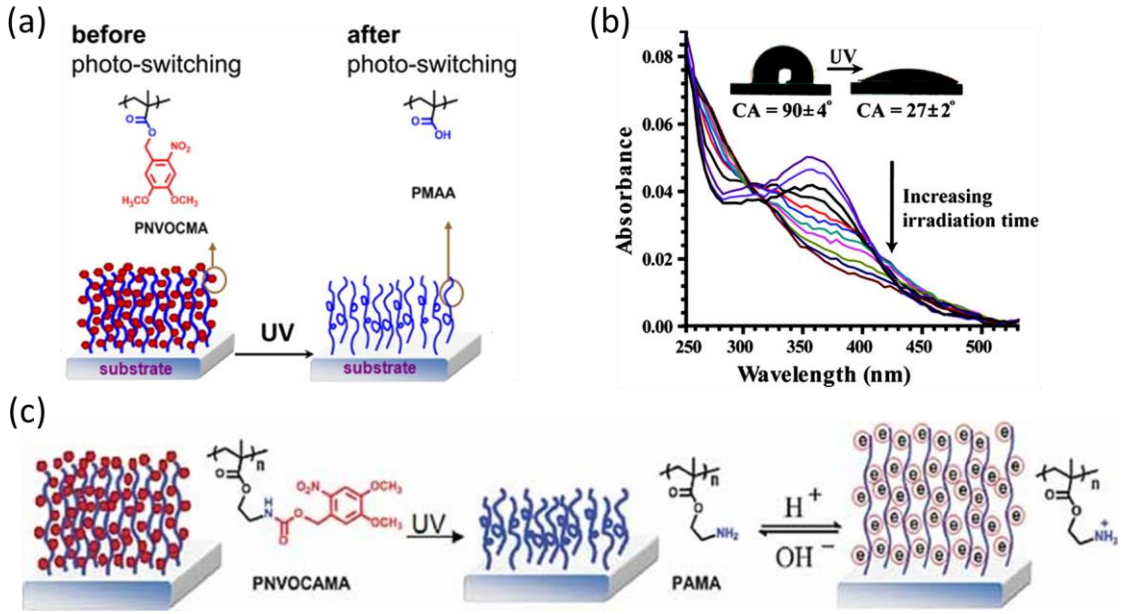

Figure 15. Photo-tuable swelling and wettability of *o*NB-derived surface. (a) Carboxylic acid caged surface. Upon UV irradiation, free acid generates. (b) Wettability changing of PNVOCMA coated surface after UV irradiation. (c) Amine caged photoresponsive surface by using PNVOCAMA as the polymer. Free amine group forms under UV illumination, which showing different swelling performances with pH response. Reproduced with permission.[43, 108-109] Copyright 2011, Wiley-VCH. Copyrights 2011,2013, American Chemical Society.

1.3 *o*NB-derived crosslinked networks

Photo-responsive *o*NB-derived polymer networks can be formed by (1) crosslinking the *o*NB-derived monomers, (2) using *o*NB derivatives as the crosslinker, and (3) tethering *o*NB moiety for post-modification within gel materials. After the cleavage of

*o*NB moiety within the network, the swelling and mechanical properties can be finely regulated. Since *o*NB-derived photodegradable materials have been detailed discussed in Section **1.1.3.3**, this property will not be discussed here.

1.3.1 Crosslinked networks with *o*NB-derived monomers

*o*NB-derived monomers with different structures and functionalities render new concepts in light-activated coatings, adhesives, inks, printing technology, and biomaterials.[59, 110] One interesting application for *o*NB-networks is as photoresist materials. Photoresists are used as thin films to produce photo-induced patterns. Light can induce degradation or crosslinking of the film, and treatment with a proper solvent dissolves either the irradiated (termed as positive photoresist) or the non-irradiated area (termed as negative photoresist), leaving a relief on the surface.[111] In a very early study, Reichmanis and co-workers introduced *o*NB cholate ester within a polymeric matrix to restrict the network's solubility. When exposed to UV irradiation, *o*NB moiety is cleaved and this allows the selective extraction of the irradiated region in an alkali developer.[112] With the development of this strategy, photoresist based organic light-emitting diode displays and protein microarrays have been fabricated.[113-114]

In very recent, *o*NB moiety is used as a "promoter" to enhance the swelling capability of the photo-irradiated region. Cui and co-workers have developed a photo-regulated localized growth of microstructure from swollen substrates, by combing photolysis, photopolymerization, and transesterification reaction together (Figure 16).[60] Upon light irradiation, the ionic groups generated by the photolysis of *o*NB moieties cause the fresh monomers selectively diffusion into the irradiation region, then are polymerized to form the inhomogeneous structures between the newly formed network and the original network, which is further homogenized by the heat triggered transesterification reaction. This spatially controllable light-regulated growth allows fine modulation in size, composition, and mechanical properties of the grown microstructures.

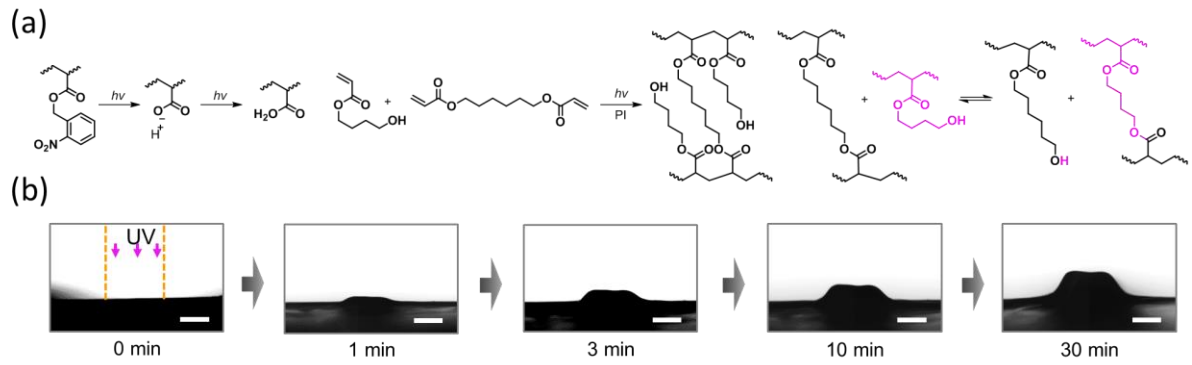

Figure 16. (a) *o*NB-based promoter for making microstructures. (b) Microstructures grown from a flat substrate by incoporate the photolysis, photopolymerization, and transesterification process. Reproduced with permission.[60] Copyrights 2020, Nature Publishing Group.

1.3.2 Crosslinked networks with *o*NB-derived crosslinkers

When introducing *o*NB-derived crosslinkers within a crosslinked network, the photolysis of *o*NB leads to the degradation of the network and the debonding of structures. Roppolo and co-workers have reported laser-triggered writing of micropatterns without any requirement of further treatment on the *o*NB-derived thiol-ene network (Figure 17a).[23] After obtaining the network consisted of multifunctional thiol and *o*NB-derived alkene, a laser beam source (375 nm) can be used to site-specific induce the photolysis of *o*NB linker, and subsequently, positive tone patterns are directly formed on the samples without using a soluble solvent to remove the photocleaved species. Furthermore, different patterned regions with carboxylic groups were obtained simply by harnessing laser energy

In recent, Batchelor et al. have integrated a 3D printing strategy to fabricate crosslinked structures and erase spatial regions of networks by only changing the wavelength emission laser sources (Figure 17b).[115] In this study, a diacrylate crosslinker with *o*NB groups has been designed, and two photons emission laser source (900 nm) is used to print micrometric structures firstly, subsequently selectively

erases the resist by using 700 nm laser wavelength emission. This approach is very useful to fabricate structured materials with wavelength selectivity.

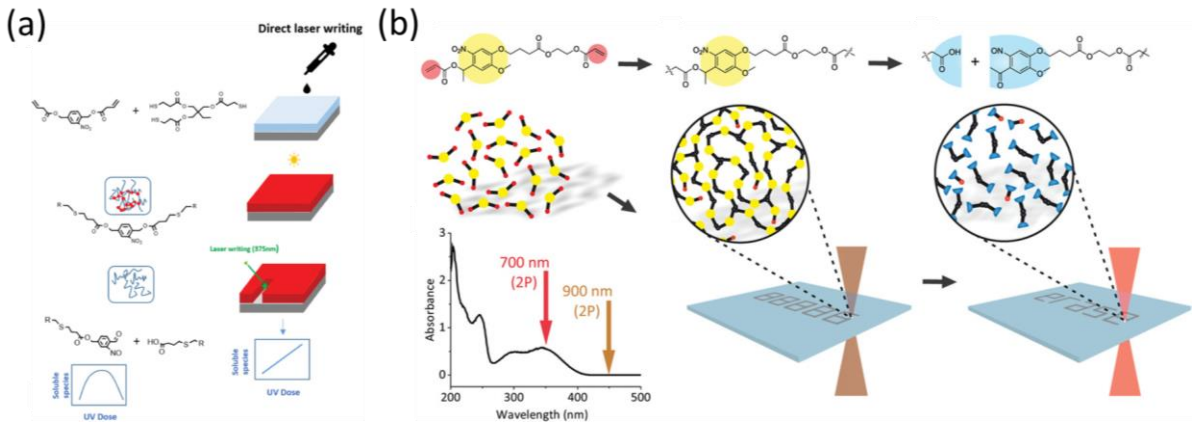

Figure 17. (a) Direct laser writing used for creating micropatterns within photolabile thiol-ene networks. (b) Schematic representation of the writing and erasing of the resist with wavelength selectivity. 900 nm wavelength was used to initiate the radical photopolymerization process, while selective removal of parts of the resist at 700 nm wavelength via *o*NB cleavage. Reproduced with permission.[23, 115] Copyrights 2019, 2020, Wiley-VCH.

1.3.3 Tethering *o*NB moiety for post-modification within gel materials

Owing to the diversity of *o*NB derivatives, functional caged groups can be released upon light irradiation, thus, it is desired to use this property for post-modification within gel materials. DeForest and co-workers have developed a series of photocaged alkoxyamines for post-conjugation of patterned proteins in gels. Based on this idea, they introduce a versatile approach to covalently decorate hydrogels with bioactive proteins to spatially control encapsulated cell fate (Figure 18a). 2-(2-Nitrophenyl) propoxycarbonyl (NPPOC)-photocaged alkoxyamine (H_2NO-) is first attached to natural gel precursor, then which can be photocleaved under UV light with a dose-dependent manner to generate alkoxyamine (Figure 18b). Then the formed alkoxyamine can localize condense with aldehyde-functionalized protein. In this case,

through photomask and laser scanning lithographic activation, 2D and 3D control over protein immobilization within based hydrogels are achieved (Figure 18c and 18d). This approach can also be used for 4D site-specifically of bioactive proteins on gel biomaterials and guidance of stem cell fate.[116-117]

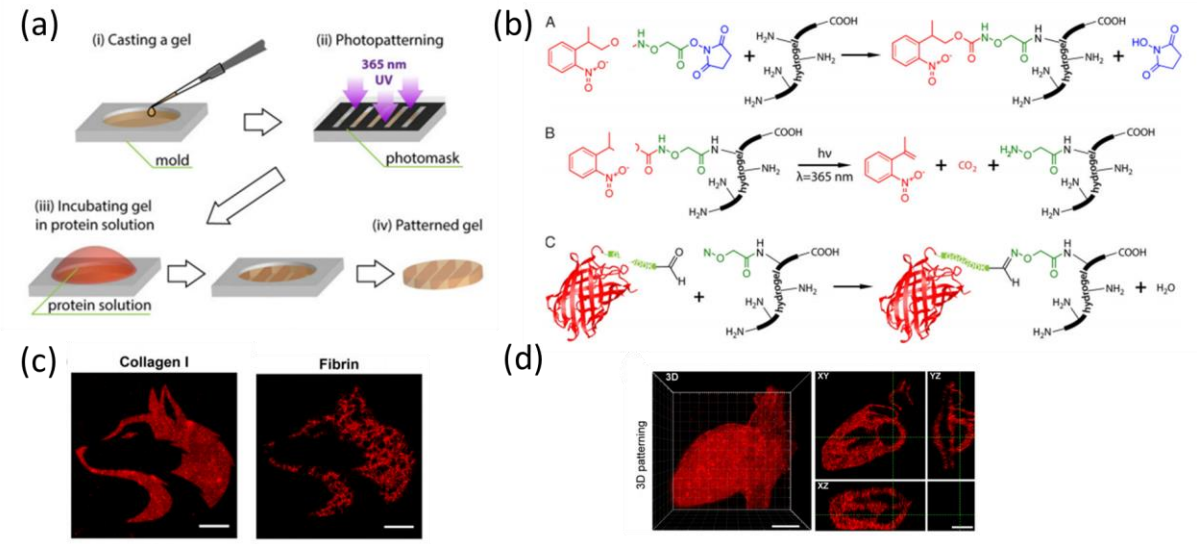

Figure 18. (a) Lithographic patterning of natural hydrogels. Gels are selectively irradiated with UV light before incubation with aldehyde-modified proteins. (b) Hydrogel modification and photopatterning through efficient photo-mediated ligation. (c) 2D protein patterns of mCherry (red) into collagen I and fibrin gels. (d) 3D pattern of an anatomical heart model. Scale bars in (c) and (d) are 50 μm. Reproduced with permission.[118] Copyright 2021, National Acad Sciences.

Moreover, N-(2-aminoethyl)-4-(4-(hydroxymethyl)-2-methoxy-5-nitrosophenoxy) butanamide (NB) linker can be introduced in hydrogels for photo-induced post-modification to generate strong adhesion between gels and tissues (Figure 19).[119] Ouyang and co-workers have developed a biomimetic tissue adhesive hydrogel that can be formed within seconds and then strongly bond to wet biological tissues after UV illumination. Methacrylated gelatin (GelMA) can form the first crosslinked network upon UV irradiation, meanwhile, the photo-induced cleavage of *o*NB linker generates an aldehyde group. The aldehyde can (1) react with amino molecules on tissue proteins to form Schiff-based, and (2) react with the amino group of GelMA to generate

a second network (Figure 19a). These two concurrent reactions lead to a high increase in wet tissue adhesion, and enhanced mechanical strength of the hydrogel. During the surgical operation process, the immediate high-pressure blood expulsion on the pig heart can be immediately covered by the formation of hydrogel with strong wet adhesion under light irradiation (Figure 19b and 19c).

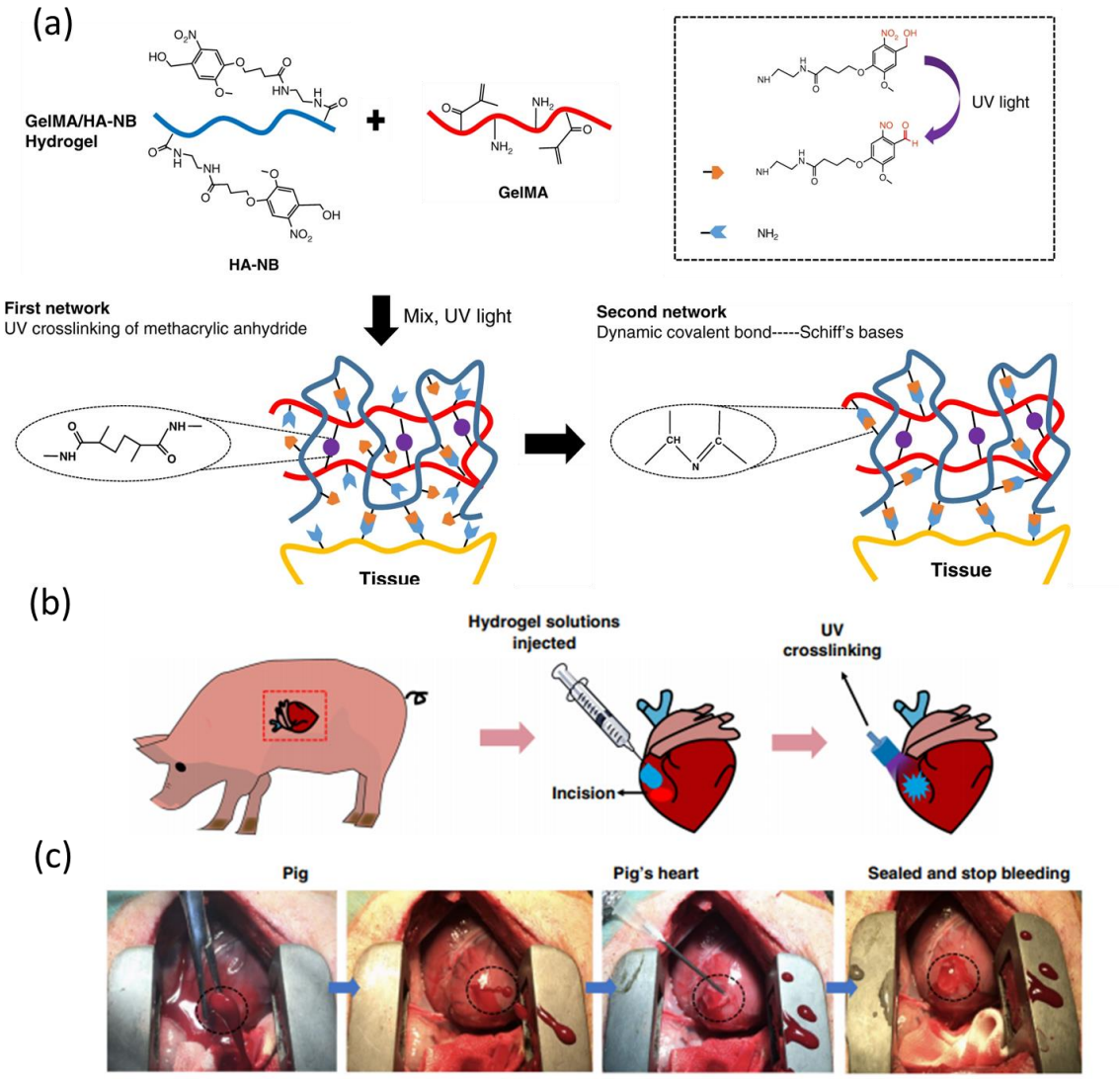

Figure 19. Strong wet adhesive hydrogel after UV irradiation. (a) The formation of the photo-triggered imine-crosslinked matrix hydrogel. (b) Schematic diagram of the surgical procedure in a pig. (c) Gross view of the rapid hemostasis and sealing of punctured injury by UV-activated hydrogel formulation. Reproduced with permission. [119] Copyright 2019, Nature Publishing Group.

Chapter 2

2. Photo-regulated growth and detachment of polymer brushes on various surfaces with wavelength-selectivity

Note: The content of this chapter has been published in: Phototriggered growth and detachment of polymer brushes with wavelength-selectivity. *ACS Macro Letters,* 2018, *7*, 239-243. X. Xiong, L. Xue, and J. Cui.

This chapter describes an approach to control the growth and detachment of polymer brushes independently by using light of different wavelengths. The approach is based on a nitrodopamine-based initiator (2-bromo-N-(2-nitro-3, 4-dihydroxyphenethyl)-2-methylpropanamide, NO_2-BDAM) which contains a catechol structure for surface modification, alkyl bromide group for radical polymerization, and *o*-nitrophenyl ethyl moiety for photolysis. When dimanganese decacarbonyl ($Mn_2(CO)_{10}$) is applied together with NO_2-BDAM as an initiating system, visible light (460 nm) can be used to trigger the site-specific growth of polymer brushes. Switching the irradiation wavelength to UV (360 nm) allows for photocleavage of the polymer chains through photolysis of the *o*-nitrophenyl ethyl group resulting in the detachment of grafted polymers from the surface. The universality of this approach is studied by using different kinds of monomers and different substrates. At last, one-step and two-steps surface patterns have been created by growing and detaching of polymer brushes, which are used to demonstrate the potential application of this facile method.

2.1 Introduction

The modification of a surface by polymer brushes is an effective strategy to tailor interface physical and chemical properties for a wide range of applications, such as

antifouling coatings, chemical sensing, and stimuli-responsive materials.[120-124] With the assistance of polymer brushes, it is convenient to provide high degrees of synthetic flexibility towards the introduction of varieties of functional groups with mechanical and chemical stabilities. For getting a high grafting density, surface-initiated radical polymerizations are often applied.[125-127] These polymerizations can be triggered by different stimuli including temperature, chemical additive, electrochemistry, light, etc.[120, 128] Among the methods currently available, light-induced surface polymerization has several advantages like spatiotemporal control, remote modulation, room-temperature operation and dose-dependent brush growth.[129-133] Photoresponsive molecules are employed to trigger in situ activation of initiating/propagating radicals for the site-specific growth of polymer chains from the surface and thus allow for patterned substrates,[129] gradient surfaces,[134] and even complex 3D structures.[135]

In addition to the growth of polymer brushes, light is also able to modulate the properties of grown polymer brushes by photo-triggered reactions to initiate catalyst,[136] activate functional groups,[24, 43, 137] and remove polymer chains,[57-58, 138] etc. When more than two chromophores that respond to the light with different wavelengths are applied together, the activity of these molecular species on surfaces can be regulated independently.[139-140] This concept of wavelength selectivity has been utilized for preparing surfaces with orthogonal properties,[141] and dragging the concept to polymer brushes is promising for design smart surfaces with photo-regulated properties.

In this chapter, a robust and facile method for regulating the growth and removal of polymer brushes independently by switching light wavelength is described. The key molecules behind the material design are $Mn_2(CO)_{10}$ and NO_2-BDAM. This methodology includes three steps: immobilizing NO_2-BDAM initiator onto the substrate

surface, conducting a surface grafting polymerization under visible light (460 nm), and then cleaving the grafted polymer brushes when exposed to UV light (360 nm). Photo-induced surface grafting and detaching are simple and rapid in producing polymer brushes at room temperature with controlled grafting layer thickness and density. This methodology can be applied to different monomers on various substrates. One-step and two-steps surface patterns are efficiently created by multi-stage light triggering of polymer brush growth and detachment processes.

2.2 Results

2.2.1 Design and synthesis of multi-functional photo-sensitive initiator

To orthogonally realize photo-initiated growth and detachment of polymer brushes with wavelength-selectivity on various substrates, a multi-functional initiator was designed. Inspired by dopamine chemistry, the nitrodopamine-based initiator, NO_2-BDAM was synthesized (Figure 1). It contains three functional moieties: (1) the catechol structure which allows for strong binding and modification on nearly all types of substrates,[142-143] (2) an alkyl bromide group for generating radical-initiating species for grafting polymerization,[144] and (3) nitrobenzyl moiety that can undergo photolysis for detaching the anchoring polymer chain.[92]

NO_2-BDAM was prepared efficiently by an amidation reaction between 6-nitrodopamine and 2-bromoisobutyryl bromide (Scheme 1). To independently control the growth of polymer chains, $Mn_2(CO)_{10}$ was selected as a visible-light (460 nm) activated initiator for surface-initiated polymerization due to its solubility in a wide variety of reactive monomers and solvents and its efficiency in generating radical species upon photolysis.[145] Upon irradiation, it generates a highly active radical $\cdot MnCO_5$ to abstract halides from organohalogen compounds to form radical

species for initiating polymerization.[146-148] Meanwhile, UV light (360 nm) irradiation can lead to a molecular cleavage on the β position of the ethylene group for debonding the tethered polymer chains.

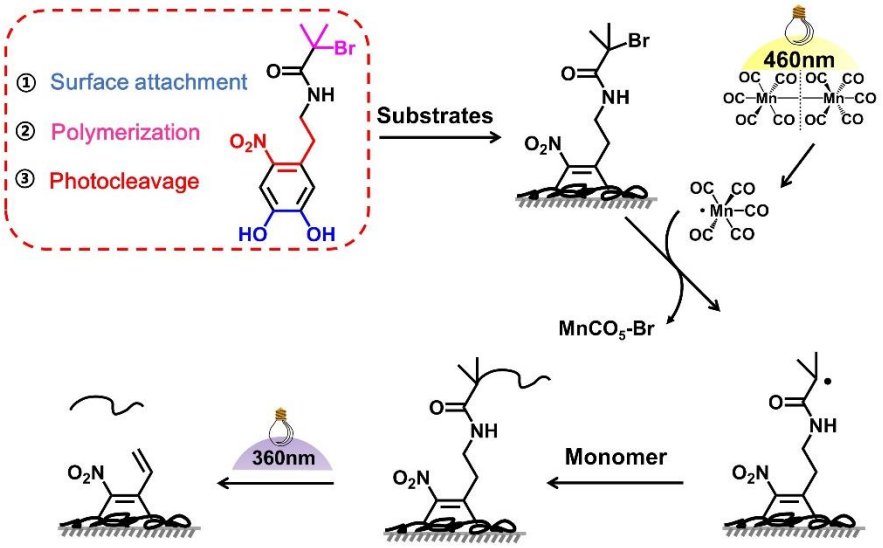

Figure 1. Schematic of the photo-regulated procedure on a surface. NO_2−BDAM, containing three functional moieties, is used for various surface attachments, in situ polymerization, and robust photocleavage.

2.2.2 Wavelength-selectivity of NO_2-BDAM and $Mn_2(CO)_{10}$

NO_2-BDAM and $Mn_2(CO)_{10}$ are firstly chosen as light-sensitive molecules and their photoactivity was evaluated under different wavelengths. The photocleavage mechanisms of NO_2-BDAM and $Mn_2(CO)_{10}$ are shown in Figure 2a. $Mn_2(CO)_{10}$ can undergo photolysis by irradiation at 460 nm to generate ·$MnCO_5$ radical while the *o*-nitrophenyl ethyl moiety of NO_2-BDAM can be photocleaved under UV light irradiation to generate *o*-nitrostyrene. The photoactivity of NO_2-BDAM and $Mn_2(CO)_{10}$ at 460 nm was investigated. Upon exposure to 460 nm at increasing time, the absorption of $Mn_2(CO)_{10}$ at 349 nm decreases rapidly due to the photolysis of $Mn_2(CO)_{10}$ which indicated a distinct degradation. At the same exposure conditions, no changes in the absorption spectrum of NO_2-BDAM were observed (Figure 2b and 2c). Photolytic

conversion of $Mn_2(CO)_{10}$ under irradiation dose of 10 J/cm^2 can reach nearly 100% while NO_2-BDAM remains stable even after higher irradiation dose (Figure 2d). These results indicate the possibility to initiate the growth of polymer chains on a surface by using 460 nm light without inducing any photodegradation of NO_2-BDAM. When UV light of 360 nm is applied, the spectrum of NO_2-BDAM shows immediate changes, implying its high photosensitivity at this wavelength (Figure 2a and 2e). The absorption at 351 nm decreases gradually and a new absorption centered at 275 nm increases finally. The photolytic reaction is almost completed at irradiation dose >80 J/cm^2 (Figure 2f). In summary, light with wavelengths of 460 and 360 nm can be used to independently control the reactivity of the $Mn_2(CO)_{10}$ and NO_2-BDAM, respectively. This feature will be used in the next section to control the growth and detachment of polymer brushes.

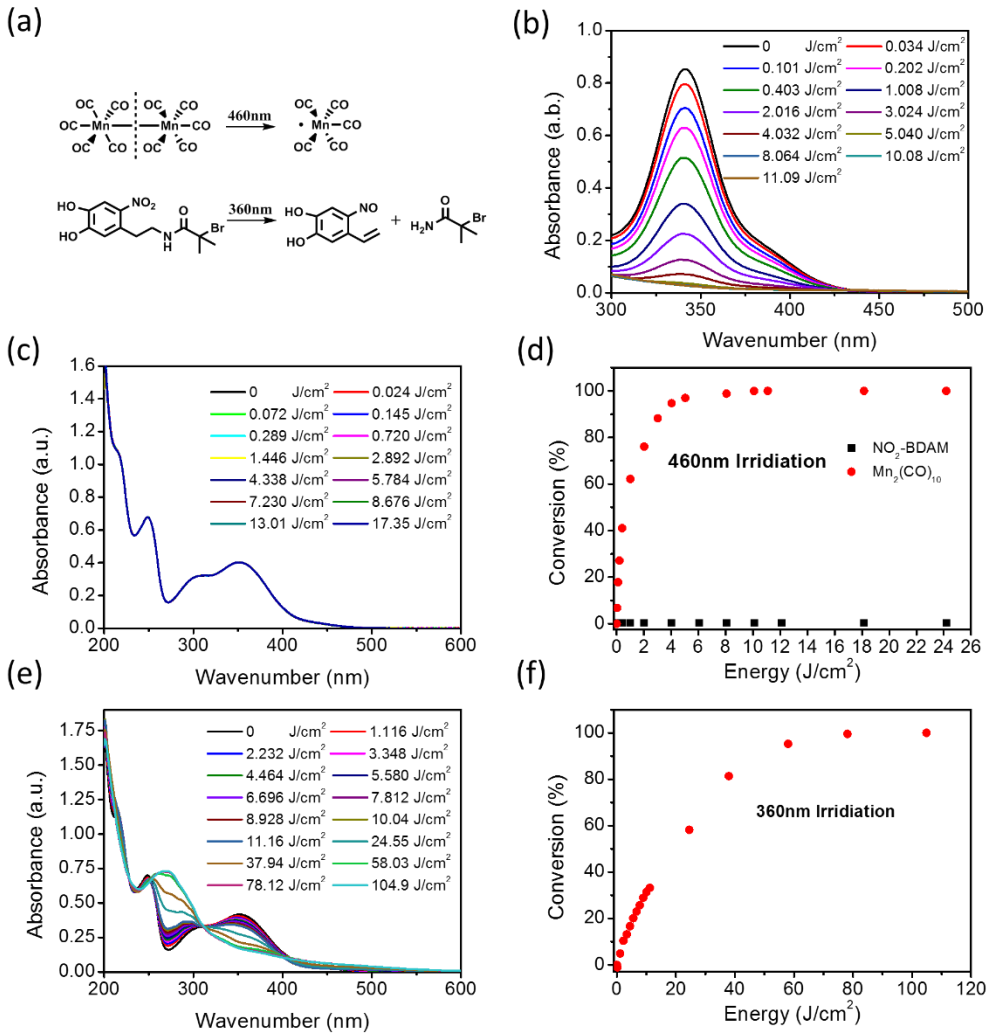

Figure 2. (a) Structures of NO_2-BDAM and $Mn_2(CO)_{10}$ and their photocleavage mechanisms. UV Spectra of (b) $Mn_2(CO)_{10}$ and (c) NO_2-BDAM after exposed to visible light of 460 nm for different irradiation doses. (d) Photolysis conversion (%) of $Mn_2(CO)_{10}$ and NO_2-BDAM in solution under different irradiation doses at 460 nm. Data were calculated from the absorbance values at λ_{max} = 349 nm by assuming 100% conversion at full photolysis. (e) UV Spectrum of NO_2-BDAM after exposure to UV light of 360 nm for different irradiation doses. (f) Photocleavage conversion (%) of NO_2-BDAM under different irradiation doses at 360 nm. Data were calculated from the absorbance values at λ_{max} = 351 nm by assuming 100% conversion at full photolysis. The concentration of $Mn_2(CO)_{10}$ used in (b)-(f) is 5.13×10^{-5} M. The concentration of NO_2-BDAM used in (b)-(f) is 5.78×10^{-5} M.

2.2.3 Visible light-induced surface grafting polymerization

NO_2-BDAM was used to modify Si and Ti substrates through different immobilizing mechanisms. NO_2-BDAM grafted Si substrates were prepared by immersion in an agitated alkaline solution (pH = 8.5) containing NO_2-BDAM. A two-step co-deposition method was tested, in which $NaIO_4$ was used as an oxidant to fabricate the initiating layer on silicon surfaces by inducing polymerization of NO_2-BDAM. The dopamine moiety of NO_2-BDAM was oxidized to create a polymerized network through the formation of quinoidal structures to immobilize NO_2-BDAM on substrates.[149] However, the oxidant is not necessary for Ti substrate since the strong chelating interaction of the catechol group with the Ti atom leads to a self-assembled monolayer (SAM) of NO_2-BDAM.[150-151] The photolabile *o*-nitrophenyl ethyl structure could be fully maintained in the SAM on Ti substrate,[151] compared to the complicated polymeric structures formed through oxidation-induced polymerization on the other substrates.[149] The introduction of *o*-nitrophenyl ethyl structure on Si and Ti substrates was confirmed by the change in water contact angle (WCA) of surfaces (Figure 3a) and signals of X-ray photoelectron spectroscopy (XPS, Figure 3b). Water contact angles of NO_2-BDAM coated Si changes from 73.4° to 32.1° and on Ti change from 70.5° to 25.5°. The appearance of a bromine signal (magnified in figure 3b) in the XPS spectrum confirmed the successful modification of NO_2-BDAM initiator on Si surface.

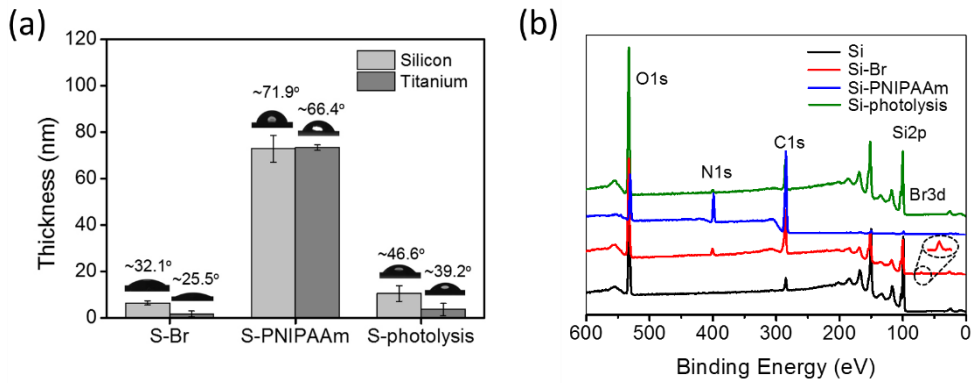

Figure 3. (a) Thickness and water contact angle of organic layers on wafers under different conditions. S-Br, S-PNIPAAm and S-photolysis mean the initiator modified substrates, PNIPAAm-modified substrates, substrates after phototriggered detachment of PNIPAAm brushes, respectively. Data are presented as the mean ± SEM. (n = 3). (b) XPS spectra of Si, Si-Br, Si-PNIPAAm, and Si-photolysis.

NO_2-BDAM-modified Si substrate (denoted as Si-Br) grafted by poly(*N*-isopropylacrylamide) (PNIPAAm) was selected as a model system to study the phototriggered growth and detachment of polymer brushes. When the substrate Si-Br was immersed in the NIPAAm solution in the presence of $Mn_2(CO)_{10}$, a polymer layer indeed formed under visible-light irradiation (460 nm, Figure 3a). The thickness of the growth of the PNIPAAm brush reached ~77.5 nm and ~78.3nm on Si and Ti surface, respectively (denoted as Si-PNIPAAm, Ti-PNIPAAm). The growth of the PNIPAAm brush alters the composition on the top properties of the surface. After PNIPAAm grafted, the content of C, N elements increased obviously due to the main elements of PNIPAAm (Figure 3b), and the WCAs of Si-PNIPAAm and Ti-PNIPAAm increased to ~71.9° and ~66.4°, respectively (Figure 3a). It was expected that the polymerization process with $Mn_2(CO)_{10}$ and alkyl bromide as the initiating system followed a free radical polymerization mechanism because of the irreversible abstract reaction between ·$MnCO_5$ and alkyl bromide,[148] which was confirmed by monitoring the molecular weight and polydispersity index (PDI) the PNIPAAm in the solution state

under different irradiation time (Figure 4a). I set the feed molar ratio of [NIPAAm]/Ethyl α-bromoisobutyrate [EBIB]/ [$Mn_2(CO)_{10}$] as 10000:1:0.8 and conducted the polymerization for 3 min, 5 min, 7 min, 10 min, 20 min, and 30 min, respectively. The obtained polymers showed similar molecular weight (2.4~2.6×10^5 g/mol) and PDI (~2.2) regardless of the irradiation time, implying a typical free radical polymerization mechanism (Figure 4b).

(a)

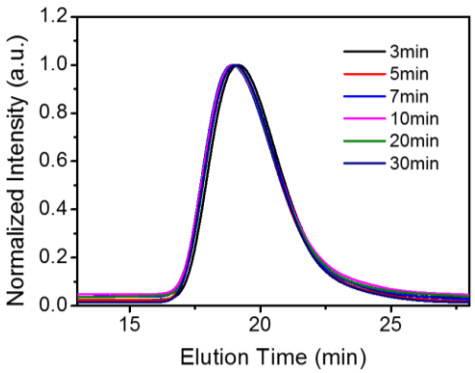

(b)

Polymerization time (min)	Mn (g/mol)	Mw/Mn
3	2.64 × 10^5	1.99
5	2.67× 10^5	2.16
7	2.71× 10^5	2.18
10	2.61× 10^5	2.21
20	2.92× 10^5	1.97
30	2.44× 10^5	2.33

Figure 4. (a) GPC traces of PNIPAAm obtained at different light irradiation time intervals during polymerization with a feed molar ratio of [NIPAAm]/[EBIB]/[$Mn_2(CO)_{10}$] = 10000:1:0.8. (b) Molecular weight and PDI of PNIPAAm under different irradiation time.

Based on this polymerization mechanism, the molecular weight of the polymer chains on substrates was then controlled by changing monomer concentration to achieve the desired film thickness (Figure 5a). It was expected that longer polymer chains would be grafted onto the substrate as increasing the concentration of monomer concentration. A nearly linear relationship between the final thickness of polymer brushes and the monomer concentration was observed. The linearity of polymerization rate as a function of monomer concentration indicated a first-order reaction kinetics, which would be expected for a “controlled” grafting polymerization reaction.[145] When the monomer concentration increased to 7 M, the grafted thickness surpassed 80 nm. Although the abstraction of bromine from the surface is irreversible, the photodecomposition of $Mn_2(CO)_{10}$ is suggested to be reversible.[152] The

obtained ·$MnCO_5$ would reform $Mn_2(CO)_{10}$ in a diffusion-limited rate under a non-irradiated state. In other words, radical species only formed under light irradiation, which implying a simple light-switchable way to regulate the growth of polymer chains. This was probed by monitoring the thickness of the polymer layers under different irradiation time. The thickness of the polymer layers increased with the irradiation energy until it reached a stable state (Figure 5b). This process also enabled a desired thickness to be easily obtained by simply regulating the exposure time. The increased thickness was attributed to the increasing of grafting density, rather than the length of polymer chains. With higher irradiation does (>2 J/cm^2), the thickness and the irradiation dose became nonlinear due to the decreasing of $Mn_2(CO)_{10}$ and monomers as well as the increase in the coverage of the substrate surface,[153] which resulted in the restricted grafting reaction. The quenching of the ·$MnCO_5$ was very fast, which even allows for a light-switched “on-off” of the grafting polymerization reaction (Figure 3c). For example, a sample irradiated for 1 min (irradiation energy: 0.2 J/cm^2) could form a grafted layer of ~9.1 nm. The thickness kept constant without obvious changing when further subjected into a dark environment for 10 min, indicating fast quenching of ·$MnCO_5$ and terminating of grafting reaction. The grafting could be then activated under visible light. In this case, the polymerization on substrates could be repeated activated and deactivated when turning on and off the light irradiation dosage. When the total irradiation energy reached 1.6 J/cm^2, the grafting thickness could achieve around 58.6nm, which is similar to the thickness grafting under continuous irradiation with the same irradiation dose.

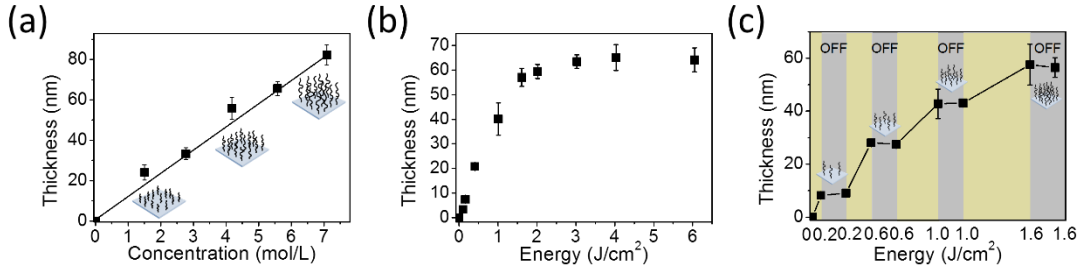

Figure 5. Photoinduced growth of PNIPAAm on silicon substrates. (a) Thicknesses of PNIPAAm layers obtained from different NIPAAm concentrations. (b) Thickness of the PNIPAAm layer on Si substrate versus irradiation dose. (c) Thickness change of the polymer layer during on-off irradiation cycles. The time off slot is 10 min. In (a), (b), and (c), the concentration of $Mn_2(CO)_{10}$ was 0.25 mM. In (b) and (c), the concentration of NIPAAm is 4.5 M. The polymerization was conducted at room temperature under 460 nm LED light irradiation. Data are presented as the mean ± SEM (n = 3).

2.2.4 Detachment of polymer brushes layer under UV irradiation

The same polymer system was used to study the detachment of tethered chains under UV light irradiation (360 nm). According to Figure 2e, NO_2-BDAM can undergo photolysis efficiently under UV irradiation, so the photocleavage of poly(NO_2-BDAM) initiator layer was first studied by UV spectroscopy. As a control, no change was observed on the absorption of the polydopamine layer, when the irradiation energy was increased to 18.6 J/cm^2 (Figure 6a). However, the absorption of poly(NO_2-BDAM) coating decreases gradually upon UV irradiation, indicating that the photocleavable behavior attributes to the *o*-nitrophenyl ethyl moiety structure and the polymer coatings possess the photocleavable properties of NO_2-BDAM (Figure 6b).[92] It is suggested that the grafted polymer brushes could be cleaved under UV irradiation. As a result, the absorption (>250 nm) of PNIPAAm brushes grafted SiO_2 surface (SiO_2-PNIPAAm) showed a similar decrease as which of poly(NO_2-BDAM) layer under irradiation (Figure 6c). Since the structure of PNIPAAm is simple and has no chromophore, it

does not show visible absorption in the region of >250 nm, indicating that the irradiation condition does not induce any damage to PNIPAAm chains (Figure 6d). This decrease was thus attributed to the photolysis that occurred on the poly(NO_2-BDAM) based bottom layer. The removal of polymer chains was further confirmed by the changes in thickness, surface wettability, and chemical composition of the organic layer (Figure 3a and 3b). After complete photolysis, the thickness of residual organic coatings of Si and Ti surfaces changed to 10.8 nm and 3.6 nm, which are very close to the original poly(NO_2-BDAM) coatings (6.5 nm and 1.8 nm), respectively. Without PNIPAAm brushes, the WCAs of Si and Ti surfaces become to 46.6° and 39.2°, respectively.

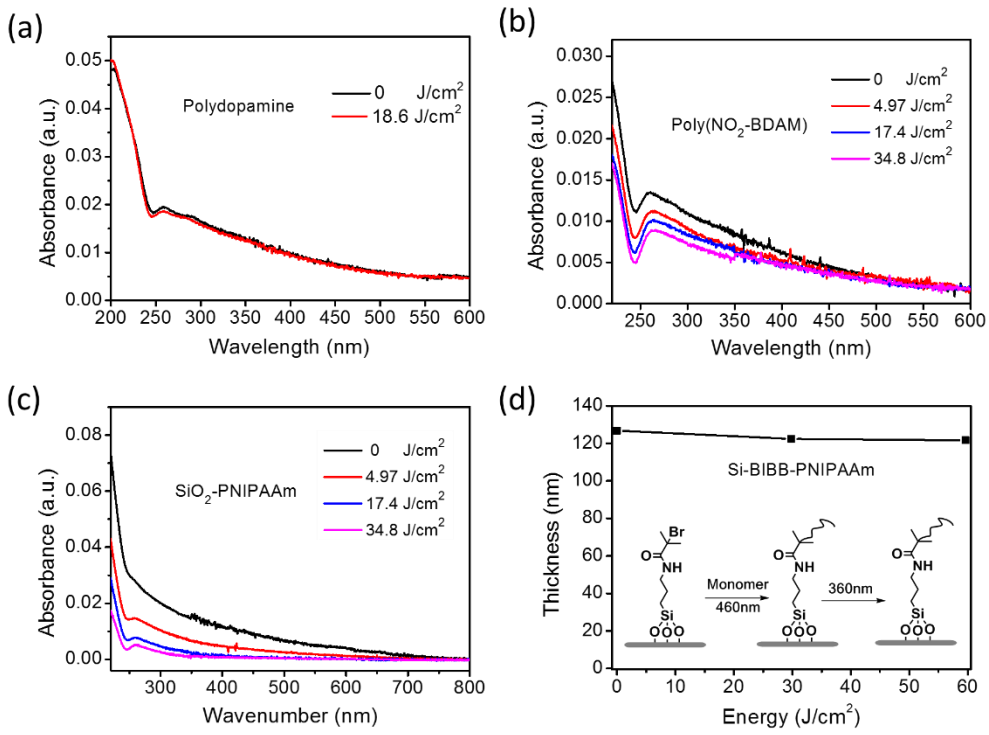

Figure 6. UV spectra of (a) polydopamine and (b) poly(NO_2-BDAM) coated SiO_2 after exposed to UV light of 360 nm for different irradiation doses. (c) UV spectra of PNIPAAm coated SiO_2 under different irradiation doses. (d) Thickness of the PNIPAAm layer on Si-BiBB surface under different UV irradiation doses. UV 360 nm LED light was used in (a), (b), (c), and (d).

After confirming the detachment of grafted polymer brushes from poly(NO_2-BDAM) based bottom layer, the degradation-induced decrease in the thickness of polymer layer under different irradiation doses was then investigated (Figure 7a). Based on this, PNIPAAm brushes on NO_2-BDAM coated Si and Ti substrates were fabricated. When gradually increasing the irradiation energy to 50 J/cm^2, the grafted PNIPAAm brushes on Si and Ti substrates (~73 nm) could be fully cleaved from the substrate. The poly(NO_2-BDAM) network layer based Si substrate shows a slightly lower photolysis efficiency (~85.5%) than NO_2-BDAM SAM layer-based Ti surface (95.1%) (Figure 7a), which was attributed to the integrated structure of o-nitrophenyl ethyl in NO_2-BDAM SAM on Ti substrate.[150]

Photo-induced detachment of polymer chains from the initiating coated layer provided a way to collect the tethered polymer chains for studying their structures. PNIPAAm coated Ti substrate with a thickness of 169 ± 3 nm was selected as an example because of its efficient photolysis performance. The detached polymers can completely dissolve in DMF, implying a non-crosslinked polymer structure (the most probable structure should be linear polymers). Gel permeation chromatography (GPC) measurement of the polymers suggests an average molecular number (Mn) of 2.41 × 10^5 g/mol and a PDI of 2.5 (Figure 7b). These polymers show smaller molecular weight and higher PDI than those from free radical polymerization in solution. It can be explained by the fact that the surface prevents monomers from delivering to the chain ends from all directions and thus reducing the effective concentration of monomers near the active chain ends.[154] The initial grafting density (γ) was estimated by using the equation $\gamma = \frac{h_{dry}\rho N_A}{M_n}$, where h_{dry} is the dry height of the polymer brushes, N_A is Avogadro's number, and ρ is the bulk volume density of polymers (1.1 g/cm^3 for PNIPAAm).[155] It has been suggested that the M_n of PNIPAAm obtained from GPC is

very close to their real molecular weight.[156] As a result, a grafting density of 0.46 chain/nm^2 is obtained, which is comparable with the grafting density of dense polymer brushes. In addition, obtained polymers contain a few short chains. These short chains might form at the end of the polymerization process where the grafted polymer chains restricted the growth of propagating chains.

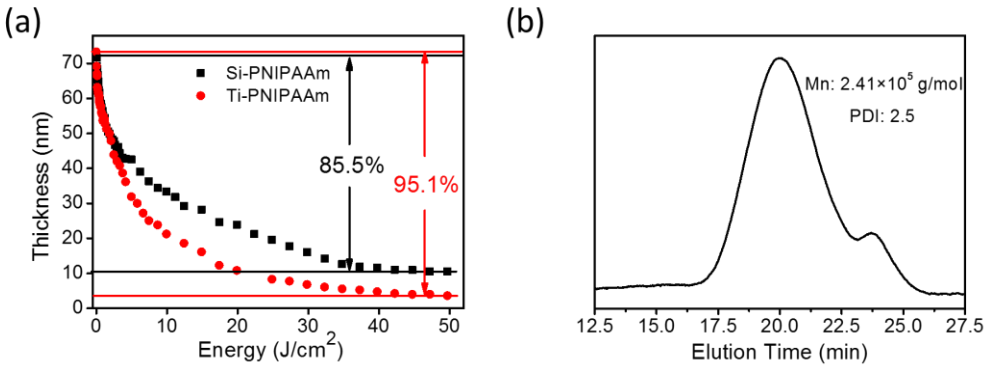

Figure 7. (a) Thickness changes of the PNIPAAm layers on Si and Ti wafers under different UV irradiation dose. (b) GPC trace of cleaved PNIPAAm polymers from Ti surface.

2.2.5 Universality of photo-regulated growth and detachment approach

To demonstrate the potential applications of this approach, the diversity of the current strategy by using different monomers and substrates was studied. In addition to NIPAAm (hydrophilic monomer), two other types of monomers including acrylic acid (AA, acidic monomer) and butyl acrylate (BA, hydrophobic monomer) were also used. All these monomers can be grown from poly(NO_2-BDAM)-coated Si wafers via visible-light-induced surface polymerization and can also be removed by UV light (Figure 8a). After grafted PBA and PAA on Si substrate, the thickness increased to 66.3 nm and 58.6 nm, while the WCA becomes hydrophobic for PBA (104.4°) and hydrophlic for PAA (38.6°), respectively. After exposed to UV light, the polymer brushes were cleaved with grafting thickness decreased to 9.3 nm and 13.5 nm, respectively. The changes

of thickness and WCA proved that the successfully grafting and detaching of polymer brushes (Figure 8a). Besides Si and Ti substrates, Au and SiO_2 wafers could also be applied in this system to conduct the grafting and detaching of PNIPAAm brushes (Figure 8a and 8b). The change of thickness and WCA for polymer grafted Au substrate (Figure 8a) and the change of UV absorption (Figure 8b) (> 250 nm) for polymer tethered SiO_2 proved the feasibility of this method. Therefore, this wavelength-selective triggered growth and detachment approach could not only be used for various monomers (NIPAAm, AA, and BA) but also could be applied to different material surfaces, such as Si, Au, Ti, and SiO_2 surfaces.

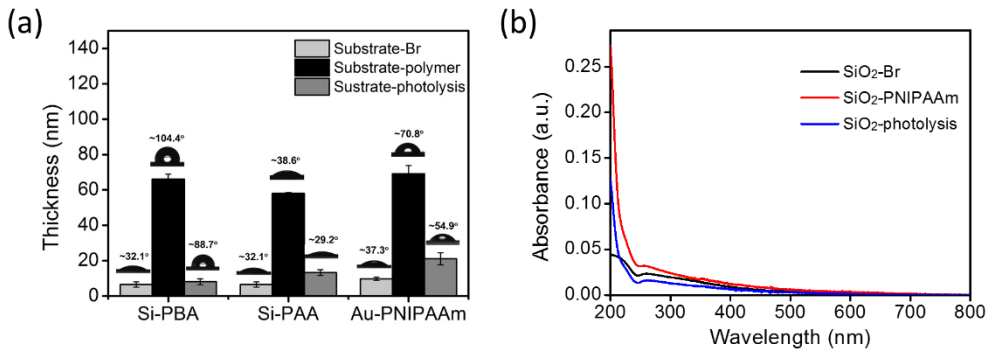

Figure 8. (a) Thickness and water contact angle tests of different polymer brushes (PBA, PAA) on silicon wafers and PNIPAAm on Au wafer under different conditions. Data are presented as the mean ± SEM (n = 3). (b) UV spectra of PNIPAAm grafted SiO_2 in different modifying processes.

2.2.6 Light-triggered growth and detachment of polymer brush for creating surface patterns

It was expected that the current strategy could be used for spatiotemporal control and post-regulation of polymer brushes to create surface patterns. To demonstrate this feasibility, patterned PNIPAAm brushes on Si and Ti substrates have been prepared. Striped and square masks were used to generate distinct polymer brush patterns (one-step patterning strategy, Figure 9a to 9d). Furthermore, the grown polymer brush

patterns could be further changed by UV light (two-steps patterning strategy, Figure 5e and 5g). After getting one-step PNIPAAm patterns on surfaces, subsequent UV irradiation of 360 nm generated new patterns by removing the polymer chains on exposed regions, implying incredible feasibility in making polymer brush patterns. Thus, the surface topologies can be continuously changed by photo-triggered growth of detachment of polymer brush approach.

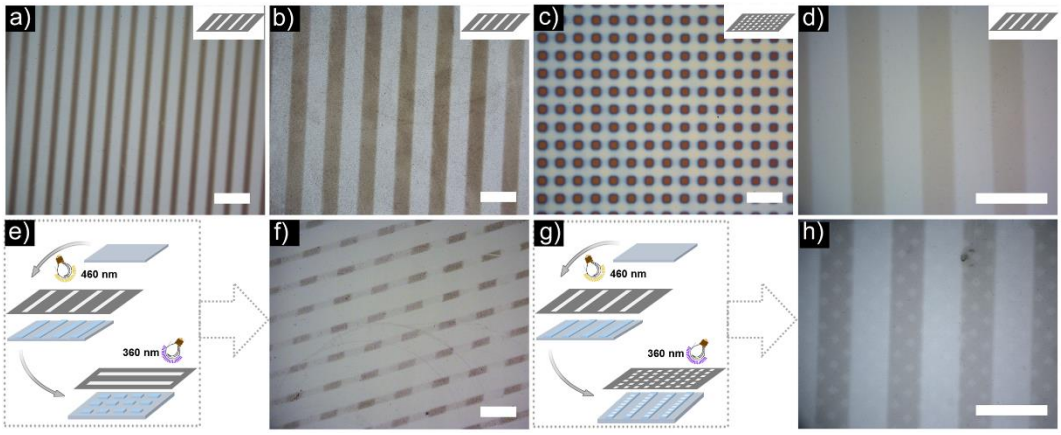

Figure 9. Photolithography demonstration of PNIPAAm brushes on (a-c,f) silicon wafers and (d,h) Ti wafers (scale bars are 400 μm). (a-d) One-step patterned brushes obtained by visible-light irradiation (460 nm) with different photomasks (a, 50 μm transparent strips with a gap of 150 μm; b,d 200 μm transparent strips with a gap of 200 μm; c, 50 × 50 μm transparent squares with a gap of 50 μm). (e, g) Schematic diagram of two-step patterning strategy by using different photomask combinations. (f) Polymer brush patterns made from the substrate shown in (a) by using a striped photomask (200 μm transparent strips with a gap of 200 μm) under UV irradiation of 360 nm. (h) Two-steps brush patterning based on the patterns formed in (d) by using a square photomask (50um squares) under UV irradiation of 360 nm.

2.3 Discussion

Over the past decades, light-induced grafting polymer brushes have become a hot topic of polymer research. The light-triggered polymerization always works by introducing chromophores which are light sensitive. The $Mn_2(CO)_{10}$-based visible light

photo-initiating system is a powerful method for the preparation of polymer brushes grafted surface due to its optical characteristics in the visible range with high quantum yield and good solubility properties.[145, 147] For example, Wu and co-authors applied a photo-initiating system for modifying polydimethylsiloxane (PDMS) surfaces. Undec-10-enyl-2-bromo-2-methylpropanoate is used as a vinyl-terminated initiator to mix with the traditional PDMS contents (Sylgard 184, base : curing agent = 10:1) to obtain the bromine functionalized PDMS surface, which could be further used to conduct visible-light-induced surface grafting polymerization with various polymers.[157] The grafting polymerization process is simple and efficient. However, since the polymer brushes are covalently bound to the substrates, the characterization of polymer brushes' properties remains challenging. For example, it is difficult to characterize the molecular weight, grafting density and PDI of the grafted polymer brushes. Based on this point, a molecule with a stimuli-cleavable unit is necessary. Compared to other cleaving methods, light-triggered molecular cleavage has received widespread interest due to its mild, clean, and easily controlled procedure.[129] The *o*-nitrobenzyl group, which undergoes selective bond cleavage upon irradiation with UV-light, has been a valuable building block to control material properties.[93] Johann Erath and co-workers have grafted photosensitive brushes (poly(6-nitroveratryl methacrylate), PNVOCMA) with a poly(acrylic acid) backbone. The main chains were modified by 6-nitroveratryloxycarbonyl (NVOC) to act as the photocleavable protecting group on Si surface by ATRP, then using UV light to remove the chromophores to expose the free COOH groups for changing the physical properties of the surface.[108] Cui and co-workers grafted photolabile polymer brushes (poly(2-[(4,5-Dimethoxy-2-nitrobenzoxy)carbonyl]aminoethyl methacryla), PNVOCAMA) with NVOC as the photoremovable protecting group, then using UV light to generate a controlled density of free amine groups (polycation (poly(2-aminoethyl methacrylate, PAMA), which were

distributed along the polymer chains and could be swelled or collapsed depending on the pH to change the surface property.[43] They provided a good manner to regulate the properties of the surface by light, but still, have limitations for the whole grafted polymer chains due to the *o*NB-based monomer with side chain photo-responsiveness. Nicholas D. Spencer and co-workers synthesized 3-(2-bromo-2-methylpropanamido)-3-(2-nitrophenyl)propanoic acid (BMNP) as a photocleaved initiator and immobilized it onto a Si surface via an amino silane linker. Poly(lauryl methacrylate) (PLM) and poly(styrene) (PS) polymers were then grafted on flat silicon surfaces via SI-ATRP, which could be cleaved off under UV irradiation. The molecular weight and PDI of the cleaved grafted polymers were characterized using size-exclusion chromatography (SEC). It was found that the grafting density of PLM is lower than PS, which was attributed to the longer side chains of PLM for causing steric interactions between neighboring chains.[58] In their system, the immobilization of the photocleavable ATRP initiator (BMNP) was relied on (3-aminopropyl) triethoxysilane (APTES), a siloxane coupling agent, which has some limitations for only Si based substrates. The single photosensitive unit always provided limited opportunities to control different material properties independently. To avoid these limitations, in this chapter, I first prepared an orthogonal surface by utilizing *o*-nitrobenzyl unit (caged surface) in terms of polymer brushes. Under my concept, a robust and facile method for regulating the growth and the removal of polymer brushes independently has been developed by switching light wavelength with combination of $Mn_2(CO)_{10}$ and NO_2-BDAM as photo-sensitive chromophores. The study reveals that the photo-triggered growth and detachment of polymer brushes with wavelength-selectivity is a versatile and efficient method to graft different monomers on various substrates, thus can be used for regulating surface property.

2.4 Conclusion

I have developed a novel wavelength-selective approach to modify surfaces by finely controlling the growth and detachment of polymer brushes, based on the combination of $Mn_2(CO)_{10}$ and NO_2-BDAM. When visible light (460 nm) was used to trigger the formation of polymer brushes, these grown polymer chains could be finely removed by UV light (360 nm). Although the photo-induced polymerization follows a free radical polymerization manner, the structure of polymer brushes can be controlled by monomer concentration (length of polymer chains) and irradiation energy (grafting density). This method can be applied with different monomers on various substrates. Moreover, one-step and two-steps patterns could be prepared. Therefore, this research provides a facile pathway of light-triggered attachment and detachment of polymer chains on material surfaces and opens new opportunities for the applications on functional surface coatings, tunable surface topologies, reactive interface engineering, photodegradable materials, and photo-induced releasing systems.

2.5 Materials and methods

2.5.1 Chemicals and materials

Silicon wafers were obtained from Si-Mat Silicon Materials, Landsberg/Lech, Germany. Gold-coated Silicon wafers (100 nm of gold deposited on a 7 nm titanium adhesion layer) and Ti-coated silicon wafers (50 nm of titanium deposited on the surface) were cut into 0.5 cm x 1.0 cm pieces. Quartz microscope slides (SiO_2) were obtained from TED PELLA, USA, and cut into 1.0 cm x 1.0 cm pieces before being used. Dimanganese decacarbonyl ($Mn_2(CO)_{10}$, 98 %), dopamine hydrochloride (DA·HCl, 98.5 %), sodium nitrite ($NaNO_2$, 98.5 %), sulfuric acid (H_2SO_4, 98 %), Sodium periodate ($NaIO_4$, 99.8 %), 2-bromoisobutyryl bromide (BIBB, 98 %), and trimethylamine (TEA, 99.5 %) were purchased from Sigma-Aldrich and used as received. *N*-isopropylacrylamide (NIPAAm, Sigma-Aldrich, 99 %) was recrystallized

from a toluene/hexane solution (1/1, v/v) and dried under vacuum prior to use. Acrylic acid (AA, Sigma-Aldrich, 99 %) and Butyl acrylate (BA, Sigma-Aldrich, 99 %) were purified by aluminum oxide to remove inhibitors before being used. Other solvents like methanol (MeOH), dichloromethane (DCM), *N,N*-dimethylformamide (DMF), ethyl acetate (EA), acetonitrile (ACN), toluene and hexane were purchased from Sigma-Aldrich and used directly.

2.5.2 Instrument

The purification of the 6-nitrodopamine was performed with a HPLC JASCO 4000 (Japan) equipped with a diode array, UV-Vis detector, and fraction collector. The combination of solvent A (MilliQ water + 0.1% TFA) and solvent B (95% CAN + 5% MilliQ water + 0.1% TFA) were used as the solvent gradients and the procedure was typically over 40 min duration. ^{1}H NMR and ^{13}C NMR spectra were recorded on a Brucker 300 MHz spectrometer, using tetramethylsilane (TMS) as an internal standard (Varian) and dimethyl sulfoxide-d6 (DMSO-$_{d6}$) as the solvent. The number-average molecular weight (Mn) and polydispersity index (Mw/Mn, PDI) of polymers were measured by a Agilent HPC 1100 gel permeation chromatography (GPC) system using a PSS-GRAM pre-column with a series of PMMA as standard samples. Mass spectra were carried out on an Agilent LC/MSD SL. Ultraviolet-visible (UV-vis) spectra were recorded with a Varian Cary 4000 (UV/Vis) spectrometer (Varian Inc. Palo Alto, USA). The chemical compositions of the pristine and modified surfaces were determined using an ESCALAB MK II X-ray photoelectron spectrometer (XPS, VG Scientific Ltd., England). The thicknesses of the grafted polymers on the Silicon, Gold, and Titanium surfaces were determined using the α-SE spectroscopic ellipsometer (J.A. Woollam Co. Inc., USA). Optical microscope images were acquired from a Nikon ECLIPSE LV100ND. The water contact angles of the surfaces were measured with a SL200C

optical contact angle meter (Solon Information Technology Co. Ltd., China). The LED-UV monochromatic lamps LTPR 460 (460 nm, 3.36 mW/cm^2) and LTPR 360 (360 nm, 0.62 mW/cm^2) (OPTO Engineering, Germany) were used to activate the grafting polymerization and cut off the polymers from the surface respectively.

2.5.3 Synthesis of 2-bromo-N-(2-nitro-3, 4-dihydroxyphenethyl)-2-methylpropanamide (NO_2-BDAM)

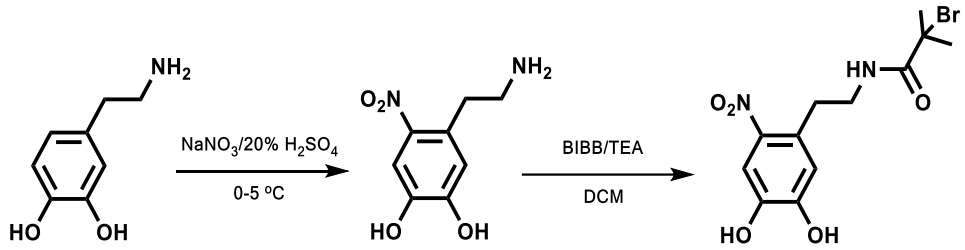

Scheme 1. Synthetic scheme of NO_2-BDAM.

NO_2-BDAM was synthesized by a two-step reaction. Firstly, 6-nitrodopamine was prepared according to previously reported protocols.[92] Briefly, to a cooled solution of dopamine hydrochloride (DA, 0.5 g, 2.63 mmol) and Sodium nitrite ($NaNO_2$, 0.63 g, 9.13 mmol) in water (15 mL) was added 20 % sulphuric acid (H_2SO_4, 2.5 mL) under vigorous stirring. Yellow precipitation formed. After collected by filtration, the precipitation was washed with cold water and cold methanol. The analytical pure 2-nitrodopamine was obtained by HPLC using gradient 0% B-100% B as yellow crystalline solid (546 mg, 70%).

And then, 6-nitrodopamine (0.2 g, 0.54 mmol) was dissolved in anhydrous DCM (50 mL) and triethylamine (6 mL) under nitrogen protection. 2-Bromoisobutyryl bromide (0.23 g, 1 mmol) was added to the solution and the mixture was stirred at room temperature for 2 hours. Ethyl acetate (100 mL) was added and then the organic layer was washed sequentially with HCl solution, water, saturated $NaHCO_3$ and dried over Na_2SO_4. After filtration, the organic solvent was removed and the product was purified

by flash column chromatography (EA/DCM: 50/50, v/v). A yellow solid product was obtained with a yield of 67 %.

^{1}H NMR (DMSO-$_{d6}$, δ, ppm): 10.32 (s, 1H, -C-O*H* aromatic), 9.73 (s, 1H, -C-O*H* aromatic), 8.09 (t, 1H, -CH_2-N*H*-), 7.49 (s, 1H, - C*H*- aromatic), 6.67 (s, 1H, - C*H*- aromatic), 3.32 (t, 2H, - C*H*$_2$-CH_2-), 2.96 (t, 2H, - C*H*$_2$-CH_2-), 1.81 (s, 6H, - C*H*$_3$-C-).

^{13}C NMR (DMSO-$_{d6}$, δ, ppm): 171.14, 151.68, 144.32, 139.87, 128.42, 119.19, 112.71, 61.15, 39.48, 32.97, 31.62.

LC-MS (*m/z*): (M + H^+) calculated 346.0, found, 347.1.

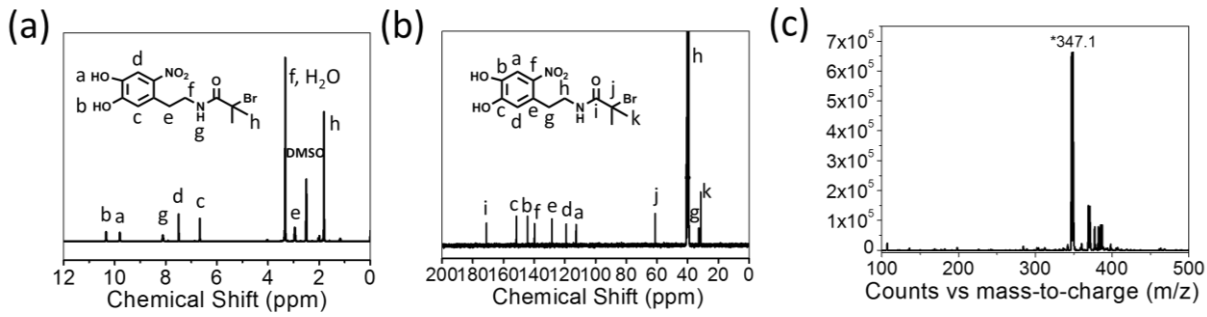

Figure 10. (a) ^{1}H NMR, (b) ^{13}C NMR and (c) LC-MS spectrum of NO_2-BDAM.

2.5.4 Preparation of alkyl bromide anchored surfaces

Before the immobilization of the alkyl bromide, Si and SiO_2 were cleaned by sonication in acetone and ethanol for 2 min, dried under the stream of nitrogen then treated in an air plasma chamber (0.3 mbar, 10 min). Au substrates were washed with water and ethanol, followed by air plasma treatment for 30 s. All the cleaned substrates (Si, Au, SiO_2) were immersed in dopamine solution (pH = 8.5, 10 mg/mL) for 30 min, washed with water and ethanol, then continued immersed in NO_2-BDAM solution (1 mg/mL) for at least 24 h with $NaIO_4$ as the oxidizing agent. After dip coating, the substrates were removed, rinsed successively with deionized water and ethanol, and dried under a stream of nitrogen (denoted as Si-Br, SiO_2-Br, and Au-Br).

Ti substrates were firstly sonicated in ethanol, acetone, and isopropanol, respectively, followed by drying under a stream of nitrogen. The substrates were immersed directly

in NO_2-BDAM solution (1 mg/mL) for 24 h at room temperature. After that, the substrates were washed with water and ethanol, dried under nitrogen (denoted as Ti-Br).

2.5.5 Visible light-initiated surface grafted polymerization

Surface grafted polymerization was carried out in a sealed flask under 460 nm LED irradiation. Grafting PNIPAAm on the Si surface was taken as an example. Firstly, NIPAAm (various amounts) and $Mn_2(CO)_{10}$ (0.1 mg, 0.25 μmol) were placed in a flask containing 1 mL methanol, and then the bromide anchored substrates were placed in the bottle and sealed with a rubber septum. The system was deoxygenated by bubbling nitrogen gas for 20 min then irradiated with a 460 nm monochromatic LED lamp for 1 h. After polymerization, the PNIPAAm grafted substrates were rinsed with ethanol and dried under a stream of nitrogen.

“On-off” irradiation experiments were conducted as follows: 10 mL methanol solution containing NIPAAm (5.085 g, 45 mmol) and $Mn_2(CO)_{10}$ (1 mg, 0.0025 mmol) were firstly bubbled to remove the oxygen, then which was transferred to cover the Si-Br substrates in a small flask carefully by syringe. After that, the solution-covered Si-Br substrates were irradiated for 1 min under a 460 nm LED lamp then washed by ethanol, dried with nitrogen gas to obtain Si-PNIPAAm-1 sample. To prove that turning off light irradiation after reaction would quench the polymerization, another sample was exposed to 460 nm light for 1 min then stored in dark for 10 min, followed by washed with ethanol and dried with nitrogen gas to get the Si-PNIPAAm-dark-1 surface. A similar procedure was applied to the second-time reaction with 2 min irradiation from Si-PNIPAAm-1 to obtain Si-PNIPAAm-2 and Si-PNIPAAm-dark-2, respectively. By varying the irradiation period to 5 min and 8 min with a similar strategy can be used for fabricating Si-PNIPAAm-3, Si-PNIPAAm-dark-3, Si-PNIPAAm-4, and Si-PNIPAAm-

dark-4, respectively.

Moreover, to demonstrate the versatility of this method, Si wafers were chosen as the model substrate to tether different functional monomers. AA (280 mg, 4 mmol) and BA (890 mg, 7.0 mmol) could be also applied to coat Si surface in a similar way above. PNIPAAm grafted different kinds of substrates, including Au, SiO_2, and Ti, could also be supported by this method.

2.5.6 Visible light-initiated polymerization of PNIPAAm in solution

NIPAAm (508.5 mg, 4.5 mmol), $Mn_2(CO)_{10}$ (0.0234 mg, 0.06 μmol), Ethyl α-bromoisobutyrate (EBIB, 0.0585 mg, 3 μmol) and 3 mL DMF were added into a 25 mL round bottle flask, then the solution was deoxygenated for 30 min before subjected to be irradiated with visible light. Polymers at reaction times of 3, 5, 7, 10, 20, and 30 min irradiation time were obtained respectively, which were precipitated in ten folds excess diethyl ether and then dried under reduced pressure. The resulting samples were dissolved in DMF (1 mg/mL) for GPC measurement.

2.5.7 UV light-mediated detachment of polymer brush from substrates

Polymer grafted substrates were placed on a small stand in a dish with a gentle stirring of water, and then were exposed to a LED light source (LTPR 360, 360 nm, 0.62 mW/cm^2) for photocleavage. After irradiation, the substrates were washed with ethanol and dried under a stream of nitrogen.

To obtain enough detached polymers for GPC measurement, PNIPAAm brushes grafted Ti substrate (Scale: 4 cm × 4 cm) was used to undergo photolysis by the above method overnight. Then polymers were collected and freeze-dried, which were then dissolved in 0.4 mL of DMF for GPC measurement.

2.5.8 Creating surface patterns through one-time and two-time engineering approach with wavelength-selectivity

One-time surface patterning process was conducted in a glass box. Firstly, NIPAAm (30.8 mg, 0.272 mmol) and $Mn_2(CO)_{10}$ (0.1 mg, 0.00025 mmol) were dissolved in 100 uL DMF, which could be used directly without degassing. Then 20 μL of the above solution was pipetted onto Si-Br or Ti-Br wafer, followed by covering it with a glass coverslip to form a thin layer of solution between the coverslip and wafer. A photomask (50 μm transparent strips with a gap of 150 μm and 200 μm transparent strips with a gap of 200 μm or 50 × 50 μm transparent squares with a gap of 50 μm) was placed on the coverslip and flushed with the substrate. After that, a glass plate was placed on the box and the edges were sealed by grease and the whole box was purged with argon for 10 minutes. Then the sample was irradiated with 460 nm monochromatic LED lamp for 15 min. The wafer was then removed from the apparatus and thoroughly rinsed with ethanol and water before dried with a stream of nitrogen to obtain a patterned surface (one-step approach).

The vertical strips patterned surface could be further exposed under 360 nm monochromatic lamps with a photomask (200 μm transparent strips with a gap of 200 μm or 50 × 50 μm transparent squares with a gap of 50 μm) on the substrate to obtain two-steps patterned surface.

Chapter 3

3. In situ variation of double network topology using wavelength-selective photolabile connector

This chapter describes a photo-controlled approach to in situ regulate the network topology of an elastomeric double network and the investigation of the effect of topology variation on mechanical properties. The approach is based on an orthogonal light-responsive inimer, vinyl-*o*NB-Br (2-((2-bromo-2-methylpropanoyl)oxy)ethyl 4-(4-(1-(acryloyloxy)ethyl)-2-methoxy-5-nitrophenoxy) butanoate). Vinyl-*o*NB-Br is composed of three functional moieties, i.e., acrylate-based double bond for incorporation within a network, Br group for further photo-induced grafting polymerization, and *o*NB moiety for photocleaving. This inimer was first used as a co-monomer to prepare a poly(di(ethylene glycol)ethyl ether acrylate) (l-PDEEA) elastomer. After soaking this elastomer into a mixture containing monomer, crosslinker, and photoinitiator, a connected-double network (c-DN) elastomer can be formed under visible light irradiation. By changing the light wavelength from visible light (460 nm) to UV light (365 nm), the obtained c-DN structure can be turned into a disconnected-double network structure (d-DN) as consequence of the photolysis of *o*NB moiety. This in situ variation of the polymer network topology results in a change in the toughness of the material, which is investigated.

3.1 Introduction

Polymer network topology, determined by the ways of the connection between network chains and crosslinked points, is an important parameter in designing advanced materials for various applications in soft actuators, self-healing materials, adhesives, and energy materials.[158-161] Crosslinked materials with different polymer network

topologies, for example, featuring different network branch functionalities,[162-164] topological polymer chains,[165-167] and multi-network topology,[168-169] show distinct mechanical properties, network dynamics, and defect tolerance.[170-172] Multi-network topologies are used to improve the mechanical properties of elastomeric polymer networks. Double network (DN) materials are one of the representative examples. They are composed of a rigid first network with densely-crosslinked structure, and a soft second network made of loosely-crosslinked long chains.[169] As the DN network is stretched, the rigid network breaks and serves as a sacrificial structure to dissipate energy while the soft network sustains stress. Thus, compared with single network materials, DN materials show high fracture strength. For example, the DN structure hydrogel consisting of poly(2-acrylamido-2-methylpropanesulfonic acid) (PAMPS gels, rigid first network) and polyacrylamide (PAAm gels, soft second network), shows anomalously high fracture energy (~1000 J/m^2) which is 100-1000 times higher than the primary gels (PAMPS gel: ~1 J/m^2 and PAAm gel: ~10 J/m^2).[169] However, during the preparation of the first network, some vinyl groups from the crosslinker of PAMPS network might remain unreacted,[173] which would lead to the formation of a connected-DN (c-DN). Thus the topology-based toughening mechanism of DN materials remains controversial. In 2009, Nakajima et al. firstly questioned the real structure of PAMPS/PAAm DN and proposed how the microstructure topology of DN (c-DN or truly independent-DN, t-DN) affects the mechanical property of DN material (Figure 1). They used photoinitiator (2-Oxoglutaric acid) (OXGA) to eliminate the residual vinyl group formed in the preparation of the first network, and prepared the t-DN structure. With low crosslinking density of the second network, the strength of c-DN is stronger than t-DN as the force can be transferred through the connecting points to realize the energy dissipation.[174] In 2014, Es-haghi et al. claimed that the t-DN prepared by eliminating the residual vinyl group with OXGA is a pseudo t-DN since the

photoinitiator procedure is not of high efficiency. In this case, a thermal initiator (2, 2'-azobis [2-(2-imidazolin-2-yl) propane] dihydrochloride, VA-044) was employed to deactivate the residual vinyl to synthesize t-DN.[175] Then a real t-DN structure hydrogel with weak mechanical property was obtained, which is contrary with the tough pseudo t-DN prepared by Nakajima et al. Although these studies have led to a better understanding of the contribution of the polymer network topology of DN structures to material properties, these reported methods do not allow for systematic investigation of the relationship between specific structure (real connecting fraction) and mechanical property due to the challenge of preparing well-defined connecting DN structures. Moreover, the c-DN and t-DN materials used for properties comparison were prepared independently, which makes the conclusion on the influence of real polymer network topology not convincing enough. Therefore, it is still desirable to develop a material system that can be continuously used for observing the effect of polymer network topologies on mechanical properties. To the best of our knowledge, if the c-DN and t-DN can be converted on the same material in situ, it will give more authentic results about the influence of polymer network topology on its mechanical performance.

In this chapter, a light wavelength-selective approach to control the connecting structure of a DN is described. The approach is based on an orthogonal light-responsive inimer (i.e. vinyl-*o*NB-Br) with multiple functions (Figure 2). Inimers, monomers containing an initiator site for polymerization, allow for post-introduction of secondary polymer into the network[167, 176-177] and have been used to spatially and temporally control the structures and properties of the resulting material.[167, 176-177] Differing from traditional inimers, the vinyl-*o*NB-Br designed here contains a photolabile spacer. Such design permits quantitative modulation of the connection between two networks. In this study, DEEA was used as the monomer to prepare the

first network and the vinyl-*o*NB-Br as the co-monomer (I-PDEEA). The vinyl group was used to synthesize the I-PDEEA elastomer and the synthesis of the DN by grafting a second network from the inimer terminal under 460 nm visible light irradiation. Owing to the connection between the first and second networks, the resulting DN material possesses a c-DN structure. Exposing the formed c-DN elastomer under UV light leads to the converting of network topology from c-DN structure to d-DN structure. The inimer units allow quantitative studies about the influence of DN topology on their mechanical properties. In this work, a small increase in toughness was observed when the double network topology changed from c-DN to d-DN. The number of connecting points showed a negligible influence on the mechanical property of the DN elastomer.

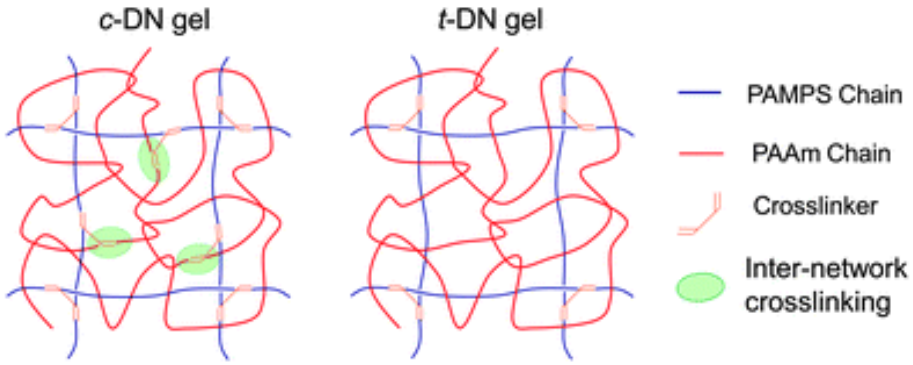

Figure 1. Illustration of chemical structures of connected-DN (c-DN) gels and truly independent-DN (t-DN) gels.[178] Reproduced with permission. Copyrights 2010, The Royal Society of Chemistry.

3.2 Results

3.2.1 Design of light-regulated polymer network topology

The design of light-regulated connection and disconnection of the second network from I-PDEEA is demonstrated in Figure 2a. Vinyl-*o*NB-Br is designed to be incorporated into the crosslinked network for the fabrication of c-DN and d-DN networks. It contains three functional parts: 1) vinyl group that is used to copolymerize with monomer to introduce the Br-based initiator into the skeleton of the first network;

2) the bromine group (Br) that can work together with $Mn_2(CO)_{10}$ to initiate the grafting polymerization to form c-DN under visible light irradiation; 3) photocleavable *o*-nitrobenzyl spacer that is UV light-sensitive and designed for light-triggered debonding of the connecting points to form d-DN in situ. In this case, a dual-wavelength selectivity was expected to independently control the grafting polymerization and debonding.

As shown in Figure 2b, I-PDEEA elastomer was prepared via the copolymerization of DEEA (monomer), 1,6-hexanediol diacrylate (HDDA, crosslinker), and vinyl-*o*NB-Br (inimer) under visible light (460 nm, 10 mW/cm^2) with Irgacure 819 (I-819) as the photoinitiator. Before subjecting it for further use, the residual vinyl groups in IDEEA elastomer were eliminated by the generation of radicals from 2,2'-azobis(2-methylpropionitrile) (AIBN) upon heating.[175] The obtained I-PDEEA was further immersed into a mixture containing DEEA (monomer, 99.795 mol%), HDDA (crosslinker, 0.2 mol%), and $Mn_2(CO)_{10}$ (visible light-sensitive additives, 0.005 mol%) to get a swollen material, followed by being subjected to visible light for 1h irradiation to get DN elastomer. Because the initiation of the secondary polymers is started from the inimer site, the resulting DN elastomer possesses a fully connected double network (c-DN) structure. When a UV light was utilized to cleave the β-position of the o-nitrophenyl ethylene group,[92] the connected second network could be debonded from the first network to form a disconnected double network (d-DN) structure. It is noteworthy that although it is difficult to ensure the formation of a complete disconnected structure,[179] a controllable, gradient decrease in connecting structure can be expected with increasing exposure dose, which should allow understanding of the relationship between polymer network topology and mechanical properties.

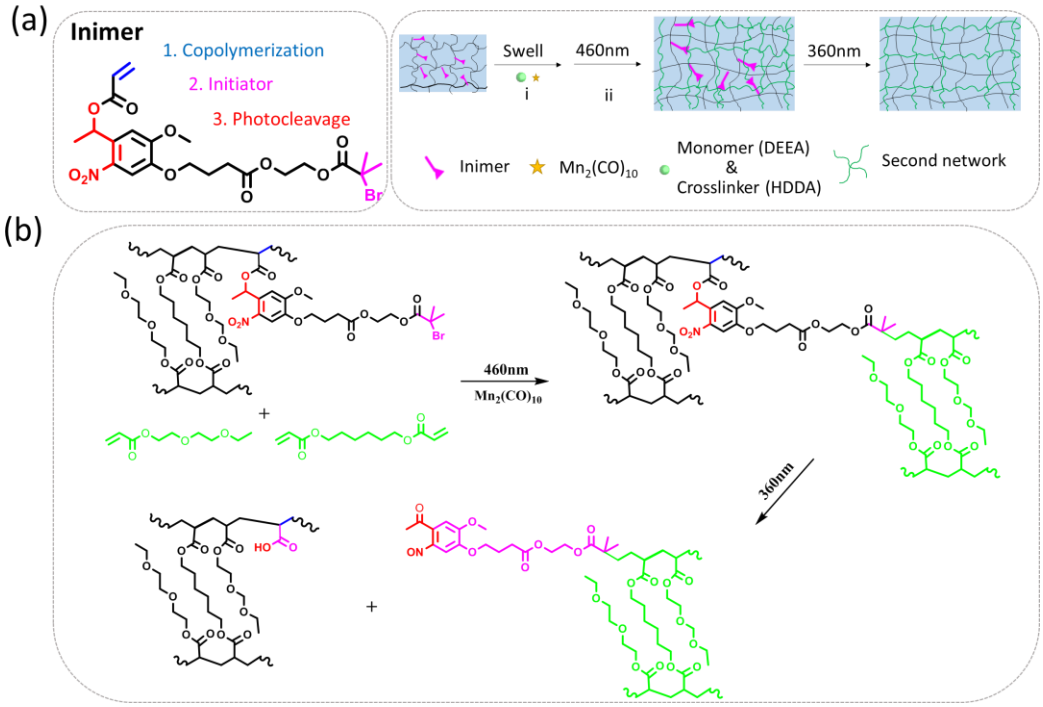

Figure 2. Schematic of light-regulated connection and disconnection of the second network from the I-PDEEA to form c-DN and d-DN topologies. (a) Vinyl-*o*NB-Br, containing three functional moieties, is polymerized together with DEEA, I-819 (photoinitiator), and HDDA (crosslinker) to form an I-PDEEA elastomer. (i) I-PDEEA elastomer was swollen in the mixture of DEEA, HDDA, and $Mn_2(CO)_{10}$. (ii) Connection of second network from the inimer (Magenta) inside I-PDEEA elastomer under 460 nm irradiation (green) to form c-DN structure. (iii) Photolysis of *o*-nitrophenyl ethyl under UV irradiation to form d-DN structure. (b) Chemical structures of components during the connecting and disconnecting process under different light wavelengths.

3.2.2 Photolysis study of $Mn_2(CO)_{10}$ and vinyl-*o*NB-Br

$Mn_2(CO)_{10}$ and vinyl-*o*NB-Br are both light-sensitive molecules. Vinyl-*o*NB-Br is expected to be inert under visible light irradiation used for the polymerization of the inimer-containing first network. To prove this concept, the photostability of vinyl-*o*NB-Br under visible light was studied by UV spectroscopy in solution. As shown in Figures 3a and 3b, irradiation at 460 nm leads to a rapid decrease in the absorption of $Mn_2(CO)_{10}$ at λ_{max} = 349 nm while no change was observed in the absorption spectrum

of vinyl-*o*NB-Br under the same exposure conditions. Even when $Mn_2(CO)_{10}$ has reached nearly 100% photolysis conversion under an irradiation dose of 10.08 J/cm^2, vinyl-*o*NB-Br still keeps 0% under a similar or higher irradiation dose (Figure 3d). These results indicate that 460 nm light could be used to selectively trigger the grafting polymerization of the second network from I-PDEEA without any degradation of the inimer.

Irradiation at 365 nm can be used to induce the decomposition of the vinyl-*o*NB-Br. As shown in Figure 3c, the characteristic absorption of vinyl-*o*NB-Br at 301 nm decreases gradually upon UV irradiation. The decomposition is complete at an irradiation dose of 3.6 J/cm^2 (Figure 3d). This implies that this reaction can be used to convert the c-DN structure into the d-DN structure upon UV exposure. Thus, the multifunctional molecule, vinyl-*o*NB-Br, is a good candidate to investigate the wavelength-selective regulation of the topology and mechanical property of crosslinked materials.

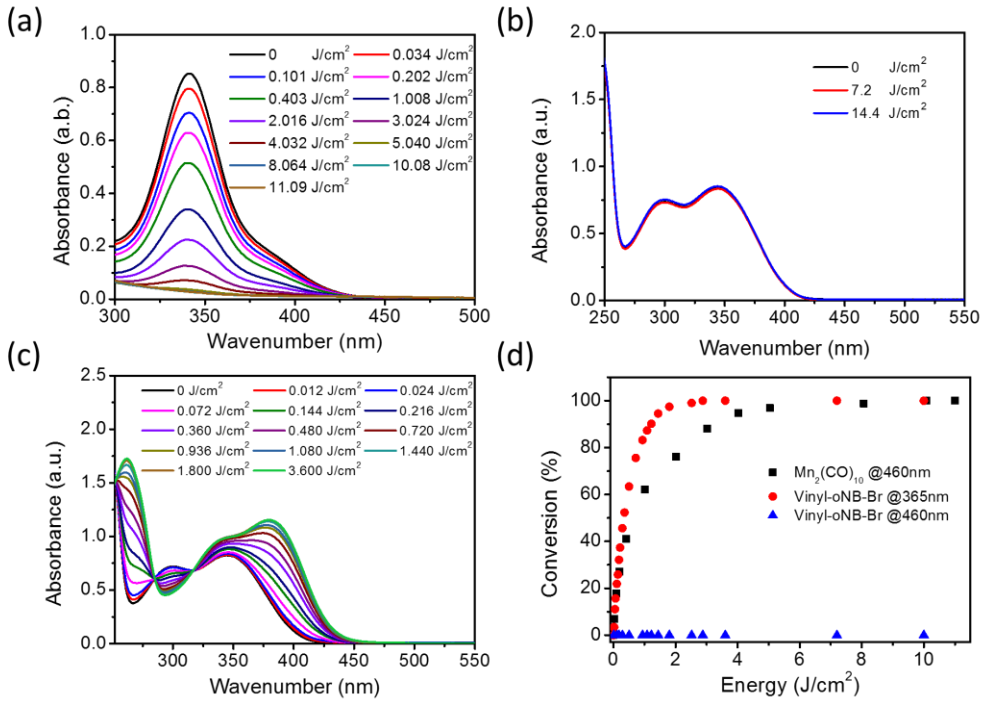

Figure 3. Wavelength-selective activation of chromophores. UV/Vis spectra of (a) $Mn_2(CO)_{10}$ solution during photolysis and (b) vinyl-*o*NB-Br solution during photolysis under 460 nm irradiation. (c) UV/Vis spectra of vinyl-*o*NB-Br solution during photolysis under 365 nm irradiation. (d) Photolysis conversion (%) of $Mn_2(CO)_{10}$ (black square) and vinyl-oNB-Br (red dot and blue triangle) in solution under different irradiation doses at 460 nm and 365 nm. Data were calculated from the absorbance values at λ_{max} = 349 nm and 301 nm by assuming 100% conversion at full photolysis of $Mn_2(CO)_{10}$ and vinyl-*o*NB-Br, respectively. The concentration of $Mn_2(CO)_{10}$ used in (a) and (d) is 5.13×10^{-5} M. The concentration of vinyl-oNB-Br used in (b)-(d) is 1.4×10^{-4} M.

3.2.3 Fabrication of I-PDEEA elastomer

I-PDEEA elastomer was fabricated by copolymerization of DEEA, HDDA, and vinyl-*o*NB-Br (inimer) under visible light (460 nm, 10 mW/cm^2) irradiation with I-819 as the photoinitiator. The crosslinker fraction can be used to tune the crosslinking degree and therefore the mechanical properties of as-prepared elastomers. As shown in Figure 4 and Table 1, when the crosslinker fraction is 0.1 mol%, the Young's modulus is around 95 kPa and the fracture strain is 207%. When increasing the crosslinker fraction to 0.5

mol%, the Young's modulus increased to 253 kPa and the fracture strain decreased to 57%. With a crosslinker fraction of 0.2 mol%, a moderate Young's modulus of 193 kPa and a fracture strain of 144% were obtained. Elastomer with high Young's modulus and low fracture strain is stiff , while the sample with low Young's modulus and high fracture strain is sticky and it is difficult to analyze or further modify it.[180] Therefore, crosslinked materials with the crosslinker fraction of 0.2 mol% were used for further study.

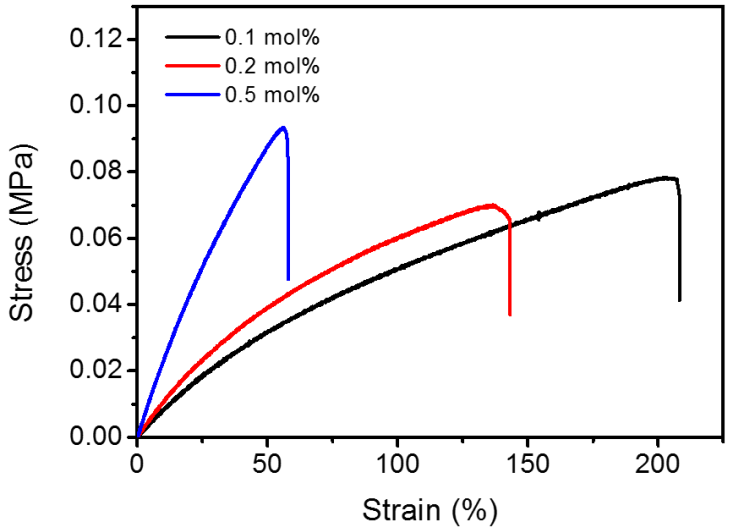

Figure 4. Tensile stress-strain curves of I-PDEEA elastomers with different crosslinker fractions.

Table 1. Young's modulus and fracture strain of I-PDEEA elastomers with different crosslinker fractions. Data are presented as the mean ±SEM (n = 3)

Crosslinker fraction / mol%	Young's Modulus/ kPa	Fracture Strain/ %
0.1	95±21	207±18
0.2	193±15	144±6
0.5	253±15	57±11

It is known that free radical polymerization of acrylic monomers leads to inhomogeneous networks in which some vinyl groups from the crosslinker remain in the cured network.[181-182] To get a well-defined DN structure without unreacted vinyl groups, the residual vinyl groups of the I-PDEEA network were removed by using the

method reported by Es-haghi.[174-175] Briefly, the I-PDEEA elastomer was immersed into DMF solution containing AIBN until equilibrium is achieved under N_2 atmosphere, followed by annealing at 65 ^oC for 5h. After processing with AIBN, the generated large amounts of radicals can react with the vinyl groups. This reaction can be monitored by the disappearance of the stretching vibration mode of the C=C bonds in the FTIR spectrum.[183] As shown in Figure 5, the band at 1630 cm^{-1} was visible after the polymerization, implying the existence of residual double bonds in the as-prepared I-PDEEA elastomer. After treatment with AIBN, the peak disappeared, indicating successful elimination of the residual vinyl groups.

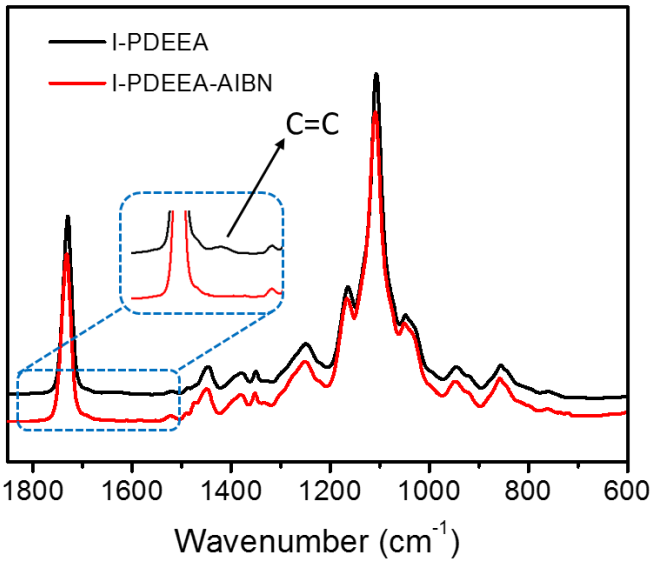

Figure 5. FTIR spectra of I-PDEEA elastomer before and after processing with AIBN to deactivate vinyl unsaturation of HDDA.

3.2.4 Connecting and disconnecting of the second network from I-PDEEA elastomer

The AIBN-treated I-PDEEA elastomer with an inimer fraction of 0.2 mol% (DEEA: HDDA: inimer: I-819=1000: 2: 2: 3) was used for further study. The sample was first immersed in the mixture of DEEA monomer, crosslinker, and photoinitiator (denoted

as feed solution, DEEA: HDDA: $Mn_2(CO)_{10}$=20000: 40:1) to get a swollen sample with an obvious increase in material size, followed by visible light (460 nm) irradiation to get the c-DN structure (Figure 6a). The c-DN structured elastomer can be further converted into the d-DN structured material by being exposed to UV light (365 nm). During irradiation, a change in color from colorless to yellow was observed, which was associated to the formation of photocleaved product, *o*-nitrobenzaldehyde, generated from the inimer (Figure 6a).[149] The photolysis process was monitored by UV-vis spectroscopy (Figure 6b). The observed changes in the spectrum of the I-PDEEA elastomer were similar to the changes observed during the irradiation of vinyl-*o*NB-Br in a solution state (Figure 2c), proving that the photolytic reaction corresponded to the cleavage of the *o*-nitrobenzyl group.

The mechanical properties of the elastomers based on these different topologies were then investigated. The as-prepared I-PDEEA elastomer shows a Young's modulus of 170 kPa with a fracture strain of 155 % (Figure 6c). Its toughness, measured as the area under the stress-strain curve, is 0.14 MJ/m^3. The sample with a c-DN structure presents higher Young's modulus (250kPa), fracture strain (240%), and toughness (0.50 MJ/m^3, Figure 6c). The strengthening phenomenon was attributed to the formation of double network topology.[184] When the inimer in the c-DN undergoes photolysis, the connected second network was debonded and a disconnected double network (d-DN) was formed. The reduction of the number of connecting points between the two networks led to an elastomer material with slightly higher fracture strain (265 %) and toughness (0.59 MJ/m^3, Figure 6c). The swelling ratio of d-DN is similar to c-DN (Figure 6d). In a DN, swelling is restricted by the stretching of the first network. The additional crosslinking structure between the first network and the second network does not seem to change the swelling ability and therefore, its disconnection did not induce visible influence on the swelling ratio.

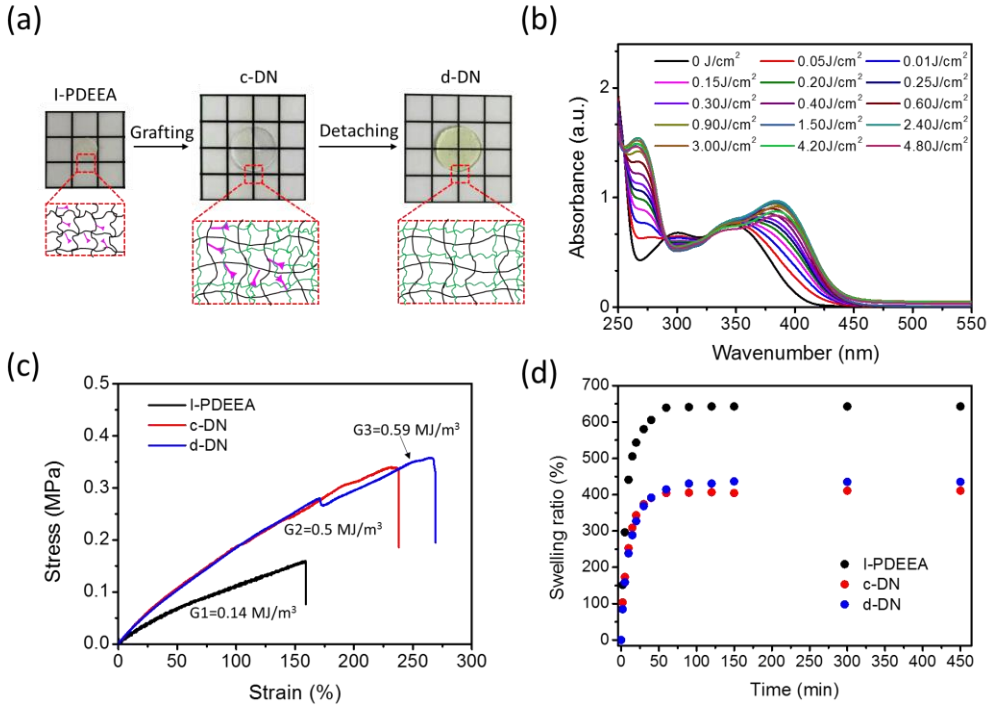

Figure 6. (a) Images of I-PDEEA elastomer, c-DN elastomer, and d-DN elastomer. (b) UV Spectrum of I-PDEEA elastomer after exposure to UV light of 365 nm for different irradiation does. (c) Tensile stress versus strain curves of I-PDEEA elastomer, c-DN elastomer, and d-DN elastomer. (d) Swelling ratio of I-PDEEA elastomer, c-DN elastomer, and d-DN elastomer. The inimer fraction of I-PDEEA used in (a), (b), (c), (d) and (e) is 0.2 mol%.

3.2.5 Influence of connecting degree between two networks on the mechanical property

The connecting degree (number of connecting points) between two networks could be tuned by the UV light irradiation dose. To prepare elastomers with different connecting degrees between two networks, the as-prepared c-DN elastomers were irradiated under UV light for different times to get different photolysis conversions of the inimer-connecting points. A series of samples with photolysis conversions 0, 10, 30, 50, 80, and 100% were used for a systematic study. As shown in Figure 7, increasing photolysis conversion results in a slight increase in toughness, which we associate to a gradual decrease in the connecting degree between the first and second network.

The result indicated that the connection between the first and the second networks did not make an important influence on the mechanical property of the DN elastomer.

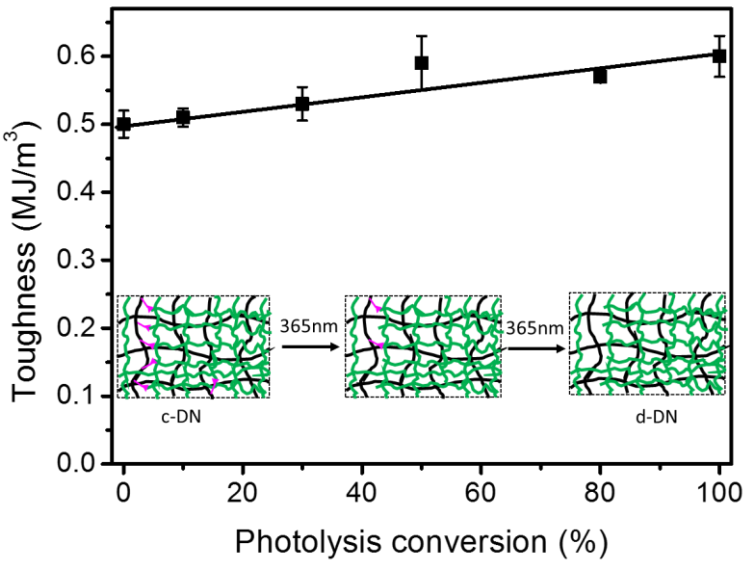

Figure 7. Toughness of DN elastomers from c-DN structure to d-DN structure with different photolysis conversions. Insert images show the topology changing from c-DN to d-DN upon UV irradiation.

3.3 Discussion

DN structure can significantly improve the mechanical property of crosslinked polymer materials including gels and elastomers.[169, 185] For example, PAMPS/PAAm DN gels show high toughness (fracture Energy ~1000 J/m^2) , compared to the single-network hydrogels made from the sample compositions.[169, 186-187] Owing to the network defects resulted from the incomplete radical polymerization, the real topologies of the DN and their influence on mechanical property still need to be explored. Nakajima et al. used excess photo-intiator (OXGA) to consume the residual vinyl groups within the network to form t-DN network.[174] Actually, they obtained a pseudo t-DN due to the inefficient deactivation of residual vinyl group by photoinitiator. To overcome this, Es-haghi and co-workers used a thermal initiator (VA-044) to completely remove the residual vinyl group to get real t-DN.[175] Although these works give a clear description on the real

topology of the DN, the connecting degree between the first and the second networks within the DN materials is hard to precisely control. This issue has been addressed by the multi-functional inimer (vinyl-*o*NB-Br) developed in this chapter. In our DN hydrogel systems, the connecting fraction between two networks is originated from the inimer units. It is well-defined and can be accurately regulated by UV irradiation dose.

The reported studies suggested that the changes in the connectivity between the two networks leading to topological variations change the material's mechanical properties. For example, Nakajima et al found that when the crosslinker fraction of the second network is >0.01 mol%, pseudo t-DN showed a high toughness and was stronger than c-DN.[174] Es-haghi and co-workers demonstrated that the real t-DN hydrogel was much brittler than pseudo t-DN prepared by Nakajima.[175] They concluded that the connection between the two networks within DN materials was good for toughness enhancement. Different results were observed in my study. When the connecting degree decreased from 100% (c-DN) to 0% (d-DN), the toughness increased slightly from 0.5 to 0.59 MJ/m^3, indicating that the connecting degree between the first and the second networks had little influence on material's toughness. This difference may due to different DN systems. In previous polyelectrolyte/PAAm DN hydrogel systems, chemical compositions and structures of the first and the second networks were different, and the c-DN and t-DN materials were different samples. However, in my system, the first and the second networks used within the PDEEA/PDEEA DN elastomer possess the same compositions and chemical structures, meanwhile the in-situ transformation from c-DN to d-DN in the single sample was used for comparison. In the other words, the same sample was used, in which the chemical compositions are the same. Based on these, the conclusion in my system that the connecting degree between two networks of similar properties has negligible influence on their mechanical properties is more convincing.

3.4 Conclusion

I have developed a novel photo-controlled approach to regulate the polymer network topology of the elastomers by varying the connecting structure between the first and the second networks in DN materials. The materials were prepared by incorporating functional inimer (vinyl-*o*NB-Br) into I-PDEEA network. After the I-PDEEA was soaked in the mixture of DEEA, HDDA and $Mn_2(CO)_{10}$, a c-DN structure elastomer could be prepared by the irradiation of visible light. Further exposure of the c-DN elastomer to UV light would in situ convert the c-DN structure to d-DN structure. Both c-DN and d-DN show similar mechanical properties and swelling abilities. Moreover, the connecting degree between two networks can be finely regulated to get a series of products with different connecting structures, but the results indicated that the change in the connecting structure showed a negligible influence on the toughness of DN elastomer.

3.5 Materials and methods

3.5.1 Chemicals and materials

4-[4-(1-Hydroxyethyl)-2-methoxy-5-nitrophenoxy]butyric acid (HO-*o*NB-COOH) (98 %, Sigma-Aldrich), trimethylamine (TEA) (99.5%, Sigma-Aldrich), ethylene glycol (EG) (99.8%, Sigma-Aldrich), pyridine (99.8%, Sigma-Aldrich), acryloyl chloride (AC) (97%, Sigma-Aldrich), tetrahydrofuran (THF) (99.9%, anhydrous, Sigma-Aldrich), 2-bromopropionyl bromide (BIBB) (97%, Sigma-Aldrich), hydrochloric acid (HCl) (36.5-38%, Sigma-Aldrich), sodium bicarbonate ($NaHCO_3$) (99.7%, Sigma-Aldrich), 4-dimethylaminopyridine (DMAP) (99%, Sigma-Aldrich), 1-(3-dimethylaminopropyl)-3-ethylcarbodiimide hydrochloride (EDC·HCl) (98%, Fluka), 1,6-hexanediol diacrylate (HDDA) (99%, Alfa Aesar), dimanganese decacarbonyl ($Mn_2(CO)_{10}$) (98%, Sigma-Aldrich), Irgacure 819 (I-819) (Ciba) were used as received. 2,2'-Azobis(2-

methylpropionitrile) (AIBN) (98%, TCI Deutschland GmbH) was recrystallized from ethanol before use. Di(ethylene glycol) ethyl ether acrylate (DEEA) (98%, TCI Deutschland GmbH) was purified by passing through a column of neutral alumina to remove the inhibitors before being used. Acetonitrile was purchased from Fluka. Other solvents like dichloromethane (DCM), petroleum ether (PE), ethyl acetate (EA), and acetone were purchased from ABCR and used without any treatment. Deionized water was purified with minimum resistivity of 18.2 MΩ cm^{-1}.

3.5.2 Instruments

The purification of the products was performed with a HPLC JASCO 4000 (Japan) equipped with a diode array, UV-Vis detector, and fraction collector. The combination of solvent A (MilliQ water + 0.1% TFA) and solvent B (95% ACN/ 5% MilliQ water + 0.1% TFA) was used as the solvent gradients and the procedure was typically over 40 min duration. ^{1}H NMR and ^{13}C NMR spectra of the products were recorded using a Bruker Advance 300 MHz nuclear magnetic resonance equipment at 25^{o}C and chloroform-d ($CDCl_3$, δ_H = 7.26 ppm) was used as the solvent. Mass spectrometry was carried out on an Agilent Technologies 1260 Infinity Liquid Chromatography/Mass Selective Detector (LC/MSD). Ultraviolet-visible (UV-vis) spectra were obtained from a Varian Cary 4000 UV/Vis spectrometer (Varian Inc. Palo Alto, USA). Optical images of as-prepared single network elastomer, c-DN elastomer, and d-DN elastomer were recorded by NIKON camera. The polymerization of the elastomer and photolysis procedure were conducted using blue 460 nm and UV 365 nm collimated LED light (Olympus BX & 1X, 1700 mA) bought from THORLABS, and during the experiments, the intensity was set as 10 mW/cm^2. FTIR spectroscopy was used to characterize residual vinyl unsaturation of l-PDEEA elastomer. A Nicolet 6700 FTIR spectrometer was used and the results were obtained with 64 scans and a resolution of 4 cm^{-1}.

3.5.3 Synthesis of photolabile initiator

3.5.3.1 Synthesis of 2-Hydroxyethyl 2-Bromopropionate (HEBiB)

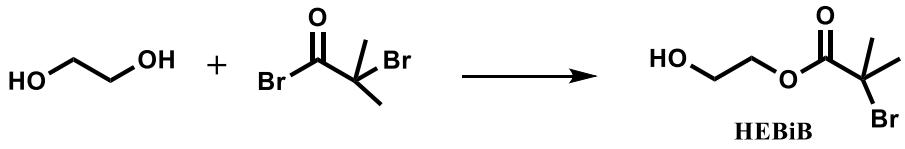

Scheme 1. Synthetic route of 2-Hydroxyethyl 2-Bromopropionate (HEBiB)

Anhydrous ethylene glycol (139.31 g, 2.02 mol) and pyridine (3.6 mL, 42.35 mmol) were diluted with dry THF (60 mL). The reaction mixture was cooled to 0 ^{o}C in an ice bath, and a solution of 2-bromopropionyl bromide (5 mL, 40.45 mmol) in dry THE (50 mL) was added dropwise. The mixture was stirred in the cooling bath for 1 h and then overnight at room temperature. The reaction solution was then acidified to pH = 2 with concentrated HCl, and extracted with DCM (3 x 100 mL). The organic fractions were washed with saturated $NaHCO_3$ solution, and evaporated to remove the solvent. The crude product was purified by silica gel column chromatography (PE / EA =1:1) to give colorless liquid. (Yield = 71.2 %) of a colorless liquid.

^{1}H NMR ($CDCl_3$, δ, ppm): 4.32 (t, 2H, HO-CH_2-CH_2-), 3.91 (t, HO-CH_2-CH_2-), 1.97 (s, 6H, - CH_3-C-Br), 2.06 (s, 1H, -O*H*).

^{13}C NMR ($CDCl_3$, δ, ppm): 171.65, 67.67, 61.05, 55.74, 30.70.

LC-MS (*m/z*): (M + Na^+) calculated 211.0, found, 211.2.

3.5.3.2 Synthesis of 2-((2-bromo-2-methylpropanoyl)oxy)ethyl 4-(4-(1-(acryloyloxy)ethyl)-2-methoxy-5-nitrophenoxy)butanoate (vinyl-oNB-Br)

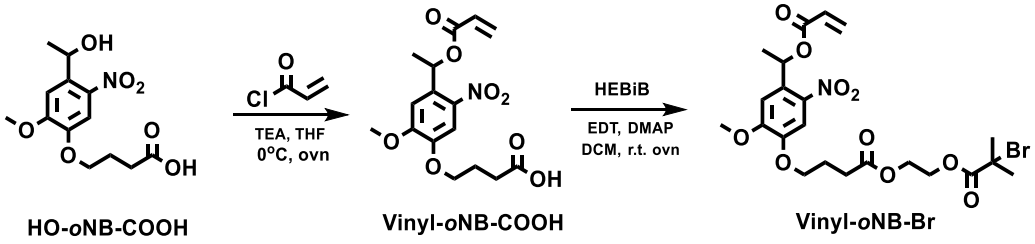

Scheme 2. Synthetic route of vinyl-*o*NB-Br.

First, the 4-(4-(acryloyloxymethyl)-2-methoxy-5-nitrophenoxy) butanoic acid (vinyl-*o*NB-COOH) was synthesized following a previously published procedure. Briefly, 4-[4-(1-hydroxyethyl)-2-methoxy-5-nitrophenoxy]butyric acid (HO-*o*NB-COOH, 150 mg, 0.5 mmol) and triethylamine (210 µL, 1.5 mmol) were dissolved in dry DCM (3 mL) at room temperature under N_2 atmosphere. The solution was cooled to 0°C with an ice bath, then acryloyl chloride (102 µL, 1.25 mmol) diluted with 1 mL dry DCM was added dropwise and reacted at room temperature overnight. The solution was then washed sequentially with $NaHCO_3$ (5 w/v % aq), dilute HCl (1 v/v % aq), and water. After that, the DCM was removed by pressure-reduced evaporation, followed by dissolving the product in an aqueous acetone solution (acetone: water =1:1) and then being stirred for 24h. Extract the reaction mixture with DCM and washed with diluted hydrochloric acid (1 v/v % aq) and water. The final product was purified by preparative HPLC (method: 30 B to 95 B, 360 nm) to obtain a pale yellow powder (124mg, Yield: 70%). The spectroscopic characterization data matched the values reported in the literature.

^{1}H NMR ($CDCl_3$, δ, ppm): δ 9.15 (s, 1H, COO*H*), 7.60 (s, 1H, - C*H*- aromatic), 7.03 (s, 1H, - C*H*- aromatic), 6.55 (m, 1H,-C*H*-CH_3), 6.45 (d, 1H, ,-CH=CH_2), 6.17 (t, 1H, ,-C*H*=CH_2), 5.88 (d,1H, -CH=CH_2), 4.14 (t, 2H,-CH_2-CH_2-CH_2-), 3.92 (s, 3H,-O-CH_3), 2.62 (t, 2H, -CH_2-CH_2-CH_2-), 2.19 (m, 2H, -CH_2-CH_2-CH_2-), 1.66 (d, 3H,-CH-CH_3).

LC-MS (*m/z*): (M + NH_4^+) calculated 371.0, found, 371.14.

The 2-((2-bromo-2-methylpropanoyl)oxy)ethyl 4-(4-(1-(acryloyloxy)ethyl)-2-methoxy-

5-nitrophenoxy) butanoate (vinyl-*o*NB-Br) was obtained by the esterification of vinyl-*o*NB-COOH with HEBiB and the synthesis procedure was conducted as followed: 4-(4-(acryloyloxymethyl)-2-methoxy-5-nitrophenoxy)butanoic acid (350 mg, 1 mmol), DMAP (36.6 mg, 0.3 mmol) and EDC·HCl (575 mg, 3 mmol) were dissolved in DCM (30 mL) under N_2 atmosphere. HEBiB (175 μL, 1.2 mmol) was added to the solution and the mixture was stirred overnight at room temperature. The solvent was then removed and the product was purified using HPLC (method: 30 B to 95 B, 360 nm). A viscous yellow liquid was obtained (327 mg, Yelid: 60%).

^{1}H NMR ($CDCl_3$, δ, ppm): 7.61 (s, 1H, - C*H*- aromatic), 7.01 (s, 1H, - C*H*- aromatic), 6.53 (m, 1H, -C*H*-CH_3), 6.43(d, 1H, -CH=C*H*$_2$), 6.17 (m, 1H, -C*H*=CH_2), 5.88 (d,1H, -CH=C*H*$_2$), 4.39 (s, 4H, -C*H*$_2$-C*H*$_2$-), 4.12 (t, 2H,-C*H*$_2$-CH_2-CH_2-), 3.94 (s, 3H,-O-C*H*$_3$), 2.59 (t, 2H, -CH_2-CH_2-C*H*$_2$-), 2.19 (m, 2H, -CH_2-C*H*$_2$-CH_2-), 1.93 (s, 6H, -C-C*H*$_3$), 1.67 (d, 3H,-C*H*-CH_3).

^{13}C NMR ($CDCl_3$, δ, ppm): 172.47, 171.29, 167.83, 153.97, 147.01, 139.56, 133.30, 131.39, 129.29, 109.97, 68.80, 68.09, 63.41, 62.11, 56.21, 55.39, 30.65, 30.43, 24.18, 22.01.

LC-MS (m/z): calculated for $C_{22}H_{28}BrNO_{10}$ ($M+NH4^+$), 564.0; found, 564.8.,

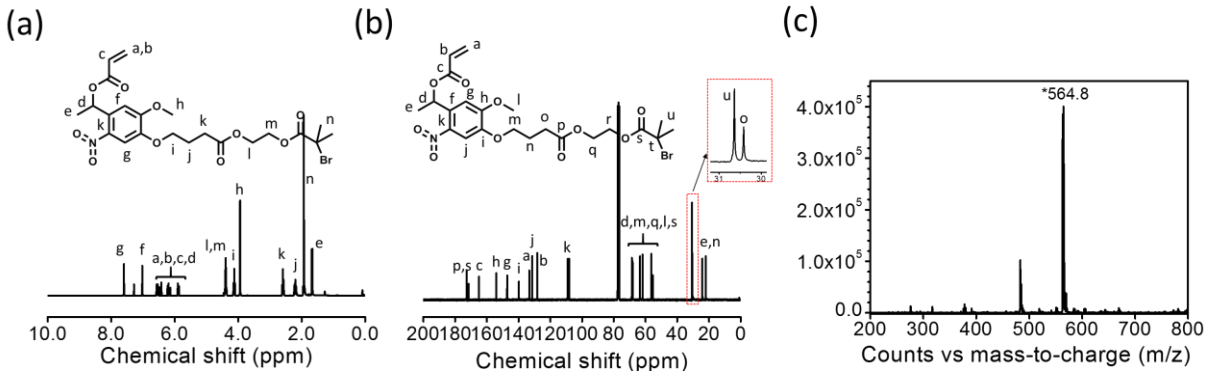

Figure 7. (a) ^{1}H NMR and (b) ^{13}C NMR and (c) Mass spectra of the vinyl-*o*NB-Br.

3.5.4 Preparation of the first network with the inimer inside (I-PDEEA elastomer) by photopolymerization

Taking the sample I-PDEEA-0.2% as an example: DEEA (monomer, 100 mol %), HDDA (crosslink-linker, 0.2 mol %), vinyl-*o*NB-Br (inimer, 0.2 mol %), and I-819 (photoinitiator, 0.3 mol %) were mixed to get the precursor solution. The precursor solution was bubbled with N_2 gas for 20 min to remove the oxygen before use. To get a well-defined material, the precursor solution was coated on a Teflon template (cut from PTFE film, thickness: 230um) covered by a glass slide. The sample was then subjected to a lamp of 460 nm (Intensity: 10mW/cm^2) for 30min to get a thin film (thickness: 230um). After the photopolymerization, the elastomer was peeled off from the glass and immersed in ethanol to remove the unreacted specimens and the ethanol solution was changed every 6 h (4 times). Then it was dried in a vacuum oven to afford the first network (I-PDEEA).

3.5.5 Eliminate the vinyl unsaturation of I-PDEEA elastomer with AIBN

The residual double bonds in the as-prepared I-PDEEA elastomer were deactivated by 2,2'-azobis(2-methylpropionitrile) (AIBN). First, AIBN (164 mg, 1 mmol) was dissolved in 10 mL DMF and it was deoxygenated with N_2 gas for 20min. Then the I-PDEEA elastomer was immersed into the solution for 24h until equilibrium swelling was achieved. Finally, the whole bottle was heated to 65^{o}C for 5h. The sample was removed from the solution and cooled to room temperature, after that the sample was washed at least 8 times with ethanol and DMF alternately to remove the excess initiator, immersed in every solvent for at least 6h then dried in a vacuum oven. The swelling and heating process were conducted in a glove box.

3.5.6 Visible light-induced grafting polymerization of the second network (c-DN elastomer)

To obtain the c-DN, the l-PDEEA elastomer which has deactivated the residual double bonds was immersed in the new deoxy precursor solution which consisted of DEEA (monomer, 99.795 mol %), HDDA (crosslinker, 0.2 mol %) and $Mn_2(CO)_{10}$ (photo-sensitive additive, 0.005 mol %) for 24h to obtain a fully swollen sample. Before conducting photopolymerization, the elastomer was wiped by tissue to remove the excess solution and then exposed to 460nm light (intensity: 10 mW/cm^2) for 30min. The swelling and polymerization processes were conducted in a glove box. Then c-DN elastomer was washed with ethanol four times to remove the unreacted specimens. Then dried in a vacuum oven.

3.5.7 UV light-induced detachment of the second network (d-DN elastomer)

c-DN elastomer was converted into d-DN elastomer using UV light irradiation. Briefly, the sample was placed on the PTFE plate and exposed to 365nm UV light (intensity 10 mW/cm^2). After 2h irradiation, the sample was turned over for another 2h irradiation to make the full cleavage of the second network.

Chapter 4

4. Regulation of the mechanical properties of an elastomer with tunable bottlebrush network topology

In this chapter, the mechanical properties of poly(di(ethylene glycol)ethyl ether acrylate) (l-PDEEA) elastomers are phototuned by light-triggered grafting on and cleavage of the network. The dual photoresponsive inimer vinyl-*o*NB-Br was first polymerized to form the first network. In a second step, PNIPAAm brushes were grafted at alkyl Br site of the inimer side chain units by photoinitiation at 460 nm light using $Mn_2(CO)_{10}$ as photo-sensitive additive forming a bottlebrush-like network topology. The grafted PNIPAAm brushes were detached by exposure at 365 nm, which photocleaves the *o*-nitrophenyl ethyl group to generate a semi-interpenetrating polymer network (SIPN) topology. Further removal of the detached PNIPAAm chains from the system leads to the formation of a polymer network topology structure similar to the original topology. The grafting efficiency of PNIPAAm brushes was studied by varying the monomer concentrations or the inimer fractions. The mechanical properties of the elastomers with different topologies were compared with the PDEEA/PNIPAAm co-network elastomer which has the same chemical composition, demonstrating the topological effect on the mechanical property of elastomers.

4.1 Introduction

Bottlebrush polymer network topologies are structures of crosslinked bottlebrush polymers. They provide elastomers and hydrogels with high deformability and high flexibility.[188-189] The steric repulsion between the side polymer chains pushes the main chain to adopt a stretched conformation and prevents side-chain fusion while maintaining elasticity.[190] This specific architecture makes bottlebrush-based networks

really soft,[188, 191] demonstrating emerging applications from sensitive pressure sensor,[192] efficient dielectric actuators,[193] biomimetic materials,[194] and photonic crystals.[195] However, most bottlebrush networks are prepared by crosslinking of the bottlebrush polymers (Figure 1a). In this method, it is difficult to regulate network topology, such as to change the length or density of the side chains.

A grafting-from method has been developed by Matyjaszewski and co-workers, which involves the use of HEMA-iBBr (inimer, Figure 1b). In their method, the latent initiator sites of inimer units are used for post-modifying the network by in-situ grafting-from polymerization, forming bottlebrush network elastomers.[167, 177] They have prepared a bottlebrush elastomer with poly(butyl methacrylate) (PBMA) as the backbone and poly(butyl acrylate) (PBA) as the side chains. They found that the Young's modulus of the elastomer decreased with PBA grafted, due to the low glass transition temperature (T_g) side PBA chains. This method is facile and effective, in which the mechanical property of the elastomer can be regulated by grafting different polymers. However, it does not allow for precise regulation of network topology after fabricated, for example, further tuning the obtained bottlebrush network topology to SIPN by using the inert inimer.

In this chapter, the multifunctional inimer vinyl-*o*NB-Br, presented in previous chapter, will be used to introduce bottlebrush structures into polymer networks for a gradual regulation of the network topology of an elastomer. The grafting and detachment of polymer brushes on the network will change the network topology from bottlebrush-like to SIPN topology, and this is expected to change the toughness of the elastomer. The concept is demonstrated in a system containing I-PDEEA as the backbone and PNIPAAm as side chains. The samples were prepared by the "grafting-from" polymerization technology at the inimer units under visible light. The obtained results show that long PNIPAAm brushes-grafted bottlebrush topology can toughen the

elastomer compared to the PDEEA/PNIPAAm based elastomers with similar chemical composition. When the grafted PNIPAAm brushes were removed by UV light irradiation, the obtained SIPN topology structure showed soften property. Interestingly, the toughened elastomer can become soft again by removing the cleaved polymer chains to generate a polymer network topology structure similar to the original one. This finding provides a topology-tunable platform for fundamentally regulating materials' toughness.

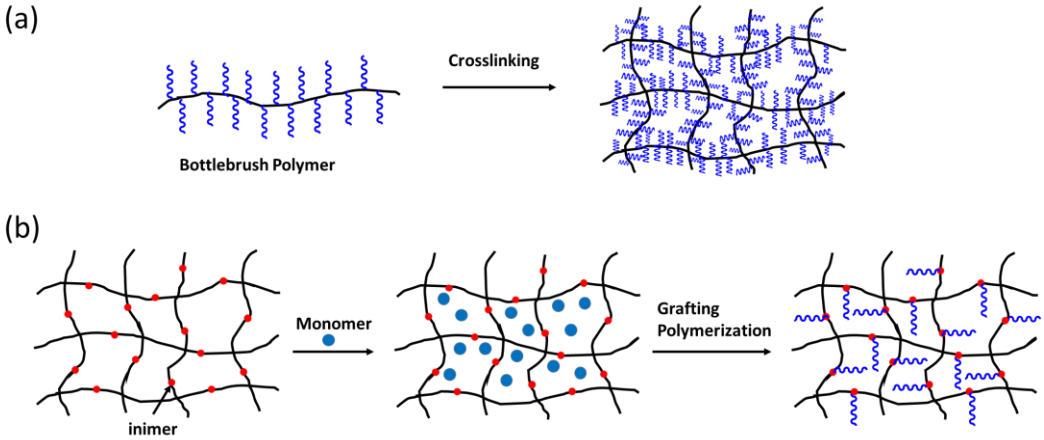

Figure 1. Synthesis of bottlebrush network. (a) Prepared by crosslinking bottlebrush polymers.[192] (b) Prepared by grafting polymer chains from inimer sites.[186] Reproduced with permission. Copyright 2016, Nature Publishing Group. Copyright 2018, American Chemical Society.

4.2 Results

4.2.1 Design of topology-tunable materials using vinyl-*o*NB-Br

The concept of the topology-tunable network is demonstrated in Figure 2. It starts with the synthesis of theI-PDEEA network followed by visible light-initiated grafting of PNIPAAm brushes and UV light-induced detachment of these obtained polymer side chains. The primary network (I-PDEEA) was prepared by copolymerization of acrylate monomer (DEEA), di(meth)acrylate crosslinker (HDDA, 0.1 mol%), and photolabile inimer (vinyl-*o*NB-Br, 0.1 mol%) under visible light (460 nm, 10 mW/cm^2) in the

presence of Irgacure 819 (I-819, 0.3 mol%) (the characterization of functional inimer was detailed described in **Chapter 3**). The inimer can be directly incorporated into the network by copolymerization. For the growth of polymer brushes, the as-prepared I-PDEEA elastomer was immersed into a DMF solution of NIPAAm (monomer) and $Mn_2(CO)_{10}$ (visible light-sensitive additive) to form a swollen substrate. Then 460 nm light was applied to initiate the grafting polymerization of PNIPAAm to form bottlebrush-like network topology (I-PDEEA-PNIPAAm).[145] For the detachment of the polymer chains, I-PDEEA-PNIPAAm was exposed to 365 nm light to debond the grafted polymer chains within the network to form SIPN structure.[196-197] The growth of polymer brushes was expected to toughen the I-PDEEA network since the stretching conformation of the polymer backbones of the original network and the presence of hard and connected PNIPAAm chains which might induce more physical entanglement between polymer chains and network.[198] Note that the force applied to a crosslinked polymer material can be transferred throughout the sample via the connected structure, especially for an elastic matrix. In the crosslinked polymer brush system, the in situ detachment allows for the study of the energy dissipation mechanism at molecular levels.

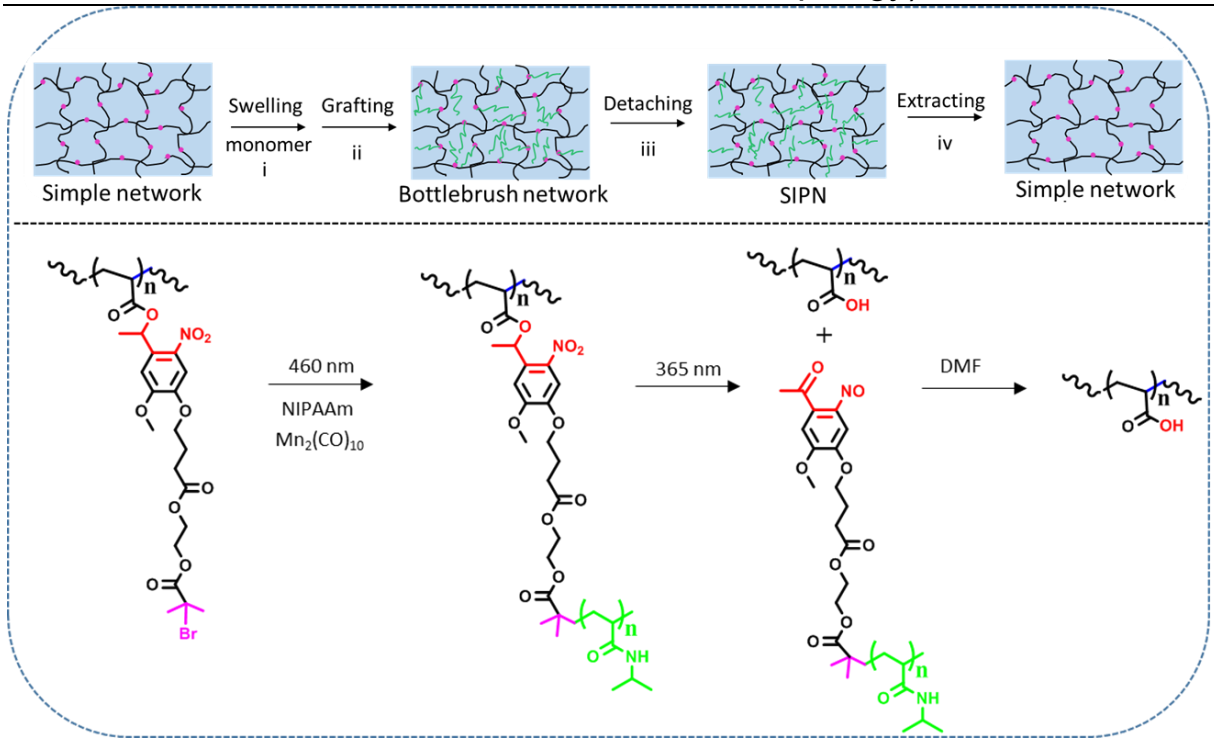

Figure 2. Schematic illustration of a topology-tunable network. PNIPAAm brushes (Green) from the networks are grafted under 460 nm irradiation together with $Mn_2(CO)_{10}$ from the inimer units (Magenta) to form bottlebrush-like network topology, then which are detached at the β position of nitrobenzyl group (red) with 365 nm light irradiation to form SIPN topology (Bottom). By further extracting out the cleaved polymer chains, the network converts into a simple network topology.

4.2.2 Visible light-initiated grafting of PNIPAAm brushes to form bottlebrush-like topological networks

A free radical polymerization mechanism was expected when the I-PEEDA network which was fully swollen of NIPAAm solution was subjected to visible light in the presence of $Mn_2(CO)_{10}$ (described in Section **2.2.2** of **chapter 2**). NIPAAm grafting was first confirmed by the increase in weight (grafting mass density, defined as the increased polymer weight per unit volume was described in section 4.5.5) directly. After grafting PNIPAAm, the grafting mass density increased from 0 mg/cm^3 to 1.2 mg/cm^3. The formation of PNIPAAm in the matrix was further studied by FTIR spectroscopy. After visible light irradiation and washing treatment, new absorptions at

1647 cm^{-1} and 1549 cm^{-1} which were assigned to the C=O stretch and N−H bending of amide groups, respectively, were observed (Figure 3a), indicating the successful growth of PNIPAAm (I-PDEEA-PNIPAAm). Moreover, the swelling ratio of I-PDEEA-PNIPAAm to water increases from 5.8% (I-PDEEA elastomer) to 60%, due to the introduction of hydrophilic PNIPAAm chains (Figure 3b).[199]

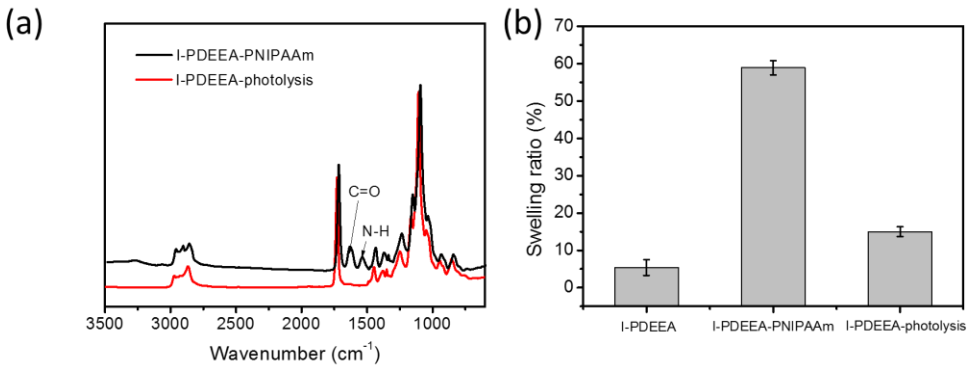

Figure 3. (a) FTIR spectra of I-PDEEA elastomer, I-PDEEA-PNIPAAm elastomer, and I-PDEEA-photolysis elastomer. (b) Swelling ratio of I-PDEEA elastomer, I-PDEEA-PNIPAAm elastomer, and I-PDEEA-photolysis elastomer. Data are presented as the mean ±SD (n = 3) The NIPAAm concentration used in (a) and (b) is 1M. The inimer fraction used in (a) and (b) is 1 mol%.

The mass density of the grafted-PNIPAAm can be regulated by different parameters such as monomer concentration and inimer fraction. As shown in Figure 4a, a linear relationship between grafted-PNIPAAm mass density and monomer concentration was observed, which is similar to the result of PNIPAAm grafted on a silicon surface in **Chapter 2**,[200] indicating that the grafting polymerization by using $Mn_2(CO)_{10}$ system works as a “controlled” polymerization mechanism. When the monomer concentration increased from 0.5 M to 3 M, the grafted PNIPAAm mass density increased from 0.05 to 0.36 mg/cm^3. Furthermore, the grafted-PNIPAAm mass density increased linearly with inimer fraction (Figure 4b). The grafted density increased from 0.08 to 0.55 mg/cm^3 when the inimer fraction increased from 0.04 mol% to 1 mol%. Note that the

increase in grafting mass density in figure 4a suggests the formation of longer PNIPAAm chains since the number of grafting chains was fixed by the inimer fraction. The increase in mass density in Figure 4b is a consequence of the generation of more PNIPAAm chains since the length of polymer chains was fixed by the monomer concentration. Therefore, both the monomer concentration and inimer fraction can be used to adjust the desired grafted-PNIPAAm bottlebrush structure with tunable polymer chains length and number.

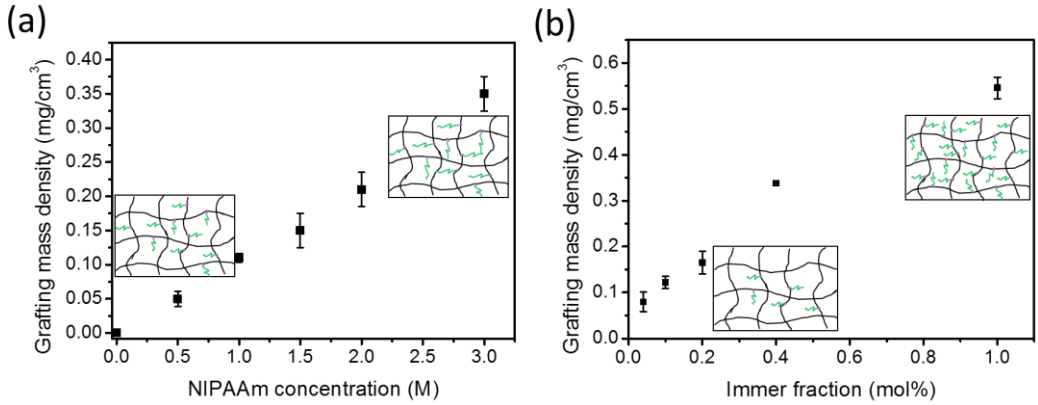

Figure 4. (a) Relationship between grafted-PNIPAAm mass density and monomer concentration. (b) Relationship between grafted PNIPAAm mass density and inimer fraction. The inimer fraction used in (a) is 0.1 mol%. The concentration of NIPAAm used in (b) is 1M. Data are presented as the mean ± SEM (n = 3)

4.2.3 UV light-induced detachment of PNIPAAm chains

The detachment of grafted PNIPAAm side chains (denoted as I-PDEEA-photolysis) was conducted under UV light irradiation. I-PDEEA-PNIPAAm shows UV absorbance bands centered at 270 nm and 350 nm, as expected from the *o*-nitrophenyl ethyl moieties of the inimer (Figure 5a).[201] After UV light irradiation and washing, a decrease in absorbance was observed due to the removal of the *o*-nitrophenyl ethyl moieties, indicating the detachment of PNIPAAm chains. The decrease in the peaks at 1647 cm^{-1} and 1549 cm^{-1} in the FTIR spectrum (Figure 3a) and the decrease in swelling

ratio of I-PDEEA-photolysis elastomer in water (Figure 3b) confirm the removal of the grafted PNIPAAm chains. By immersion of the swollen I-PDEEA-PNIPAAm elastomer in DMF followed by UV light exposure detachment and diffusion of the PNIPAAm chains out of the gel is expected. Indeed, Figure 5b shows that the size of the I-PDEEA-photolysis sample is smaller than the swollen I-PDEEA-PNIPAAm sample, and the color of the concentrated DMF solution changes from colorless to yellow color due to the nitrobenzaldehyde byproducts generated during the photolysis process. These results indicated the removal of grafted PNIPAAm chains from the I-PDEEA network.

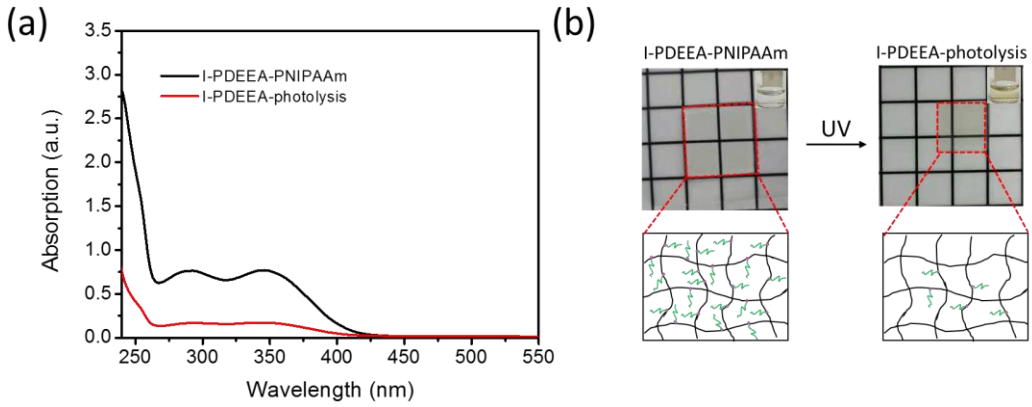

Figure 5. (a) UV Spectra of I-PDEEA-PNIPAAm elastomer and I-PDEEA-photolysis elastomer. (b) UV light-induced cleavage and extracting out of PNIPAAm chains from networks into solution. Photograph of fully swollen I-PDEEA-PNIPAAm before and after exposure to UV light of 365 nm in DMF.

The removal of PNIPAAm polymers can be further proved by the decrease in grafting mass density directly. The grafting mass density of PNIPAAm decreased from 1.2 to 0.2 mg/cm^3 due to the removal of PNIPAAm chains (Figure 6a). The relationship between the length of polymer chains and photolysis efficiency was studied. Longer polymer chains could be grafted by polymerization at higher monomer concentration (Figure 4a), and after photocleaved process, the physical entanglement effect between the cleaved free linear PNIPAAm chains and I-PDEEA network was

increased,[174, 183, 198] thus resulting in decreased photolysis efficiency of detaching PNIPAAm (Figure 6a). Meanwhile, the influence of the number of polymer chains on photolysis efficiency was also investigated. More polymer chains and *o*NB moieties could be obtained from higher inimer fraction network (Figure 4b), which would generate more nitrobenzaldehyde-terminated polymers upon UV irradiation. The intermolecular reaction of nitrobenzaldehyde-terminated polymers may generate complicated structures and affect the extraction of detached polymer chains, resulting in decreased photolysis efficiency (Figure 6b).[202]

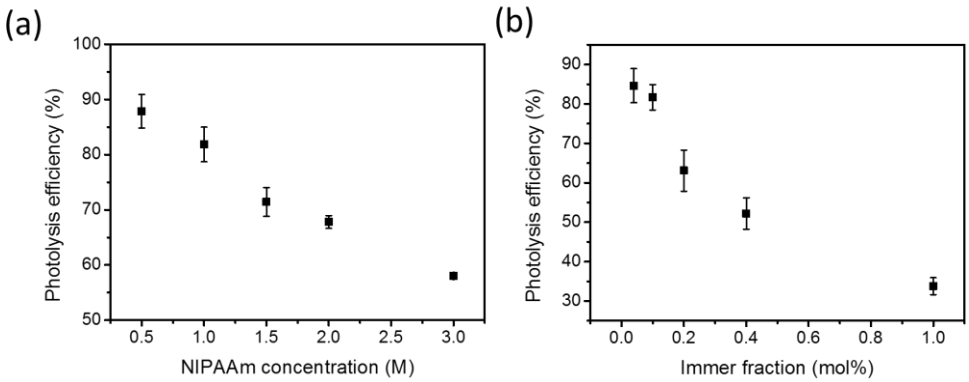

Figure 6. (a) Photolysis efficiency versus monomer concentration and (b) Photolysis efficiency versus inimer fraction. The inimer fraction used in (a) is 0.1 mol%. The concentration of NIPAAm used in (b) is 1M. Data are presented as the mean ± SEM (n = 3)

4.2.4 Regulation of the mechanical properties of materials with tunable topological structures

The mechanical properties of PNIPAAm grafted elastomers with the same chemical compositions (grafting mass density of 0.36 mg/cm^3, NIPAAm mass fraction of 36%) but different topologies were further evaluated. The topologies of the I-PDEEA-PNIPAAm elastomers were schematically illustrated in Figure 6a. As PNIPAAm is a stiff polymer with a high T_g,[203] which may strengthen the elastomer, thus a PNIPAAm/PDEEA co-network elastomer made by the copolymerization of NIPAAM

and DEEA was used as a control sample (donated as PDEEA/PNIAAm co-network, schematically illustrated as Sample 1 in Figure 7a) to evaluate the influence of chemical compositions. NIPAAm concentration of 1M and inimer fraction of 0.4 mol% were used to get a PNIPAAm grafted bottlebrush-like topology with short but dense PNIPAAm chains (donated as 0.4 mol% inimer-1M NIPAAm, schematically illustrated as Sample 2 in Figure 6a), while NIPAAm concentration of 3M and inimer fraction of 0.1 mol% were used to prepare the elastomer with a bottlebrush-like topology with long but relatively dilute PNIPAAm chains (donated as 0.1 mol% inimer-3M NIPAAm, schematic illustrated as Sample 3 in Figure 7a). Moreover, sample 3 was further exposed to UV light to form a SIPN topology (donated as 0.1 mol% inimer-3M NIPAAm-photolysis-SIPN, schematically illustrated as Sample 4 in Figure 7a). The mechanical properties of these samples were then studied. As shown in Figure 7b and Table 1, the PDEEA/PNIAAm co-network elastomer (Sample 1) and 0.4 mol% inimer-1M NIPAAm elastomer (Sample 2) showed much soft properties with toughness (the area under the stress-strain curve) of 1.09 and 1.45 MJ/m^3. And 0.1 mol% inimer-3M NIPAAm elastomer (Sample 3) showed a Young's modulus of 5.62 MPa and toughness of 18.43 MJ/m^3. The results indicate that the longer PNIPAAm chains connected to PDEEA elastomer would enhance the entanglement between grafted polymer chains and network, which is more efficient for dissipating energy during stretching, leading to the toughening of networks.[174-175] However, when Sample 3 exposed under UV light changed to SIPN topology, the toughness decreased to 5.62 MJ/m^3 which may be due to the loss of connecting points. All the above results revealed that the network's toughness can be regulated by changing the topological structures, and the topology structure with long polymer chains and covalently connecting to I-PDEEA network is the most efficient topology for toughness enhancement.

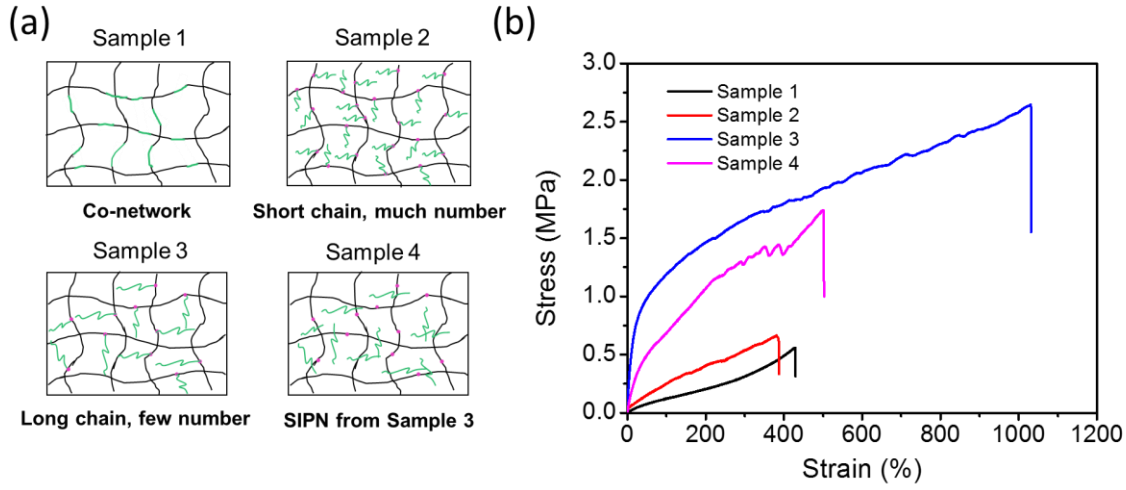

Figure 7. (a) Schematic illustration of PDEEA/PNIPAAm elastomers with different topologies. (b) Tensile stress versus strain curves of different topological DEEA/PNIPAAm elastomers with same PNIPAAm mass fraction in (a). Sample 1: copolymerization from NIPAAM and DEEA. Sample 2: inimer fraction, 0.4 mol%; NIPAAm concentration, 1M. Sample 3: inimer fraction, 0.1 mol%; NIPAAm concentration, 3M. Sample 4: Photolysis sample from Sample 3. The NIPAAm mass fraction is kept as 36% in all the samples.

Table 1. Summarization of mechanical properties of Sample 1, Sample 2, Sample 3 and Sample 4 from figure 6. Data are presented as the mean ± SEM. (n = 3)

Sample	Young's Modulus/ MPa	Fracture Strain/ %	Toughness/ MJ/m^3
1	0.21±0.32	418±30	1.09±0.21
2	0.27±0.45	376±11	1.45±0.16
3	4.92±0.61	917±124	18.43±1.94
4	1.89±0.26	476±64	5.62±1.08

After the investigation of the mechanical property of topology-tunable materials, the mechanical property of the sample after washing (to remove the free PNIPAAm chains) was further studied. In this study, the condition of an inimer fraction of 0.1 mol% and a NIPAAm concentration of 1M was used, in which more than 80% PNIPAAm chains can be removed out. As shown in Figure 8, the I-PDEEA with a simple network

structure shows a toughness of 0.15±0.06 MJ/m^3, and the value was increased to 1.18 ± 0.29 MJ/m^3 after the PNIPAAm side chains were introduced (I-PDEEA-PNIPAAm). Interestingly, once the grafted PNIPAAm chains were removed from the elastomer, the toughness of the I-PDEEA-photolysis sample changed to 0.25±0.10 MJ/m^3, which is slightly higher than the as-prepared one. It was attributed to the residual PNIPAAm chains that could not be fully cleaved upon UV irradiation.[179]

Generally, the visible light-initiated growth of PNIPAAm chains to form bottlebrush-like topology can toughen the elastomer, and the toughness decreased after the bottlebrush-like topology was converted to SIPN topology. These changes indicated that it is efficient to tune the mechanical property of crosslinked materials by regulating polymer network topology. Furthermore, the toughened elastomer can further become soft again by removing the detached PNIPAAm chains, which indicating the feasibility of the light wavelength-selective approach to modify materials.

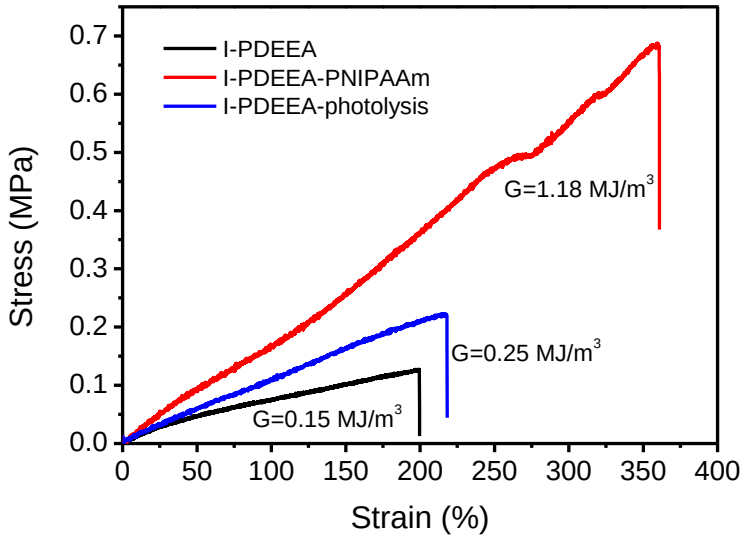

Figure 8. Tensile stress versus strain curves of I-PDEEA elastomer, I-PDEEA-PNIPAAm elastomer, and I-PDEEA-photolysis elastomer. Condition: inimer fraction, 0.1 mol%; NIPAAm concentration, 1M.

4.3 Discussion

Introducing linear polymer chains into a given polymer network to form bottlebrush

network or SIPN can efficiently change their mechanical properties. For example, Matyjaszewski and co-workers fabricated a bottlebrush network by grafting PBA linear chains via ATRP from inimer sites into PMBA network. After forming the PMBA-PBA bottlebrush network, the Young's modulus decreased from 8.6 MPa to 0.5 MPa.[186] And Es-haghi and co-workers prepared bottlebrush network hydrogel and SIPN hydrogel by polymerization of poly(acrylamide) (PAAm, High T_g and stiff polymer) in poly(3-sulfopropyl acrylate) (PSAPS) hydrogel with or without the residual vinyl group.[175] They found that PSAPS-PAAm hydrogels with bottlebrush network topology are tough while which with SIPN topology are brittle. However, the mechanical property of current systems with bottlebrush or SIPN topologies can't be further regulated because the inert connecting points between linear polymers and networks are stable and cannot be changed after fabrication. In this chapter, this issue has been improved by incorporating photo-responsive inimer (vinyl-oNB-Br) into a given network. The formed bottlebrush network topology can further be converted into SIPN by UV irradiation and as a result, the tough bottlebrush network showed a soften behavior.

In my PDEEA-PNIPAAm system, the bottlebrush topology could toughen the network, which is different from the soften effect of PMBA-PBA system developed by Matyjaszewski and co-workers.[186] I suspect it may because different side chains were used (PBA in Matyjaszewski's study but PNIPAAm here). PNIPAAm has a high T_g (133 ^oC) and acts as a stiff chain at room temperature, while PBA has a low T_g (-50 ^oC) and acts as a soft chain at room temperature. But the toughening phenomenon is similar to the PSAPS-PAAm bottlebrush system due to the similar property of PNIPAAm and PAAm (T_g: 165 ^oC). Hence, the physical property of grafted linear polymer chains can significantly influence the mechanical property of the formed bottlebrush network.

When exposed to UV light, the bottlebrush topological network could be transferred

into SIPN in my system. The resulting SIPN is still tougher than PDEEA network (SIPN: 5.62 MJ/m^3, PDEEA network: 0.15 MJ/m^3), which is different from that in PSAPS-PAAm SIPN system (SIPN: brittle, PSAPS network: brittle). That's because the mobility of free polymer chains in a dry state is worse than PSAPS-PAAm hydrogel. The restricted mobility of PNIPAAm chains may help to sustain the force during stretching, while the flexible PAAm chains can't. Note that it is impossible for them to change their bottlebrush network topologies (for regulating mechanical property). But here, in my system, the bottlebrush network could change to SIPN in situ. Therefore, the incorporation of *o*NB-derived inimer into the network suggests a facile way to regulate polymer network topology and its mechanical property on demand.

4.4 Conclusion

I have developed a novel wavelength-selective approach to regulate the toughness of elastomer by controlling the growth and detachment of PNIPAAm brushes with a photolabile inimer in PDEEA network. 460 nm light can trigger the grafting polymerization of PNIPAAm brushes at the alkyl Br site from inimer units to form bottlebrush-like topology in a network. The obtained polymer side chains can be further detached under UV light to form SIPN topology. After the removal of the detached PNIPAAm polymer chains from the network, simple network topology was obtained again. The grafted PNIPAAm mass density can be controlled by the monomer concentration (length of polymer chains) and inimer fraction (number of polymer chains). The introduction of grafted PNIPAAm side chains can enhance the toughness of an elastomer, while their detachment would weaken the toughness. What's more, with the same grafted PNIPAAm mass density, longer polymer chains with less polymer number can tough the elastomer efficiently rather than short chains with more polymer chains. Interestingly, after the removal of the detached polymer

chains, the materials can be turned back into the network topology as that of the original sample. Therefore, the research in this chapter provides a facial photo-regulated way to tune crosslinked material's topology by growing and detaching polymer side chains from an elastomer.

4.5 Materials and methods

4.5.1 Chemicals and materials

1,6-Hexanediol diacrylate (HDDA) (99%, Alfa Aesar), dimanganese decacarbonyl ($Mn_2(CO)_{10}$) (98%, Sigma-Aldrich), Irgacure 819 (I-819) (Ciba) were used as received. 2,2'-Azobis(2-methylpropionitrile) (AIBN) (98%, TCI Deutschland GmbH) was recrystallized from ethanol before use. Di(ethylene glycol) ethyl ether acrylate (DEEA) (98%, TCI Deutschland GmbH) was purified by passing through a column of neutral alumina to remove the inhibitors before being used. *N*-Isopropylacrylamide (NIPAAm, Sigma-Aldrich, 99 %) was recrystallized from a toluene/hexane solution (1/1, v/v) and dried under vacuum before use. Other solvents like ethanol (ETOH), *N,N*-dimethylformamide (DMF), and toluene were purchased from Sigma-Aldrich and used without any treatment. Deionized water was purified with minimum resistivity of 18.2 $M\Omega\ cm^{-1}$.

4.5.2 Instruments

Ultraviolet-visible (UV-vis) spectra were obtained from a Varian Cary 4000 UV/Vis spectrometer (Varian Inc. Palo Alto, USA). The polymerization of the elastomer and photolysis procedure were conducted using UV 365 nm and blue 460 nm collimated LED light (Olympus BX & 1X, 1700 mA) bought from THORLABS, and during the experiments, the intensity was set as 10 mW/cm^2. The results of Attenuated total reflection-Fourier transform infrared (ATR-FTIR) spectroscopy were recorded with a

Bruker VERTEX 70v FTIR spectrometer under a measurement condition of 64 scans and a resolution of 4 cm^{-1}. Optical images of I-PDEEA-PNIPAAm elastomer before and after photolysis were recorded by NIKON camera. An analytical balance (Mettler Toledo XS105 Dualrange) was used to measure the grafting mass density of the grafted PNIPAAm brushes inside I-PDEEA elastomer. Samples were washed at least six times with DMF and ethanol to remove any unreacted monomer/or cleaved polymers and then dried before the next characterization.

4.5.3 Fabrication of the inimer-containing network (I-PDEEA elastomer)

I-PDEEA elastomer was fabricated by a simple photopolymerization. Briefly, DEEA (monomer, 99.5 mol%), HDDA (crosslink-linker, 0.1 mol%), vinyl-*o*NB-Br (inimer, 0.1 mol%), and I-819 (photoinitiator, 0.3 mol%) were mixed, and then the precursor solution was deoxidized with N_2 gas for 20min. The precursor solution was coated on a Teflon template (cut from PTFE film, thickness: 230um) covered by glass slid and cured under 460nm (Intensity: 10mW/cm^2) for 30min to obtain a thin film. After polymerization, the elastomer was peeled off from the glass and immersed in ethanol to remove the unreacted specimens and the ethanol solution was changed every 6 h (4 times). Then it was dried in a vacuum oven to afford the I-PDEEA elastomer.

During this fabrication process, the fraction of inimer can be changed to 0.04 mol%, or 0.2 wt%, or 0.4 wt%, or 1 wt% to obtain I-PDEEA elastomers with different connecting points (Br).

The PNIPAAm/PDEEA co-network elastomer with PNIPAAm fraction of 36% was prepared similarly: NIPAAm (360 mg, 3.2 mmol), DEEA (1.0g, 5.3 mmol), HDDA (1.9mg, 8.5 μmol), and I-819 (12.4mg, 25.5 μmol) were mixed and bubbled with N_2 for

20min to remove the oxygen. Then the cured process is the same as the l-PDEEA elastomer.

4.5.4 Eliminate the residual vinyl group of l-PDEEA elastomer with AIBN

The procedure is the same as described in **Section 3.5.5** of **Chapter 3**.

4.5.5 Visible light-induced grafting polymerization of PNIPAAm in l-PDEEA elastomer

For the grafting polymerization of PNIPAAm brushes to obtain a bottlebrush-like network, the l-PDEEA elastomer which has deactivated the residual double bonds was fully swelled in a deoxy solution which consisted of NIPAAm (565 mg, 0.5 mmol), $Mn_2(CO)_{10}$ (0.2 mg, 0.5 μmol) and 5 mL DMF. Before conducting photopolymerization, the elastomer was wiped by tissue to remove the excess solution, and then exposed to 460nm light (intensity: 10mW/cm^2) for 30min. The swelling and polymerization process were finished in a glove box. Then PNIPAAm grafted elastomer (l-PDEEA-PNIPAAm) was immersed in ethanol and changed every 6 h (4 times) to remove the unreacted monomers.

During this grafting process, the NIPAAm concentration can be changed to 0.5M, or 1.5M, or 2M, or 3M to obtain PNIPAAm grafted l-PDEEA elastomers with different polymer-chain lengths.

The grafting mass density of PNIPAAm was obtained according to the following equation:

$$\text{Grafting mass density} = \frac{(Wt - Wo)}{\text{V}}$$

where W_o and W_t are the masses of the I-PDEEA elastomer, I-PDEEA-PNIPAAm elastomer or I-PDEEA-PNIPAAm-photolysis elastomer, and V is the volume of the elastomer.

4.5.6 UV light-induced detachment of PNIPAAm brush from I-PDEEA elastomer

I-PDEEA-PNIPAAm elastomers were fully swelled in DMF and then exposed to 365nm UV light with an intensity of 10mw/cm^2. After 1h irradiation, the samples were immersed into a fresh DMF solution and sonicated for 10min to fully remove the cleaved polymers. Repeating three times of the UV irradiation and sonication processes mentioned above, then dried in a vacuum oven (I-PDEEA-photolysis).

For the semi-interpenetrating elastomer, the I-PDEEA-PNIPAAm elastomer was conducted in a dry state. Briefly, the sample was placed on the PTFE plate and exposed to 365nm UV light. After 2h irradiation, the sample was turned over to let the backside be exposed to the UV light for 2h to make the full cleavage of the polymer side chains.

Chapter 5

5. Conclusions and outlook

In this thesis, I have developed several light-mediated approaches to regulate the properties of polymer-based systems. The approaches are based on the design and synthesis of *o*NB derivatives with multitasking functionalities. Briefly, an approach to attach and detach polymer chains on various surfaces using light of different wavelengths has been presented and used for modulating surface topologies and making desired surface patterns. This wavelength-selective concept was applied to polymer networks, and applied to regulate the connection between the first and second networks and exchange between connected and disconnected double network structures. In addition, the same approach was used to tune the attachment and detachment of polymer brushes to form bottlebrush-like and semi-interpenetrating topologies, and therefore regulate material mechanical properties.

Here are the major conclusions and outlook of this thesis:

- Photo-regulated growth and detachment of polymer brushes are developed by the combination of $Mn_2(CO)_{10}$ and NO_2-BDAM with wavelength-selectivity (**Chapter 2**). Visible light (460 nm) irradiation enables formation of different functional polymer brushes on various types of substrates, while UV light (360 nm) illumination contributes to removal of the grafted polymer brushes. This strategy is promising to create one-step and two-steps surface patterns.
- Photo-controlled regulation of DN elastomers' topology by varying the connection between the first and the second networks is described (**Chapter 3**). The c-DN topology can be prepared via the grafting polymerization of the monomer and crosslinker entrapped in the inimer-

containing I-PDEEA networks under visible light irradiation, which can be further in situ converted into d-DN using UV light. By controlling the photodegradation degree of inimer, the connecting degree between the first network and the second network can be finely tuned. It was found that this topological transition induces a negligible change in material mechanical properties. These results are inspirable in the understanding of the energy dissipation mechanism of DN structures at molecular levels. From the viewpoint of polymer networks, the c-DN has a significantly higher crosslinking degree than that of d-DN but they show similar mechanical properties. It indicated that no force or energy was transferred or dissipated through these connecting points. In other words, in a crosslinked polymer, only some crosslinking points are effective. These mechanistic insights can be helpful in the design of various crosslinked polymer systems.

- Wavelength-selective approach for regulating the toughness of elastomer was developed by finely controlling the growth and detachment of PNIPAAm brushes using the combination of $Mn_2(CO)_{10}$ and vinyl-*o*NB-Br. 460 nm light can trigger the grafting from polymerization of PNIPAAm brushes to form a bottlebrush-like topology network which enhances the toughness of the elastomer. Further exposed under UV light, the detachment of the grafted polymer brushes to form a SIPN topology that will weaken the sample. It is also found that with the same compositions, a sample with longer PNIPAAm chains shows better mechanical properties (modulus, strain, and toughness). Interestingly, after the removal of the detached polymer chains, the materials can be turned back to a soft state as that of the original sample. The work opens the window

of a new method to mediate material properties.

Although I have established several wavelength-selective systems for tailing the properties of polymer-based materials, many issues should be focused on and addressed in further researches. The main outlook presents as follows:

- Current study indicates the efficiency of tuning the surface property under light irradiation by using functional irreversible *o*NB derivatives. Because of the diversity of chromophores, further developments can make a focus on the rational design and integration of photo-reversible moieties to fabricate photo-responsive interfaces. Considering the energy-saving control, material surfaces with repeatable usage are highly recommended.
- The mechanism of force transfer through the connecting structure at molecular levels within double network materials is still unclear. Further study in this direction is highly desirable and the concept of degradable inimers might be a direction for this study since it allows for fine modulation of the polymer network topologies. Moreover, the concept of tunable polymer network topology can inspire more insights into design of topology-switchable materials by introducing dynamic linkages.
- Bottlebrush-like topology is a splendid structure for toughening crosslinked materials. However, many questions are raised in the current study, including the energy dissipation mechanism in this system (how the force is transferred through the covalent bonds and the physical entanglement), the change in both chemical structure and polymer conformation of the networks during photolysis, what's the difference between elastic and glassy polymer chains in roughening materials, etc. Further studies should concentrate on these issues and thus provide more fundamental understanding over toughening mechanisms.

List of scientific contributions of X. Xiong

Articles

1. **X. Xiong**, L. Xue, L. Yang, S. Dong and J. Cui. Bio-inspired semi-infused adaptive surface with reconfigurable topography for on-demand droplet manipulation. *Mater. Chem. Front.*, **2021**, DOI: 10.1039/D1QM00399B.
2. **X. Xiong**, J. Cui and A. del Campo. Photoresponsive polymers. *Smart Polymers and their Applications*, **2019**, 87-153.
3. **X. Xiong**, L. Xue and J. Cui. Phototriggered Growth and Detachment of Polymer Brushes with Wavelength Selectivity. *ACS Macro Lett.*, **2018**, *7*, 239-243.
4. L. Xue, **X. Xiong**, B. Krishnan, F. Puza, S. Wang and J. Cui. Light-regulated growth from dynamic swollen substrates for making rough surfaces. *Nat. Commun.*, **2020**, *11*, 963.
5. B. Krishnan, L. Xue, **X. Xiong** and J. Cui. Photoinduced strain-assisted synthesis of a stiff-stilbene polymer by ring-opening metathesis polymerization. *Chem. Eur. J.*, **2020**, *26*, 14828.
6. Y. Zheng, X. Liu, J. Xu, H. Zhao, **X. Xiong**, X. Hou and J. Cui. Thermoresponsive mobile interfaces with switchable wettability, optical properties, and penetrability. *ACS Appl. Mater. Inter.*, **2017,** *9*, 35483-35491.
7. L. Xue^{+}, S. Wang^{+}, **X. Xiong**$^{+}$ and J. Cui. Growing Polymer Materials with Updatable Bulky Properties. **2021**, CCS Chemistry, under review.

Conference and seminar

1. Photo-Regulated Growth and Detachment of Polymer Brushes with Wavelength-Selectivity. INM Colloquium Biointerfaces, June 06. 2017, INM-Leibniz Institute for New Materials, Saarbrücken, Germany (Talk).

2. Magnet-actuated Droplet Manipulation on a Ferrofluidimpregnated Surface. Bioinspired and Biomimetic Hydrogels, October 04. 2017, Julich, Germany (Poster presentation).

Curriculum Vitae

Xinhong Xiong,

Date of Brith: 06. 01. 1992

Nationality: P. R. China

EDUCATION

PhD 2016-present

- Doctorate studies at Leibniz Institute for New Materials and Saarland University, Saarbrücken, Germany
- Tentative title of the Thesis: *o*-Nitrobenzyl-based polymer materials with light-regulated multi-functions
- Supervisor: Prof. Dr. Aránzazu del Campo, second supervisor: Prof. Dr. Tobias Kraus, adviser: Dr. Jiaxi Cui
- Major: Chemistry

Master of Science 2013-2016

- Master studies at Soochow University, Suzhou, P. R. China
- Supervisor: Prof. Dr. Zhaoqiang Wu and Prof. Dr. Hong Chen
- Major: Chemistry

Bachelor of Engineering 2009-2013

- HuBei University, Wuhan, P. R. China
- Major: Chemical Engineering and Technology

References

1. Krauss, U.; Lee, J.; Benkovic, S. J.; Jaeger, K.-E., LOVely enzymes – towards engineering light-controllable biocatalysts. *Microbial Biotechnology* **2010,** *3* (1), 15-23.

2. Shibaev, V.; Bobrovsky, A.; Boiko, N., Photoactive liquid crystalline polymer systems with light-controllable structure and optical properties. *Progress in Polymer Science* **2003,** *28* (5), 729-836.

3. Zhao, Y., Rational design of light-controllable polymer micelles. *The Chemical Record* **2007,** *7* (5), 286-294.

4. Shinkai, S.; Hidefumi, K,; Osamu M. Photoresponsive complexation of metal cations with an azobenzene-crown-azobenzene bridge immobilized in polymer supports. *Journal of the American Chemical Society* **1982,** *104* (10), 2933-2934.

5. Everlof, G. J.; Jaycox, G. D., Stimuli-responsive polymers. 4. Photo- and thermo-regulated chiroptical behavior in azobenzene-modified polymers fitted with main chain spirobiindane turns and chiral binaphthyl bends. *Polymer* **2000,** *41* (17), 6527-6536.

6. Gupta, S.; Uhlmann, P.; Agrawal, M.; Chapuis, S.; Oertel, U.; Stamm, M., Immobilization of Silver Nanoparticles on Responsive Polymer Brushes. *Macromolecules* **2008,** *41* (8), 2874-2879.

7. Lai, C.-T.; Hong, J.-L., Aggregation-Induced Emission in Tetraphenylthiophene-Derived Organic Molecules and Vinyl Polymer. *The Journal of Physical Chemistry B* **2010,** *114* (32), 10302-10310.

8. Chen, C.; Liu, G.; Liu, X.; Pang, S.; Zhu, C.; Lv, L.; Ji, J., Photo-responsive, biocompatible polymeric micelles self-assembled from hyperbranched polyphosphate-based polymers. *Polymer Chemistry* **2011,** *2* (6), 1389-1397.

9. Chen, C.-J.; Liu, G.-Y.; Liu, X.-S.; Li, D.-D.; Ji, J., Construction of photo-responsive micelles from azobenzene-modified hyperbranched polyphosphates and study of their reversible self-assembly and disassembly behaviours. *New Journal of Chemistry* **2012,** *36* (3), 694-701.

10. Han, D.; Tong, X.; Zhao, Y., Block Copolymer Micelles with a Dual-Stimuli-Responsive Core for Fast or Slow Degradation. *Langmuir* **2012,** *28* (5), 2327-2331.

11. Pandey, S.; Kolli, B.; Mishra, S. P.; Samui, A. B., Siloxane polymers containing azo moieties synthesized by click chemistry for photo responsive and liquid crystalline applications. *Journal of Polymer Science Part A: Polymer Chemistry* **2012,** *50* (6), 1205-

1215.

12. Wang, Y.; Lin, S.; Zang, M.; Xing, Y.; He, X.; Lin, J.; Chen, T., Self-assembly and photo-responsive behavior of novel ABC2-type block copolymers containing azobenzene moieties. *Soft Matter* **2012,** *8* (11), 3131-3138.

13. Wu, Y.; Zhang, Q.; Kanazawa, A.; Shiono, T.; Ikeda, T.; Nagase, Y., Photoinduced Alignment of Polymer Liquid Crystals Containing Azobenzene Moieties in the Side Chain. 5. Effect of the Azo Contents on Alignment Behavior and Enhanced Response. *Macromolecules* **1999,** *32* (12), 3951-3956.

14. Byrne, R.; Ventura, C.; Benito Lopez, F.; Walther, A.; Heise, A.; Diamond, D., Characterisation and analytical potential of a photo-responsive polymeric material based on spiropyran. *Biosensors and Bioelectronics* **2010,** *26* (4), 1392-1398.

15. De Sousa, F. B.; Guerreiro, J. D. T.; Ma, M.; Anderson, D. G.; Drum, C. L.; Sinisterra, R. D.; Langer, R., Photo-response behavior of electrospun nanofibers based on spiropyran-cyclodextrin modified polymer. *Journal of Materials Chemistry* **2010,** *20* (44), 9910-9917.

16. Fries, K. H.; Driskell, J. D.; Samanta, S.; Locklin, J., Spectroscopic Analysis of Metal Ion Binding in Spiropyran Containing Copolymer Thin Films. *Analytical Chemistry* **2010,** *82* (8), 3306-3314.

17. Mayer, S.; Zentel, R., A new chiral polyisocyanate: an optical switch triggered by a small amount of photochromic side groups. *Macromolecular Chemistry and Physics* **1998,** *199* (8), 1675-1682.

18. Zhang, W.; Yoshida, K.; Fujiki, M.; Zhu, X., Unpolarized-Light-Driven Amplified Chiroptical Modulation Between Chiral Aggregation and Achiral Disaggregation of an Azobenzene-alt-Fluorene Copolymer in Limonene. *Macromolecules* **2011,** *44* (13), 5105-5111.

19. Uchida, K.; Takata, A.; Ryo, S.-i.; Saito, M.; Murakami, M.; Ishibashi, Y.; Miyasaka, H.; Irie, M., Picosecond laser photolysis studies on a photochromic oxidation polymer film consisting of diarylethene molecules. *Journal of Materials Chemistry* **2005,** *15* (21), 2128-2133.

20. Lendlein, A.; Jiang, H.; Jünger, O.; Langer, R., Light-induced shape-memory polymers. *Nature* **2005,** *434* (7035), 879-882.

21. Rosario, R.; Gust, D.; Garcia, A. A.; Hayes, M.; Taraci, J. L.; Clement, T.; Dailey, J. W.; Picraux, S. T., Lotus Effect Amplifies Light-Induced Contact Angle Switching. *The Journal of Physical Chemistry B* **2004,** *108* (34), 12640-12642.

22. Ryplida, B.; Lee, K. D.; In, I.; Park, S. Y., Light-Induced Swelling-Responsive Conductive, Adhesive, and Stretchable Wireless Film Hydrogel as Electronic Artificial Skin. *Advanced Functional Materials* **2019,** *29* (32), 1903209.

23. Romano, A.; Angelini, A.; Rossegger, E.; Palmara, G.; Castellino, M.; Frascella, F.; Chiappone, A.; Chiadò, A.; Sangermano, M.; Schlögl, S.; Roppolo, I., Laser-Triggered Writing and Biofunctionalization of Thiol-Ene Networks. *Macromolecular Rapid Communications* **2020,** *41* (10), 2000084.

24. Cui, J.; Nguyen, T.-H.; Ceolín, M.; Berger, R.; Azzaroni, O.; del Campo, A., Phototunable Response in Caged Polymer Brushes. *Macromolecules* **2012,** *45* (7), 3213-3220.

25. Ding, T.; Yang, W.; Luo, Z.; Liu, J.; Zhang, J.; Cai, K., Preparation of cell pattern on titanium substrates based on upconvertion nanoparticles. *Materials Letters* **2017,** *209*, 392-395.

26. Li, L.; Deng, X.-X.; Li, Z.-L.; Du, F.-S.; Li, Z.-C., Multifunctional Photodegradable Polymers for Reactive Micropatterns. *Macromolecules* **2014,** *47* (14), 4660-4667.

27. Tsang, K. M. C.; Annabi, N.; Ercole, F.; Zhou, K.; Karst, D. J.; Li, F.; Haynes, J. M.; Evans, R. A.; Thissen, H.; Khademhosseini, A.; Forsythe, J. S., Facile One-Step Micropatterning Using Photodegradable Gelatin Hydrogels for Improved Cardiomyocyte Organization and Alignment. *Advanced Functional Materials* **2015,** *25* (6), 977-986.

28. Radl, S. V.; Schipfer, C.; Kaiser, S.; Moser, A.; Kaynak, B.; Kern, W.; Schlögl, S., Photo-responsive thiol–ene networks for the design of switchable polymer patterns. *Polymer Chemistry* **2017,** *8* (9), 1562-1572.

29. Yesilyurt, V.; Ramireddy, R.; Thayumanavan, S., Photoregulated Release of Noncovalent Guests from Dendritic Amphiphilic Nanocontainers. *Angewandte Chemie International Edition* **2011,** *50* (13), 3038-3042.

30. Kloxin, A. M.; Kasko, A. M.; Salinas, C. N.; Anseth, K. S., Photodegradable Hydrogels for Dynamic Tuning of Physical and Chemical Properties. *Science* **2009,** *324* (5923), 59.

31. Kubota, S.; Tanaka, Y.; Moriwaki, T.; Eto, S., Positive Working Photosensitive Polyimide: The Effect of Some Properties on Sensitivity. *Journal of The Electrochemical Society* **1991,** *138* (4), 1080-1084.

32. García-Fernández, L.; Specht, A.; del Campo, A., A Polyurethane-Based Positive Photoresist. *Macromolecular Rapid Communications* **2014,** *35* (20), 1801-1807.

33. Doi, N.; Yamauchi, Y.; Ikegami, R.; Kuzuya, M.; Sasai, Y.; Kondo, S.-i., Photo-responsive polymer micelles from o-nitrobenzyl ester-based amphiphilic block copolymers

synthesized by mechanochemical solid-state copolymerization. *Polymer Journal* **2020,** *52* (12), 1375-1385.

34. Yan, B.; Boyer, J.-C.; Branda, N. R.; Zhao, Y., Near-Infrared Light-Triggered Dissociation of Block Copolymer Micelles Using Upconverting Nanoparticles. *Journal of the American Chemical Society* **2011,** *133* (49), 19714-19717.

35. Gupta, M. K.; Balikov, D. A.; Lee, Y.; Ko, E.; Yu, C.; Chun, Y. W.; Sawyer, D. B.; Kim, W. S.; Sung, H.-J., Gradient release of cardiac morphogens by photo-responsive polymer micelles for gradient-mediated variation of embryoid body differentiation. *Journal of Materials Chemistry B* **2017,** *5* (26), 5206-5217.

36. Lee, J.-E.; Ahn, E.; Bak, J. M.; Jung, S.-H.; Park, J. M.; Kim, B.-S.; Lee, H.-i., Polymeric micelles based on photocleavable linkers tethered with a model drug. *Polymer* **2014,** *55* (6), 1436-1442.

37. Zhao, Y., Light-Responsive Block Copolymer Micelles. *Macromolecules* **2012,** *45* (9), 3647-3657.

38. Zhao, Y., Photocontrollable block copolymer micelles: what can we control? *Journal of Materials Chemistry* **2009,** *19* (28), 4887-4895.

39. Zhang, Q.; Re Ko, N.; Kwon Oh, J., Recent advances in stimuli-responsive degradable block copolymer micelles: synthesis and controlled drug delivery applications. *Chemical Communications* **2012,** *48* (61), 7542-7552.

40. Villiou, M.; Paez, J. I.; del Campo, A., Photodegradable Hydrogels for Cell Encapsulation and Tissue Adhesion. *ACS Applied Materials & Interfaces* **2020,** *12* (34), 37862-37872.

41. Käpylä, E.; Delgado, S. M.; Kasko, A. M., Shape-Changing Photodegradable Hydrogels for Dynamic 3D Cell Culture. *ACS Applied Materials & Interfaces* **2016,** *8* (28), 17885-17893.

42. Yanagawa, F.; Sugiura, S.; Takagi, T.; Sumaru, K.; Camci-Unal, G.; Patel, A.; Khademhosseini, A.; Kanamori, T., Activated-Ester-Type Photocleavable Crosslinker for Preparation of Photodegradable Hydrogels Using a Two-Component Mixing Reaction. *Advanced Healthcare Materials* **2015,** *4* (2), 246-254.

43. Cui, J.; Azzaroni, O.; del Campo, A., Polymer Brushes with Phototriggered and Phototunable Swelling and pH Response. *Macromolecular Rapid Communications* **2011,** *32* (21), 1699-1703.

44. Mayer, G.; Heckel, A., Biologically Active Molecules with a "Light Switch". *Angewandte Chemie International Edition* **2006,** *45* (30), 4900-4921.

45. Theato, P., One is Enough: Influencing Polymer Properties with a Single Chromophoric Unit. *Angewandte Chemie International Edition* **2011,** *50* (26), 5804-5806.

46. Barltrop, J. A.; Plant, P. J.; Schofield, P. Photosensitive protective groups. *Chemical Communications* **1966,** 22, 822-823.

47. M. Goeldner and R. Givens, Dynamic Studies in Biology: Phototriggers, Photoswitches and Caged Biomolecules, Wiley, VCH, Weinheim, **2005,** p. 159.

48. Inomata, K.; Kawasaki, S.; Kameyama, A.; Nishikubo, T., Synthesis of photo-functional polymers with both pendant phenacyl ester and spiro ortho ester groups and photochemical properties of the resulting polymers. *Reactive and Functional Polymers* **2000,** *45* (1), 1-9.

49. Iwamura, M.; Ishikawa, T.; Koyama, Y.; Sakuma, K.; Iwamura, H., 1-Pyrenylmethyl esters, photolabile protecting groups for carboxylic acids. *Tetrahedron Letters* **1987,** *28* (6), 679-682.

50. Arumugam, S.; Orski, S. V.; Locklin, J.; Popik, V. V., Photoreactive Polymer Brushes for High-Density Patterned Surface Derivatization Using a Diels–Alder Photoclick Reaction. *Journal of the American Chemical Society* **2012,** *134* (1), 179-182.

51. Bertrand, O.; Fustin, C.-A.; Gohy, J.-F., Multiresponsive Micellar Systems from Photocleavable Block Copolymers. *ACS Macro Letters* **2012,** *1* (8), 949-953.

52. Amit, B.; Zehavi, U.; Patchornik, A. Photosensitive Protecting Groups—A Review. *Israel Journal of Chemistry* **1974,** *12* (1-2), 103–113.

53. Tyler, D. R., Photochemically degradable polymers containing metal–metal bonds along their backbones. *Coordination Chemistry Reviews* **2003,** *246* (1), 291-303.

54. Kloxin, A. M.; Benton, J. A.; Anseth, K. S., In situ elasticity modulation with dynamic substrates to direct cell phenotype. *Biomaterials* **2010,** *31* (1), 1-8.

55. Tibbitt, M. W.; Kloxin, A. M.; Sawicki, L. A.; Anseth, K. S., Mechanical Properties and Degradation of Chain and Step-Polymerized Photodegradable Hydrogels. *Macromolecules* **2013,** *46* (7), 2785-2792.

56. Karthik, S.; Prashanth Kumar, B. N.; Gangopadhyay, M.; Mandal, M.; Singh, N. D. P., A targeted, image-guided and dually locked photoresponsive drug delivery system. *Journal of Materials Chemistry B* **2015,** *3* (5), 728-732.

57. Cui, J.; Miguel, V. S.; del Campo, A., Light-Triggered Multifunctionality at Surfaces Mediated by Photolabile Protecting Groups. *Macromolecular Rapid Communications* **2013,** *34* (4), 310-329.

58. Kang, C.; Crockett, R. M.; Spencer, N. D., Molecular-Weight Determination of Polymer Brushes Generated by SI-ATRP on Flat Surfaces. *Macromolecules* **2014,** *47* (1), 269-275.

59. Romano, A.; Roppolo, I.; Rossegger, E.; Schlogl, S.; Sangermano, M., Recent Trends in Applying Rrtho-Nitrobenzyl Esters for the Design of Photo-Responsive Polymer Networks. *Materials (Basel)* **2020,** *13* (12).

60. Xue, L.; Xiong, X.; Krishnan, B. P.; Puza, F.; Wang, S.; Zheng, Y.; Cui, J., Light-regulated growth from dynamic swollen substrates for making rough surfaces. *Nature Communications* **2020,** *11* (1), 963.

61. Wang, P., Photolabile Protecting Groups: Structure and Reactivity. *Asian Journal of Organic Chemistry* **2013,** *2* (6), 452-464.

62. Šolomek, T.; Mercier, S.; Bally, T.; Bochet, C. G., Photolysis of ortho-nitrobenzylic derivatives: the importance of the leaving group. *Photochemical & Photobiological Sciences* **2012,** *11* (3), 548-555.

63. Petropoulos, C. C., Synthesis of novel photodegradable poly(o-nitrobenzaldehyde acetal) polymers. *Journal of Polymer Science: Polymer Chemistry Edition* **1977,** *15* (7), 1637-1644.

64. Bachmann, J.; Petit, C.; Michalek, L.; Catel, Y.; Blasco, E.; Blinco, J. P.; Unterreiner, A.-N.; Barner-Kowollik, C., Chain-Length-Dependent Photolysis of ortho-Nitrobenzyl-Centered Polymers. *ACS Macro Letters* **2021,** *10* (4), 447-452.

65. Mrlik, M.; Sobolciak, P.; Krupa, I.; Kasak, P., Light-controllable viscoelastic properties of a photolabile carboxybetaine ester-based polymer with mucus and cellulose sulfate. *Emergent Materials* **2018,** *1* (1), 35-45.

66. Radl, S.; Kreimer, M.; Manhart, J.; Griesser, T.; Moser, A.; Pinter, G.; Kalinka, G.; Kern, W.; Schlögl, S., Photocleavable epoxy based materials. *Polymer* **2015,** *69*, 159-168.

67. Wong, C.-H.; Zimmerman, S. C., Orthogonality in organic, polymer, and supramolecular chemistry: from Merrifield to click chemistry. *Chemical Communications* **2013,** *49* (17), 1679-1695.

68. de Gracia Lux, C.; McFearin, C. L.; Joshi-Barr, S.; Sankaranarayanan, J.; Fomina, N.; Almutairi, A., A Single UV or Near IR Triggering Event Leads to Polymer Degradation into Small Molecules. *ACS Macro Lett* **2012,** *1* (7), 922-926.

69. Liu, G.; Wang, X.; Hu, J.; Zhang, G.; Liu, S., Self-Immolative Polymersomes for High-Efficiency Triggered Release and Programmed Enzymatic Reactions. *Journal of the American Chemical Society* **2014,** *136* (20), 7492-7497.

70. Li, Y.; Jia, X.; Gao, M.; He, H.; Kuang, G.; Wei, Y., Photoresponsive nanocarriers based on PAMAM dendrimers with a o-nitrobenzyl shell. *Journal of Polymer Science Part A: Polymer Chemistry* **2010,** *48* (3), 551-557.

71. Schumers, J.-M.; Fustin, C.-A.; Can, A.; Hoogenboom, R.; Schubert, U. S.; Gohy, J.-F., Are o-nitrobenzyl (meth)acrylate monomers polymerizable by controlled-radical polymerization? *Journal of Polymer Science Part A: Polymer Chemistry* **2009,** *47* (23), 6504-6513.

72. Gumbley, P.; Koylu, D.; Thomas, S. W., Photoresponsive Polymers Containing Nitrobenzyl Esters via Ring-Opening Metathesis Polymerization. *Macromolecules* **2011,** *44* (20), 7956-7961.

73. Schmatz, B.; Yuan, Z.; Lang, A. W.; Hernandez, J. L.; Reichmanis, E.; Reynolds, J. R., Aqueous Processing for Printed Organic Electronics: Conjugated Polymers with Multistage Cleavable Side Chains. *ACS Central Science* **2017,** *3* (9), 961-967.

74. Zhu, W.; Zhang, L.; Chen, Y.; Zhang, K., A UV-Cleavable Bottlebrush Polymer with o-Nitrobenzyl-Linked Side Chains. *Macromolecular Rapid Communications* **2017,** *38* (11), 1700007.

75. Sasaki, T.; Yoneyama, T.; Hashimoto, S.; Takemura, S.; Naka, Y., Photoinduced depolymerization of poly(olefin sulfone)s possessing photobase generator side-chains: Effect of spacer-chain length. *Journal of Polymer Science Part A: Polymer Chemistry* **2013,** *51* (18), 3873-3880.

76. Li, S.; Ji, S.; Zhou, Z.; Chen, G.; Li, Q., Synthesis and Self-Assembly of o-Nitrobenzyl-Based Amphiphilic Hybrid Polymer with Light and pH Dual Response. *Macromolecular Chemistry and Physics* **2015,** *216* (11), 1192-1200.

77. Morris, D. Toward photocontrolled release using light-dissociable block copolymer micelles. *Macromolecules* **2006,** *39*, 4633-4640.

78. Green, M. D.; Foster, A. A.; Greco, C. T.; Roy, R.; Lehr, R. M.; Epps, I. I. I. T. H.; Sullivan, M. O., Catch and release: photocleavable cationic diblock copolymers as a potential platform for nucleic acid delivery. *Polymer Chemistry* **2014,** *5* (19), 5535-5541.

79. Takada, T.; Nishioka, Y.; Baba, T., The Ultraviolet-Induced Functionalization of Multi-Walled Carbon Nanotubes with Polymer Radicals Generated from Polyvinyl Benzoate Derivatives. *C* **2017,** *3* (3), 28.

80. Schumers, J.-M.; Gohy, J.-F.; Fustin, C.-A., A versatile strategy for the synthesis of block copolymers bearing a photocleavable junction. *Polymer Chemistry* **2010,** *1* (2), 161-163.

81. Srivastava, S.; Agarwal, P.; Archer, L. A., Tethered Nanoparticle–Polymer Composites: Phase Stability and Curvature. *Langmuir* **2012,** *28* (15), 6276-6281.

82. Fang, J.-Y.; Lin, Y.-K.; Wang, S.-W.; Li, Y.-C.; Lee, R.-S., Synthesis and characterization of dual-stimuli-responsive micelles based on poly(N-isopropylacrylamide) and polycarbonate with photocleavable moieties. *Reactive and Functional Polymers* **2015,** *95*, 46-54.

83. Zhang, Y.; Cao, X.; Liang, T.; Tong, Z., Acid/light dual-responsive biodegradable polymeric nanocarriers for efficient intracellular drug delivery. *Polymer Bulletin* **2019,** *76* (4), 1775-1792.

84. Folmer, B. J.B.; Cavini, E. Photo-induced depolymerization of reversible supramolecular polymers. *Chemical Communications* **1998,** *17*, 1847-1848.

85. Sijbesma, R. P.; Beijer, F. H.; Brunsveld, L.; Folmer, B. J. B.; Hirschberg, J. H. K. K.; Lange, R. F. M.; Lowe, J. K. L.; Meijer, E. W., Reversible Polymers Formed from Self-Complementary Monomers Using Quadruple Hydrogen Bonding. *Science* **1997,** *278* (5343), 1601.

86. Cui, J.; Campo, A. d., Multivalent H-bonds for self-healing hydrogels. *Chemical Communications* **2012,** *48* (74), 9302-9304.

87. Cui, J.; Wang, D.; Koynov, K.; del Campo, A., 2-Ureido-4-Pyrimidone-Based Hydrogels with Multiple Responses. *ChemPhysChem* **2013,** *14* (13), 2932-2938.

88. Albu, A. M.; Draghicescu, W.; Munteanu, T.; Ion, R.; Mitran, V.; Cimpean, A.; Popescu, S.; Pirvu, C., Nitrodopamine vs dopamine as an intermediate layer for bone regeneration applications. *Materials Science and Engineering: C* **2019,** *98*, 461-471.

89. Coumes, F.; Woisel, P.; Fournier, D., Facile Access to Multistimuli-Responsive Self-Assembled Block Copolymers via a Catechol/Boronic Acid Ligation. *Macromolecules* **2016,** *49* (23), 8925-8932.

90. Ding, X.; Vegesna, G. K.; Meng, H.; Winter, A.; Lee, B. P., Nitro-Group Functionalization of Dopamine and its Contribution to the Viscoelastic Properties of Catechol-Containing Nanocomposite Hydrogels. *Macromolecular Chemistry and Physics* **2015,** *216* (10), 1109-1119.

91. Paez, J. I.; Ustahüseyin, O.; Serrano, C.; Ton, X.-A.; Shafiq, Z.; Auernhammer, G. K.; d'Ischia, M.; del Campo, A., Gauging and Tuning Cross-Linking Kinetics of Catechol-PEG Adhesives via Catecholamine Functionalization. *Biomacromolecules* **2015,** *16* (12), 3811-3818.

92. Shafiq, Z.; Cui, J.; Pastor-Pérez, L.; San Miguel, V.; Gropeanu, R. A.; Serrano, C.; del

Campo, A., Bioinspired Underwater Bonding and Debonding on Demand. *Angewandte Chemie International Edition* **2012,** *51* (18), 4332-4335.

93. Zhao, H.; Sterner, E. S.; Coughlin, E. B.; Theato, P., o-Nitrobenzyl Alcohol Derivatives: Opportunities in Polymer and Materials Science. *Macromolecules* **2012,** *45* (4), 1723-1736.

94. Zhao, H.; Gu, W.; Sterner, E.; Russell, T. P.; Coughlin, E. B.; Theato, P., Highly Ordered Nanoporous Thin Films from Photocleavable Block Copolymers. *Macromolecules* **2011,** *44* (16), 6433-6440.

95. Yamamoto, S.; Tochigi, H.; Yamazaki, S.; Nakahama, S.; Yamaguchi, K., Synthesis of Amphiphilic Diblock Copolymer Using Heterobifunctional Linkers, Connected by a Photodegradable N-(2-Nitrobenzyl)imide Structure and Available for Two Different Click Chemistries. *Bulletin of the Chemical Society of Japan* **2016,** *89* (4), 481-489.

96. Kloxin, A. M.; Tibbitt, M. W.; Kasko, A. M.; Fairbairn, J. A.; Anseth, K. S., Tunable Hydrogels for External Manipulation of Cellular Microenvironments through Controlled Photodegradation. *Advanced Materials* **2010,** *22* (1), 61-66.

97. Kharkar, P. M.; Kiick, K. L.; Kloxin, A. M., Design of thiol- and light-sensitive degradable hydrogels using Michael-type addition reactions. *Polymer Chemistry* **2015,** *6* (31), 5565-5574.

98. Shah, S.; Sasmal, P. K.; Lee, K.-B., Photo-triggerable hydrogel–nanoparticle hybrid scaffolds for remotely controlled drug delivery. *Journal of Materials Chemistry B* **2014,** *2* (44), 7685-7693.

99. Arakawa, C. K.; Badeau, B. A.; Zheng, Y.; DeForest, C. A., Multicellular Vascularized Engineered Tissues through User-Programmable Biomaterial Photodegradation. *Advanced Materials* **2017,** *29* (37), 1703156.

100. Shin, D.-S.; You, J.; Rahimian, A.; Vu, T.; Siltanen, C.; Ehsanipour, A.; Stybayeva, G.; Sutcliffe, J.; Revzin, A., Photodegradable Hydrogels for Capture, Detection, and Release of Live Cells. *Angewandte Chemie International Edition* **2014,** *53* (31), 8221-8224.

101. Siltanen, C.; Shin, D.-S.; Sutcliffe, J.; Revzin, A., Micropatterned Photodegradable Hydrogels for the Sorting of Microbeads and Cells. *Angewandte Chemie International Edition* **2013,** *52* (35), 9224-9228.

102. Yang, C.; Tibbitt, M. W.; Basta, L.; Anseth, K. S., Mechanical memory and dosing influence stem cell fate. *Nature Materials* **2014,** *13* (6), 645-652.

103. Norris, S. C. P.; Tseng, P.; Kasko, A. M., Direct Gradient Photolithography of

Photodegradable Hydrogels with Patterned Stiffness Control with Submicrometer Resolution. *ACS Biomaterials Science & Engineering* **2016,** *2* (8), 1309-1318.

104. Milner, S. T., Polymer Brushes. *Science* **1991,** *251* (4996), 905.

105. Fromel, M.; Li, M.; Pester, C. W., Surface Engineering with Polymer Brush Photolithography. *Macromolecular Rapid Communications* **2020,** *41* (18), 2000177.

106. van der Waarden, M., Adsorption of aromatic hydrocarbons in nonaromatic media on carbon black. *Journal of Colloid Science* **1951,** *6* (5), 443-449.

107. Gungor, E.; Armani, A. M., Photocleavage of Covalently Immobilized Amphiphilic Block Copolymer: From Bilayer to Monolayer. *Macromolecules* **2016,** *49* (16), 5773-5781.

108. Erath, J.; Cui, J.; Schmid, J.; Kappl, M.; Campo, A. d.; Fery, A., Phototunable Surface Interactions. *Langmuir* **2013,** *29* (39), 12138-12144.

109. Kumar, S.; Dory, Y. L.; Lepage, M.; Zhao, Y., Surface-Grafted Stimuli-Responsive Block Copolymer Brushes for the Thermo-, Photo- and pH-Sensitive Release of Dye Molecules. *Macromolecules* **2011,** *44* (18), 7385-7393.

110. Thomas Iii, S. W., New Applications of Photolabile Nitrobenzyl Groups in Polymers. *Macromolecular Chemistry and Physics* **2012,** *213* (23), 2443-2449.

111. Franssila, S. Introduction to Microfabrication. John Wiley & Sons, **2010,** 5–15.

112. Reichmanis, E.; Gooden, R.; Wilkins Jr, C. W.; Schonhorn, H., A study of the photochemical response of o-nitrobenzyl cholate derivatives in P(MMA-MAA) matrices. *Journal of Polymer Science: Polymer Chemistry Edition* **1983,** *21* (4), 1075-1083.

113. Doh, J.; Irvine, D. J., Photogenerated Polyelectrolyte Bilayers from an Aqueous-Processible Photoresist for Multicomponent Protein Patterning. *Journal of the American Chemical Society* **2004,** *126* (30), 9170-9171.

114. Taylor, P. G.; Lee, J.-K.; Zakhidov, A. A.; Chatzichristidi, M.; Fong, H. H.; DeFranco, J. A.; Malliaras, G. G.; Ober, C. K., Orthogonal Patterning of PEDOT:PSS for Organic Electronics using Hydrofluoroether Solvents. *Advanced Materials* **2009,** *21* (22), 2314-2317.

115. Batchelor, R.; Messer, T.; Hippler, M.; Wegener, M.; Barner-Kowollik, C.; Blasco, E., Two in One: Light as a Tool for 3D Printing and Erasing at the Microscale. *Advanced Materials* **2019,** *31* (40), 1904085.

116. DeForest, C. A.; Tirrell, D. A., A photoreversible protein-patterning approach for guiding stem cell fate in three-dimensional gels. *Nature Materials* **2015,** *14* (5), 523-531.

117. Shadish, J. A.; Benuska, G. M.; DeForest, C. A., Bioactive site-specifically modified proteins for 4D patterning of gel biomaterials. *Nature Materials* **2019,** *18* (9), 1005-1014.

118. Batalov, I.; Stevens, K. R.; DeForest, C. A., Photopatterned biomolecule immobilization to guide three-dimensional cell fate in natural protein-based hydrogels. *Proc Natl Acad Sci U S A* **2021,** *118* (4).

119. Hong, Y.; Zhou, F.; Hua, Y.; Zhang, X.; Ni, C.; Pan, D.; Zhang, Y.; Jiang, D.; Yang, L.; Lin, Q.; Zou, Y.; Yu, D.; Arnot, D. E.; Zou, X.; Zhu, L.; Zhang, S.; Ouyang, H., A strongly adhesive hemostatic hydrogel for the repair of arterial and heart bleeds. *Nature Communications* **2019,** *10* (1), 2060.

120. Li, B.; Yu, B.; Ye, Q.; Zhou, F., Tapping the Potential of Polymer Brushes through Synthesis. *Accounts of Chemical Research* **2015,** *48* (2), 229-237.

121. Krishnamoorthy, M.; Hakobyan, S.; Ramstedt, M.; Gautrot, J. E., Surface-Initiated Polymer Brushes in the Biomedical Field: Applications in Membrane Science, Biosensing, Cell Culture, Regenerative Medicine and Antibacterial Coatings. *Chemical Reviews* **2014,** *114* (21), 10976-11026.

122. Azzaroni, O., Polymer brushes here, there, and everywhere: Recent advances in their practical applications and emerging opportunities in multiple research fields. *Journal of Polymer Science Part A: Polymer Chemistry* **2012,** *50* (16), 3225-3258.

123. Barbey, R.; Lavanant, L.; Paripovic, D.; Schüwer, N.; Sugnaux, C.; Tugulu, S.; Klok, H.-A., Polymer Brushes via Surface-Initiated Controlled Radical Polymerization: Synthesis, Characterization, Properties, and Applications. *Chemical Reviews* **2009,** *109* (11), 5437-5527.

124. Zhao, B.; Brittain, W. J., Polymer brushes: surface-immobilized macromolecules. *Progress in Polymer Science* **2000,** *25* (5), 677-710.

125. Olivier, A.; Meyer, F.; Raquez, J.-M.; Damman, P.; Dubois, P., Surface-initiated controlled polymerization as a convenient method for designing functional polymer brushes: From self-assembled monolayers to patterned surfaces. *Progress in Polymer Science* **2012,** *37* (1), 157-181.

126. Tsujii, Y.; Ohno, K.; Yamamoto, S.; Goto, A.; Fukuda, T., Structure and Properties of High-Density Polymer Brushes Prepared by Surface-InitiatedLiving Radical Polymerization. *In Surface-Initiated Polymerization I*, Jordan, R., Ed. Springer Berlin Heidelberg: Berlin, Heidelberg, 2006; pp 1-45.

127. Edmondson, S.; Osborne, V. L.; Huck, W. T. S., Polymer brushes via surface-initiated polymerizations. *Chemical Society Reviews* **2004,** *33* (1), 14-22.

128. Zoppe, J. O.; Ataman, N. C.; Mocny, P.; Wang, J.; Moraes, J.; Klok, H.-A., Surface-

Initiated Controlled Radical Polymerization: State-of-the-Art, Opportunities, and Challenges in Surface and Interface Engineering with Polymer Brushes. *Chemical Reviews* **2017,** *117* (3), 1105-1318.

129. Discekici, E. H.; Pester, C. W.; Treat, N. J.; Lawrence, J.; Mattson, K. M.; Narupai, B.; Toumayan, E. P.; Luo, Y.; McGrath, A. J.; Clark, P. G.; Read de Alaniz, J.; Hawker, C. J., Simple Benchtop Approach to Polymer Brush Nanostructures Using Visible-Light-Mediated Metal-Free Atom Transfer Radical Polymerization. *ACS Macro Letters* **2016,** *5* (2), 258-262.

130. Heeb, R.; Bielecki, R. M.; Lee, S.; Spencer, N. D., Room-Temperature, Aqueous-Phase Fabrication of Poly(methacrylic acid) Brushes by UV-LED-Induced, Controlled Radical Polymerization with High Selectivity for Surface-Bound Species. *Macromolecules* **2009,** *42* (22), 9124-9132.

131. Pester, C. W.; Poelma, J. E.; Narupai, B.; Patel, S. N.; Su, G. M.; Mates, T. E.; Luo, Y.; Ober, C. K.; Hawker, C. J.; Kramer, E. J., Ambiguous anti-fouling surfaces: Facile synthesis by light-mediated radical polymerization. *Journal of Polymer Science Part A: Polymer Chemistry* **2016,** *54* (2), 253-262.

132. Xiong, X.; Wu, Z.; Yu, Q.; Xue, L.; Du, J.; Chen, H., Reversible Bacterial Adhesion on Mixed Poly(dimethylaminoethyl methacrylate)/Poly(acrylamidophenyl boronic acid) Brush Surfaces. *Langmuir* **2015,** *31* (44), 12054-12060.

133. Yan, J.; Li, B.; Zhou, F.; Liu, W., Ultraviolet Light-Induced Surface-Initiated Atom-Transfer Radical Polymerization. *ACS Macro Letters* **2013,** *2* (7), 592-596.

134. Bhat, R. R.; Tomlinson, M. R.; Wu, T.; Genzer, J., Surface-Grafted Polymer Gradients: Formation, Characterization, and Applications. *In Surface-Initiated Polymerization II*, Jordan, R., Ed. Springer Berlin Heidelberg: Berlin, Heidelberg, 2006; pp 51-124.

135. Poelma, J. E.; Fors, B. P.; Meyers, G. F.; Kramer, J. W.; Hawker, C. J., Fabrication of Complex Three-Dimensional Polymer Brush Nanostructures through Light-Mediated Living Radical Polymerization. *Angewandte Chemie International Edition* **2013,** *52* (27), 6844-6848.

136. Brown, A. A.; Azzaroni, O.; Fidalgo, L. M.; Huck, W. T. S., Polymer brush resist for responsive wettability. *Soft Matter* **2009,** *5* (14), 2738-2745.

137. Brown, A. A.; Azzaroni, O.; Huck, W. T. S., Photoresponsive Polymer Brushes for Hydrophilic Patterning. *Langmuir* **2009,** *25* (3), 1744-1749.

138. Kang, C.; Crockett, R.; Spencer, N. D., The influence of surface grafting on the

growth rate of polymer chains. *Polymer Chemistry* **2016,** *7* (2), 302-309.

139. San Miguel, V.; Bochet, C. G.; del Campo, A., Wavelength-Selective Caged Surfaces: How Many Functional Levels Are Possible? *Journal of the American Chemical Society* **2011,** *133* (14), 5380-5388.

140. Stegmaier, P.; Alonso, J. M.; Campo, A. d., Photoresponsive Surfaces with Two Independent Wavelength-Selective Functional Levels. *Langmuir* **2008,** *24* (20), 11872-11879.

141. del Campo, A.; Boos, D.; Spiess, H. W.; Jonas, U., Surface Modification with Orthogonal Photosensitive Silanes for Sequential Chemical Lithography and Site-Selective Particle Deposition. *Angewandte Chemie International Edition* **2005,** *44* (30), 4707-4712.

142. Holten-Andersen, N.; Harrington, M. J.; Birkedal, H.; Lee, B. P.; Messersmith, P. B.; Lee, K. Y. C.; Waite, J. H., pH-induced metal-ligand cross-links inspired by mussel yield self-healing polymer networks with near-covalent elastic moduli. *Proceedings of the National Academy of Sciences* **2011,** *108* (7), 2651.

143. Ye, Q.; Zhou, F.; Liu, W., Bioinspired catecholic chemistry for surface modification. *Chemical Society Reviews* **2011,** *40* (7), 4244-4258.

144. Ciftci, M.; Arslan, M.; Buchmeiser, M.; Yagci, Y., Polyethylene-g-Polystyrene Copolymers by Combination of ROMP, Mn2(CO)10-Assisted TEMPO Substitution and NMRP. *ACS Macro Letters* **2016,** *5* (8), 946-949.

145. Xiong, X.; Liu, W.; Luan, Y.; Du, J.; Wu, Z.; Chen, H., A Versatile, Fast, and Efficient Method of Visible-Light-Induced Surface Grafting Polymerization. *Langmuir* **2014,** *30* (19), 5474-5480.

146. Asandei, A. D.; Adebolu, O. I.; Simpson, C. P., Mild-Temperature Mn2(CO)10-Photomediated Controlled Radical Polymerization of Vinylidene Fluoride and Synthesis of Well-Defined Poly(vinylidene fluoride) Block Copolymers. *Journal of the American Chemical Society* **2012,** *134* (14), 6080-6083.

147. Ciftci, M.; Batat, P.; Demirel, A. L.; Xu, G.; Buchmeiser, M.; Yagci, Y., Visible Light-Induced Grafting from Polyolefins. *Macromolecules* **2013,** *46* (16), 6395-6401.

148. Bektas, S.; Ciftci, M.; Yagci, Y., Hyperbranched Polymers by Visible Light Induced Self-Condensing Vinyl Polymerization and Their Modifications. *Macromolecules* **2013,** *46* (17), 6751-6757.

149. Cui, J.; Iturri, J.; Paez, J.; Shafiq, Z.; Serrano, C.; d'Ischia, M.; del Campo, A., Dopamine-Based Coatings and Hydrogels: Toward Substitution-Related Structure–

Property Relationships. *Macromolecular Chemistry and Physics* **2014,** *215* (24), 2403-2413.

150. Dalsin, J. L.; Hu, B.-H.; Lee, B. P.; Messersmith, P. B., Mussel Adhesive Protein Mimetic Polymers for the Preparation of Nonfouling Surfaces. *Journal of the American Chemical Society* **2003,** *125* (14), 4253-4258.

151. Xu, L. Q.; Jiang, H.; Neoh, K.-G.; Kang, E.-T.; Fu, G. D., Poly(dopamine acrylamide)-co-poly(propargyl acrylamide)-modified titanium surfaces for 'click' functionalization. *Polymer Chemistry* **2012,** *3* (4), 920-927.

152. Hughey, J. L.; Anderson, C. P.; Meyer, T. J., Photochemistry of Mn2(CO)10. *Journal of Organometallic Chemistry* **1977,** *125* (2), C49-C52.

153. Bai, H.; Huang, Z.; Yang, W., Visible light-induced living surface grafting polymerization for the potential biological applications. *Journal of Polymer Science Part A: Polymer Chemistry* **2009,** *47* (24), 6852-6862.

154. Turgman-Cohen, S.; Genzer, J., Simultaneous Bulk- and Surface-Initiated Controlled Radical Polymerization from Planar Substrates. *Journal of the American Chemical Society* **2011,** *133* (44), 17567-17569.

155. Wu, T.; Efimenko, K.; Vlček, P.; Šubr, V.; Genzer, J., Formation and Properties of Anchored Polymers with a Gradual Variation of Grafting Densities on Flat Substrates. *Macromolecules* **2003,** *36* (7), 2448-2453.

156. Ganachaud, F.; Monteiro, M. J.; Gilbert, R. G.; Dourges, M.-A.; Thang, S. H.; Rizzardo, E., Molecular Weight Characterization of Poly(N-isopropylacrylamide) Prepared by Living Free-Radical Polymerization. *Macromolecules* **2000,** *33* (18), 6738-6745.

157. Xiong, X.; Wu, Z.; Pan, J.; Xue, L.; Xu, Y.; Chen, H., A facile approach to modify poly(dimethylsiloxane) surfaces via visible light-induced grafting polymerization. *Journal of Materials Chemistry B* **2015,** *3* (4), 629-634.

158. Keplinger, C.; Sun, J.-Y.; Foo, C. C.; Rothemund, P.; Whitesides, G. M.; Suo, Z., Stretchable, Transparent, Ionic Conductors. *Science* **2013,** *341* (6149), 984.

159. Martinez, R. V.; Glavan, A. C.; Keplinger, C.; Oyetibo, A. I.; Whitesides, G. M., Soft Actuators and Robots that Are Resistant to Mechanical Damage. *Advanced Functional Materials* **2014,** *24* (20), 3003-3010.

160. Yu, K.; Xin, A.; Feng, Z.; Lee, K. H.; Wang, Q., Mechanics of self-healing thermoplastic elastomers. *Journal of the Mechanics and Physics of Solids* **2020,** *137*, 103831.

161. Zhao, X., Designing toughness and strength for soft materials. *Proceedings of the National Academy of Sciences* **2017,** *114* (31), 8138.

162. Tuncaboylu, D. C.; Sari, M.; Oppermann, W.; Okay, O., Tough and Self-Healing Hydrogels Formed via Hydrophobic Interactions. *Macromolecules* **2011,** *44* (12), 4997-5005.

163. Zhao, X.; Chen, X.; Yuk, H.; Lin, S.; Liu, X.; Parada, G., Soft Materials by Design: Unconventional Polymer Networks Give Extreme Properties. *Chemical Reviews* **2021,** *121* (8), 4309-4372.

164. Puza, F.; Zheng, Y.; Han, L.; Xue, L.; Cui, J., Physical entanglement hydrogels: ultrahigh water content but good toughness and stretchability. *Polymer Chemistry* **2020,** *11* (13), 2339-2345.

165. Zhang, G.; Peng, W.; Wu, J.; Zhao, Q.; Xie, T., Digital coding of mechanical stress in a dynamic covalent shape memory polymer network. *Nature Communications* **2018,** *9* (1), 4002.

166. Zhang, K.; Lackey, M. A.; Cui, J.; Tew, G. N., Gels Based on Cyclic Polymers. *Journal of the American Chemical Society* **2011,** *133* (11), 4140-4148.

167. Cuthbert, J.; Balazs, A. C.; Kowalewski, T.; Matyjaszewski, K., STEM Gels by Controlled Radical Polymerization. *Trends in Chemistry* **2020,** *2* (4), 341-353.

168. Zheng, N.; Xu, Y.; Zhao, Q.; Xie, T., Dynamic Covalent Polymer Networks: A Molecular Platform for Designing Functions beyond Chemical Recycling and Self-Healing. *Chemical Reviews* **2021,** *121* (3), 1716-1745.

169. Gong, J. P.; Katsuyama, Y.; Kurokawa, T.; Osada, Y., Double-Network Hydrogels with Extremely High Mechanical Strength. *Advanced Materials* **2003,** *15* (14), 1155-1158.

170. Wang, R.; Lin, T.-S.; Johnson, J. A.; Olsen, B. D., Kinetic Monte Carlo Simulation for Quantification of the Gel Point of Polymer Networks. *ACS Macro Letters* **2017,** *6* (12), 1414-1419.

171. Noda, Y.; Hayashi, Y.; Ito, K., From topological gels to slide-ring materials. *Journal of Applied Polymer Science* **2014,** *131* (15).

172. Zhukhovitskiy, A. V.; Zhong, M.; Keeler, E. G.; Michaelis, V. K.; Sun, J. E. P.; Hore, M. J. A.; Pochan, D. J.; Griffin, R. G.; Willard, A. P.; Johnson, J. A., Highly branched and loop-rich gels via formation of metal–organic cages linked by polymers. *Nature Chemistry* **2016,** *8* (1), 33-41.

173. Brown, H. R., A Model of the Fracture of Double Network Gels. *Macromolecules*

2007, *40* (10), 3815-3818.

174. Nakajima, T.; Furukawa, H.; Tanaka, Y.; Kurokawa, T.; Osada, Y.; Gong, J. P., True Chemical Structure of Double Network Hydrogels. *Macromolecules* **2009,** *42* (6), 2184-2189.

175. Shams Es-haghi, S.; Leonov, A. I.; Weiss, R. A., Deconstructing the Double-Network Hydrogels: The Importance of Grafted Chains for Achieving Toughness. *Macromolecules* **2014,** *47* (14), 4769-4777.

176. Beziau, A.; Fortney, A.; Fu, L.; Nishiura, C.; Wang, H.; Cuthbert, J.; Gottlieb, E.; Balazs, A. C.; Kowalewski, T.; Matyjaszewski, K., Photoactivated Structurally Tailored and Engineered Macromolecular (STEM) gels as precursors for materials with spatially differentiated mechanical properties. *Polymer* **2017,** *126*, 224-230.

177. Cuthbert, J.; Beziau, A.; Gottlieb, E.; Fu, L.; Yuan, R.; Balazs, A. C.; Kowalewski, T.; Matyjaszewski, K., Transformable Materials: Structurally Tailored and Engineered Macromolecular (STEM) Gels by Controlled Radical Polymerization. *Macromolecules* **2018,** *51* (10), 3808-3817.

178. Gong, J. P., Why are double network hydrogels so tough? *Soft Matter* **2010,** *6* (12), 2583-2590.

179. Wirkner, M.; Weis, S.; San Miguel, V.; Alvarez, M.; Gropeanu, R. A.; Salierno, M.; Sartoris, A.; Unger, R. E.; Kirkpatrick, C. J.; del Campo, A., Photoactivatable caged cyclic RGD peptide for triggering integrin binding and cell adhesion to surfaces. *Chembiochem* **2011,** *12* (17), 2623-9.

180. Shams Es-haghi, S.; Weiss, R. A., Fabrication of Tough Hydrogels from Chemically Cross-Linked Multiple Neutral Networks. *Macromolecules* **2016,** *49* (23), 8980-8987.

181. Dušek, K.; Galina, H.; Mikeš, J., Features of network formation in the chain crosslinking (co)polymerization. *Polymer Bulletin* **1980,** *3* (1), 19-25.

182. Tobita, H.; Hamielec, A. E., Crosslinking kinetics in polyacrylamide networks. *Polymer* **1990,** *31* (8), 1546-1552.

183. Es-haghi, S. S.; Leonov, A. I.; Weiss, R. A., On the Necking Phenomenon in Pseudo-Semi-Interpenetrating Double-Network Hydrogels. *Macromolecules* **2013,** *46* (15), 6203-6208.

184. King, D. R.; Okumura, T.; Takahashi, R.; Kurokawa, T.; Gong, J. P., Macroscale Double Networks: Design Criteria for Optimizing Strength and Toughness. *ACS Applied Material & Interfaces* **2019,** *11* (38), 35343-35353.

185. Ducrot, E.; Chen, Y.; Bulters, M.; Sijbesma, R. P.; Creton, C., Toughening Elastomers with Sacrificial Bonds and Watching Them Break. *Science* **2014,** *344* (6180), 186.

186. Na, Y.-H.; Kurokawa, T.; Katsuyama, Y.; Tsukeshiba, H.; Gong, J. P.; Osada, Y.; Okabe, S.; Karino, T.; Shibayama, M., Structural Characteristics of Double Network Gels with Extremely High Mechanical Strength. *Macromolecules* **2004,** *37* (14), 5370-5374.

187. Tanaka, Y.; Kuwabara, R.; Na, Y.-H.; Kurokawa, T.; Gong, J. P.; Osada, Y., Determination of Fracture Energy of High Strength Double Network Hydrogels. *The Journal of Physical Chemistry B* **2005,** *109* (23), 11559-11562.

188. Daniel, W. F. M.; Burdyńska, J.; Vatankhah-Varnoosfaderani, M.; Matyjaszewski, K.; Paturej, J.; Rubinstein, M.; Dobrynin, A. V.; Sheiko, S. S., Solvent-free, supersoft and superelastic bottlebrush melts and networks. *Nature Materials* **2016,** *15* (2), 183-189.

189. Keith, A. N.; Vatankhah-Varnosfaderani, M.; Clair, C.; Fahimipour, F.; Dashtimoghadam, E.; Lallam, A.; Sztucki, M.; Ivanov, D. A.; Liang, H.; Dobrynin, A. V.; Sheiko, S. S., Bottlebrush Bridge between Soft Gels and Firm Tissues. *ACS Central Science* **2020,** *6* (3), 413-419.

190. Self, J. L.; Sample, C. S.; Levi, A. E.; Li, K.; Xie, R.; de Alaniz, J. R.; Bates, C. M., Dynamic Bottlebrush Polymer Networks: Self-Healing in Super-Soft Materials. *Journal of the American Chemical Society* **2020,** *142* (16), 7567-7573.

191. Yamauchi, Y.; Samitsu, S.; Goto, K.; Takeuchi, M., Bottlebrush polymer-reinforced transparent multiphase plastics with enhanced thermal stability. *Chemical Communications* **2020,** *56* (93), 14641-14644.

192. Reynolds, V. G.; Mukherjee, S.; Xie, R.; Levi, A. E.; Atassi, A.; Uchiyama, T.; Wang, H.; Chabinyc, M. L.; Bates, C. M., Super-soft solvent-free bottlebrush elastomers for touch sensing. *Materials Horizons* **2020,** *7* (1), 181-187.

193. Vatankhah-Varnoosfaderani, M.; Daniel, W. F. M.; Zhushma, A. P.; Li, Q.; Morgan, B. J.; Matyjaszewski, K.; Armstrong, D. P.; Spontak, R. J.; Dobrynin, A. V.; Sheiko, S. S., Bottlebrush Elastomers: A New Platform for Freestanding Electroactuation. *Advanced Materials* **2017,** *29* (2), 1604209.

194. Vatankhah-Varnosfaderani, M.; Daniel, W. F. M.; Everhart, M. H.; Pandya, A. A.; Liang, H.; Matyjaszewski, K.; Dobrynin, A. V.; Sheiko, S. S., Mimicking biological stress–strain behaviour with synthetic elastomers. *Nature* **2017,** *549* (7673), 497-501.

195. Xia, Y.; Olsen, B. D.; Kornfield, J. A.; Grubbs, R. H., Efficient Synthesis of Narrowly Dispersed Brush Copolymers and Study of Their Assemblies: The Importance of Side

Chain Arrangement. *Journal of the American Chemical Society* **2009,** *131* (51), 18525-18532.

196. DeForest, C. A.; Anseth, K. S., Cytocompatible click-based hydrogels with dynamically tunable properties through orthogonal photoconjugation and photocleavage reactions. *Nature Chemistry* **2011,** *3* (12), 925-931.

197. Brown, T. E.; Anseth, K. S., Spatiotemporal hydrogel biomaterials for regenerative medicine. *Chemical Society Reviews* **2017,** *46* (21), 6532-6552.

198. Shams Es-haghi, S.; Weiss, R. A., Finite strain damage-elastoplasticity in double-network hydrogels. *Polymer* **2016,** *103*, 277-287.

199. Chen, J.-K.; Wang, J.-H.; Fan, S.-K.; Chang, J.-Y., Reversible Hydrophobic/Hydrophilic Adhesive of PS-b-PNIPAAm Copolymer Brush Nanopillar Arrays for Mimicking the Climbing Aptitude of Geckos. *The Journal of Physical Chemistry C* **2012,** *116* (12), 6980-6992.

200. Xiong, X.; Xue, L.; Cui, J., Phototriggered Growth and Detachment of Polymer Brushes with Wavelength Selectivity. *ACS Macro Letters* **2018,** *7* (2), 239-243.

201. Álvarez, M.; Best, A.; Pradhan-Kadam, S.; Koynov, K.; Jonas, U.; Kreiter, M., Single-Photon and Two-Photon Induced Photocleavage for Monolayers of an Alkyltriethoxysilane with a Photoprotected Carboxylic Ester. *Advanced Materials* **2008,** *20* (23), 4563-4567.

202. Fuentes de Arriba, Á. L.; Simón, L.; Raposo, C.; Alcázar, V.; Sanz, F.; Muñiz, F. M.; Morán, J. R., Imidazolidinone intermediates in prolinamide-catalyzed aldol reactions. *Organic & Biomolecular Chemistry* **2010,** *8* (13), 2979-2985.

203. Shinde, V. S.; Girme, M. R.; Pawar, V. U. Thermoresponsive polystyrene-b-poly (N-isopropylacrylamide) copolymers by atom transfer radical polymerization. **2011.**